Doctoral theses at NTNU, 2021:298

Erlend Sandø Kiel

Methods for quantifying and communicating risks and uncertainties related to extraordinary events in power systems

Doctoral thesis

NTNU
Norwegian University of Science and Technology
Thesis for the Degree of Philosophiae Doctor
Faculty of Information Technology and Electrical Engineering
Department of Electric Power Engineering

NTNU
Norwegian University of Science and Technology

Erlend Sandø Kiel

Methods for quantifying and communicating risks and uncertainties related to extraordinary events in power systems

Thesis for the Degree of Philosophiae Doctor

Trondheim, September 2021

Norwegian University of Science and Technology
Faculty of Information Technology and Electrical Engineering
Department of Electric Power Engineering

NTNU
Norwegian University of
Science and Technology

NTNU
Norwegian University of Science and Technology

Thesis for the Degree of Philosophiae Doctor

Faculty of Information Technology and Electrical Engineering
Department of Electric Power Engineering

ISBN 978-82-326-6111-4 (printed ver.)
ISBN 978-82-326-6358-3 (electronic ver.)
ISSN 1503-8181 (printed ver.)
ISSN 2703-8084 (online ver.)

Doctoral theses at NTNU, 2021:298

Printed by NTNU Grafisk senter

The PhD was funded through the project “Analysis of extraordinary events in power systems” (HILP) (Grant No. 255226), co-funded by the Research Council of Norway, Statnett and Fingrid.

Acknowledgements

The writing of this thesis has been a long and demanding affair, and has sometimes felt like solitary work. There are however many others that have contributed with help, guidance and support throughout the process, and for that I am grateful. First and foremost, I would like to thank my supervisor, Gerd Hovin Kjølle, for her constant support, depth of knowledge, good humor and patience that have most certainly contributed to this thesis being finalized. I also want to thank my co-supervisor, Kjetil Uhlen, for his valuable input and support – sometimes on topics unknown to me. A special mention should also be reserved for Iver Bakken Sperstad for his depth of knowledge and the many good discussions we have had.

I want to extend a special thanks to my fellow PhD students at NTNU. We have had a lot of fun, and you have brightened my days throughout these past few years. I would also thank my new colleagues at SINTEF Energy Research for their support during the final stages of writing this thesis, and the opportunities that you have given me.

Finally, I want to thank my friends and family for their support throughout this whole affair. You are too many to mention but I believe you know who you are. I could not have done this without you.

Erlend Sandø Kiel
Trondheim
August 2021

Summary

Society is dependent on a reliable electricity supply for its normal operation. Blackouts can have severe societal consequences and are sometimes termed extraordinary events. These events are often associated with a high impact and a low probability of occurring. Extraordinary events can have consequences that are deemed unacceptable, yet due to their low probability of occurrence they are not sufficiently identified and communicated through the means of traditional reliability analysis. Operators need tools to plan and operate the power system to ensure that the risk of extraordinary events is reduced in a cost-efficient manner. As a response to this, it is necessary to develop new methods to understand, analyze and communicate the risks and uncertainties related to extraordinary events in power systems.

This thesis contributes to this task in four ways:

- A method of calculating transmission line unavailability due to correlated threat exposure is proposed. The method contributes to an improved understanding of the probability of an unwanted event.
- Protection system misoperation can further weaken the power system following an initial event, and is an important part of many extraordinary events. A compact and generalized method of including protection system failures and misoperation in power system reliability analysis is developed. The method is used to study the interaction between adverse weather and protection system misoperations.
- Extraordinary events that are caused by natural hazards are often associated with long outage durations due to physical infrastructure damage. However, limitations in the available data can make it difficult to parameterize models which include outage durations. A model to predict transmission line down-times is constructed as a possible solution to this challenge.
- Appropriate communication of risk is necessary for stakeholders to make sound risk-informed decisions. The thesis develops novel risk visualizations to support this. The risk visualizations incorporates both the consequences in terms of energy not supplied and also a measure of the criticality for the affected end-users.

List of Figures

List of Tables

List of Symbols

Table 1: List of Symbols 1/3.

3.1 Time-series of failure probability	
$p(y\|\lambda)$	Probability of y given λ
y	Vector of annual failure rates
n	Number of years of observation
λ	Exponential distribution rate parameter
$l(y\|\lambda)$	Likelihood of y given λ
β	Gamma distribution rate parameter
α	Gamma distribution shape parameter
$\Gamma(*)$	Gamma function
IM	Intensity Measure
w	Wind speed [m/s]
t	Time identifier [h]
d	Transmission line length [m]
l	Transmission line identifier
s	Line segment identifier
$erf(*)$	Error function
p	Probability of failure
μ	Log-normal distribution scale parameter
σ	Log-normal distribution shape parameter
k	Time period under consideration [years]

Table 2: List of Symbols 2/3.

3.2 Unavailability	
r	Outage duration [h]
R	Random variable of outage duration
n	Number of observations
μ	Log-normal distribution scale parameter
σ	Log-normal distribution shape parameter
$E(*)$	Expected value of random variable *
$Var(*)$	Variance of random variable *
$F(*)$	Cumulative distribution function
$S(*)$	Survival function
Δ	Difference between two observations
P	Number of intervals
a	Interval identifier
o	Offset
t	Time identifier
k	Inflation factor
CS	A set of components
P(U)	Probability of unavailability
3.3 Dependent failures: Protection systems	
$FT1 - FT4$	Fault Type(s)
G	A graph
V	A vertex set
E	An edge set
b	Bus identifier
$l = \{u, v\}$	Edge element, representing a transmission line between bus u and v
n	Total number of buses
m	Total number of transmission lines
c	Bus connecting two adjacent transmission lines
$s = \{a, b\}$	Set of a- and b- side identifiers of transmission lines
P_l^s	Protection system of line l on its s-side
$p_l^{s,\lambda}$	Specific annual failure rate of a protection system
$p_l^{s,m}$	Conditional probability of missing operation of the protection system
$p_l^{s,u}$	Conditional probability of unwanted non-selective tripping of the protection system
$\cup$	Union (probability)
i	Target line
j	Source line
$A = [a_{i,j}]$	Adjacency matrix between source lines and target lines
$PT3 - PT4$	Probability matrices
λ	Failure rate
λ'	Equivalent failure rate
λ^D	Dependency mode failure rate
U	Unavailability
r	Outage duration [h]
$\oslash$	Element-wise Hadamard division

Table 3: List of Symbols 3/3.

3.4 Restoration times due to permanent faults	
α	Dirichlet concentration parameters
k	Number of categories in α
y	Vector of observations for each category
3.5 Visualization and communication	
$p(\lambda_{i,t})$	Probability of failure of line i at time t
i	Line identifier
t	Time identifier [h]
y	Number of years of observations
POR	Permanent Outage Rate
w	Share of failures due to wind
ρ	Spearman's correlation coefficient
J	Set of system states
$p(u)$	Probability of unavailability
$p(\lambda)$	Probability of failure
n	Number of components in the set
$F(*)$	Cumulative distribution function
$c(r)$	Cost function at reference time
f	CENS correction factor
r	Outage duration
U	Unavailability
λ	Failure rate
$\lambda_{\{x,y\},:}$	Time-series of failure probability for the set $\{x,y\}$
b	Bus identifier
$P_{interr,b,t}$	Interrupted power at bus b at time t
$E(*)$	Expected value of random variable *

Abbreviations

AUD	Australian Dollars
BN	Bayesian Network
CDF	Cumulative Density Function
CENS	Cost of Energy Not Supplied
ENS	Energy Not Supplied
ENTSO-E	European Network of Transmission System Operators
FASIT	Fault And Supply Interruption information Tool
FOR	Forced Outage Rate
FT	Fault Type
HILP	High Impact Low Probability
IEC	International Electrotechnical Commission
IEEE	Institute of Electrical and Electronics Engineers
IEV	International Electrotechnical Vocabulary
IM	Intensity Measure
MC	Markov Chain
MLE	Maximum Likelihood Estimator
MoM	Method of Moments
NERC	North American Electric Reliability Corporation
NOK	Norwegian Kroner
PDF	Probability Density Function
POR	Permanent Outage Rate
RBTS	Roy Billinton Test System
RTS	Reliability Test System
SF	Survival Function
SHELF	SHeffield ELicitation Framework
TSO	Transmission System Operator
USD	U.S. dollars
VOLL	Value of Lost Load

Contents

1 Introduction

Society is dependent on a reliable supply of electricity for its normal operation. The power system is an important and critical infrastructure, and blackouts can have severe consequences for society. There are many examples of historical blackouts that have had a significant societal impact. Malfunctioning software and inadequate operator awareness caused the 2003 U.S. - Canada blackout which affected an estimated 50 million people, and had an estimated total cost between $4 billion and $10 billion USD in the U.S. alone [1, 2]. The storm Dagmar swept across Norway, Sweden and Finland in 2011, causing 1.7 million end-users to experience interrupted power, which for some lasted for more than 25 days [3]. Renewable energy penetration, lack of system inertia and severe weather caused the disconnection of 850 thousand customers in South Australia, and a subsequent estimated cost of $367 million AUD [4, 5].

Extraordinary events, such as blackouts with high societal consequences, have a high impact and a low probability, and are often referred to as HILP events [6]. Such events can be considered tail-end events, and is considered not well enough covered by traditional reliability analysis [7–9]. Operators need tools to plan and operate the power system to ensure both a reliable and resilient power system, reducing the risk of HILP events in a cost-efficient manner. As a response to this, it is necessary to develop new methods to understand, analyze and communicate the risks and uncertainties related to extraordinary events in power systems.

1.1 Motivation

The transmission system is usually operated within the N-1 criterion, i.e., the system is able to withstand the failure of one component without any interruption of service. The power system is a highly reliable system, and the occurrence of multiple simultaneous or near simultaneous failures of its components due to random and independent events is very unlikely although not impossible. A more likely scenario is that the system is subject to a threat which multiple

components are exposed to simultaneously, e.g. due to extreme weather. This causes a correlated threat exposure and higher failure probability for the exposed components within a compressed period of time. Another typical scenario is dependent failures, due to shared infrastructure or failure propagation. The former causes multiple component outages due to a common cause, such as two overhead transmission lines experiencing the collapse of a shared tower, while the latter causes multiple outages due to a fault at one location propagating to another component, e.g. through protection system misoperation. One or more power system failures can be understood as an *unwanted event* which may lead to interruption of electricity supply [6].

Natural hazards are of particular interest when it comes to HILP events. Environmental factors are by far the largest contributor to Energy Not Supplied (ENS) in the Norwegian transmission system in the 33-420kV grid, and are more generally a major factor affecting the reliability of supply [10,11]. Although there are different taxonomies and cause analyses available, natural hazards stands out as a prominent cause of major blackouts [3,12–15]. A distinction between natural hazard events and power system initiated events is offered in [16] where *natural hazard events* are understood to be caused mainly by factors related to the environment, while *power system initiated events* are mainly caused by technical or operational failures in the power system.

This is a useful initial differentiation as natural hazard events are often faced with unique challenges. Extreme weather can cause multiple components in the power system in certain geographical areas to be under high stress from external forces at the same time. This spatial and temporal correlation in exposure can increase the probability of simultaneous or near simultaneous multiple outages of exposed components in a limited geographical area, leading to the failure bunching phenomenon [17]. Natural hazards can also cause extensive physical damage to components in the system which must be repaired before supply can be restored. Reparation and restoration following a natural hazard event may be further hampered by, for instance, continued adverse weather, debris after a disaster or damages to other critical infrastructures [16, 18, 19]. Out of the 66 major blackouts surveyed in [20] it is found that most power system blackouts are initiated due to bad weather.

A common theme in the analysis of extraordinary events is cascading failures. Cascading failures starts with a "trigger" event, e.g. one or multiple component outages, which continues with generations of dependent events [21]. Dependencies can cause some weaknesses to be realized only after an initiating event [13, 22–26]. One example is protection system failures [27], where misoperation of the protection system may cause a further weakening of the system following an initial failure. This weakening can lead to more complex sequences of events such as uncontrolled cascades and subsequent blackouts. A useful observation is that mitigating risk of the initiating event can reduce the frequency of blackouts, while

limiting propagating can reduce their size [21].

One example of a cascading event is the 2019 UK blackout. The event is most commonly thought to have been initiated by a lightning strike to a transmission line. The protection system of the line operated correctly to clear the fault. Nonetheless, the event was immediately followed by 1480 MW of generation losses, in part attributed to unexpected behavior of control and protection systems following the lightning strike. The event itself did not cause any major physical damage to the power system and the system was restored within approximately 40 minutes [28, 29].

The criticality of historical extraordinary events has previously been illustrated along the axes of duration and magnitude of the event [16,30]. Figure 1.1 provides an overview of some notable historical extraordinary events in the period of 1965-2021, categorized by cause of the event (details can be found in Appendix A). In particular the duration of the event is usually longer when it comes to natural hazard events, which often entail large societal consequences. Long restoration times are often associated with major storms, earthquakes or other events which cause damage to infrastructure. The two natural hazard events with the shortest average interruption duration (UK 2019 and US 1998) in the figure are both initiated by lightning strikes. Other events with long average interruption durations are associated with severe infrastructure damage such as the Canadian ice storm in 1998, the cyclone in France in 1999, and the storm Gudrun in Sweden in 2005. The criticality of extraordinary events is however not only dependent on the magnitude and duration of the events but is also affected by the impact on health and life, and the social and economic consequences due to the event [6]. Considerable work has been performed in valuating lost load for customers, in terms of economic consequences, incorporating elements such as which customers are affected and when the power interruption occurs [31–33].

Due to their significant consequences it is important to better understand the risk of extraordinary events. A traditional definition of risk put forward in [34] is that risk is a function of a scenario, a probability and a consequence. Traditional reliability indices in power systems are often derived from expected values, where failure rates, outage durations and interrupted power are important variables. Relying on expected value can lead to the fallacy of the expected value, where low probability events are consumed into the mean [35]. As noted in [36], expected loss does not adequately capture events with low probabilities and high consequences - which are often the case for blackouts in the modern power system. Some consequences of blackouts may be unacceptable, even if they are not reflected into the expected value. This risk aversion among consumers and policy-makers may justify grid investments beyond the theoretical optimum [9]. Thus it is also important to incorporate uncertainty and the distributions of the relevant variables into the risk assessment.

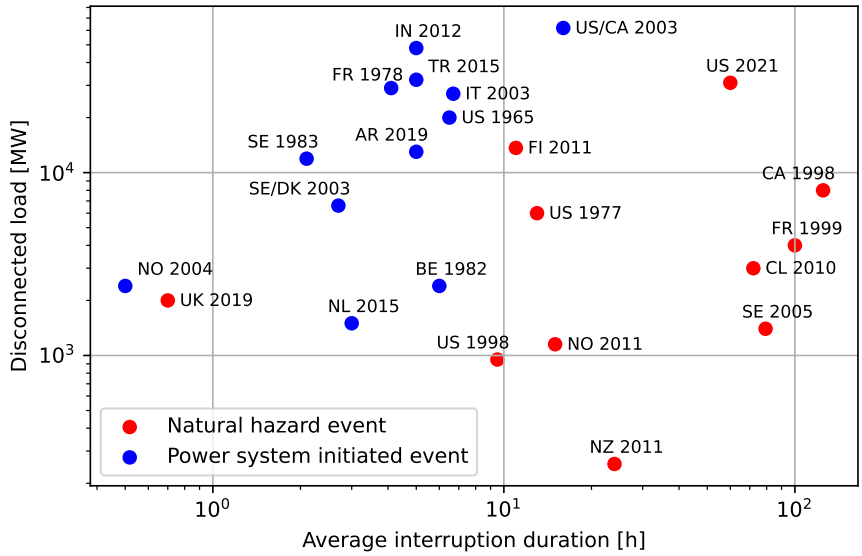

Figure 1.1: Historical extraordinary events, categorized by cause of the event.

Uncertainty can broadly be classified into two categories [37]: Aleatory uncertainty is associated with natural variability or randomness and is considered irreducible. Epistemic uncertainty is associated with lack of knowledge, and knowledge acquisition contributes to reducing this form of uncertainty. There are ways in which aleatory uncertainty can become epistemic, e.g. through advances in science, and there are epistemic uncertainties that are known but can be reduced to random behavior in detailed analysis. These two forms of uncertainty affect power system reliability evaluations [38]. Changing weather conditions, seasonal supply and demand, and inherent variability are just some of the parameters which can potentially produce outcomes which are worse than expected.

Identifying, understanding and communicating risks associated with extraordinary events can thus be an important part of risk-informed decisions among relevant decision makers. This thesis is a contribution to this.

1.2 Objective, scope and limitations

The objective of the thesis is to develop methodologies for understanding and communicating uncertainties and risks related to extraordinary events. The following research questions have been defined to reach the objective:

1 How do time-varying failure rates affect the rate of unwanted events?

2 How do interactions between the failure bunching phenomena and protection misoperation contribute to unwanted events?

3 What are the contributions to long restoration times caused by natural hazard events?

4 How can risk of extraordinary events be communicated and visualized?

This thesis limits itself to considering the risk of extraordinary events from a transmission system operator (TSO) perspective. The work considers the risk, uncertainty and communication of extraordinary events from a planning perspective, largely avoiding the operational perspective.

1.3 Contributions.

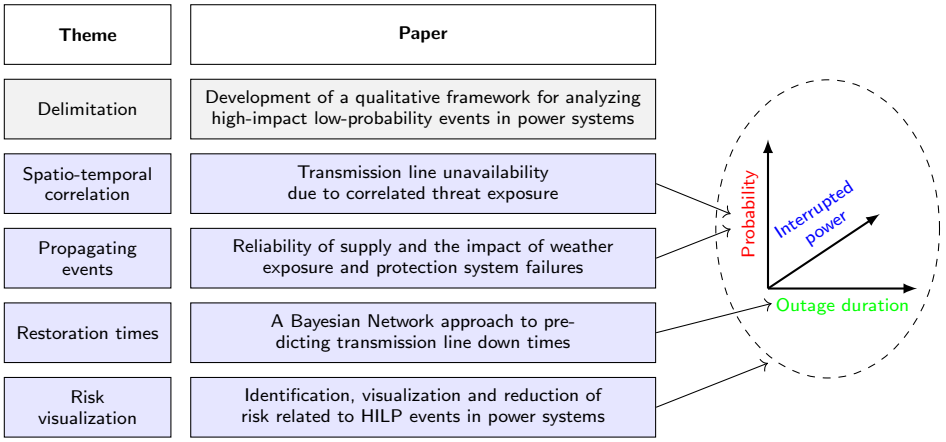

Figure 1.2: Contributions

Initially, a qualitative framework for analyzing HILP events was developed (see **Paper A** in Table 1.1). It is acknowledged that it is impossible to model all aspects relevant to HILP events accurately in a single analysis, and the framework is a tool to define, decompose and delimit the analysis according to which problem the analysis is trying to respond to. A delimitation is performed according to the objective and the associated research questions. This paper is not considered part of the thesis but is included as an appendix.

To answer the first research question, a new method of calculating time-series for component unavailability due to time-varying threats, such as for example, wind or lightning, was developed in **Paper 1**. The model is based on historical time-series of failure probabilities for overhead transmission lines, and distributions of outage durations. This gives a more realistic view of the probability of overlapping outages. The model is transferable to other components or threats. The motivation behind developing the approach is to estimate how the probability of reaching an unwanted event consisting of one or more overlapping component outages changes when there is spatio-temporal correlation in threat exposure. Using time-series of unavailability of components also enables simple comparison with corresponding time-series of consequences due to the unwanted event. This paper contributes to an improved understanding of the probability of the unwanted event.

Paper 2 combines the effects of spatio-temporal correlation in threat exposure, with an early stage of propagating events: dependent failures through protection system misoperation. Further weakening of the power system following a failure can cause the system to quickly move from a secure, to an alert one, to a state of thermal overloads or instability. As extreme weather can cause periods with a high probability of failure, dependent protection misoperation will cluster in the same time periods. This paper develops a generalized method for incorporating propagating failures between adjacent transmission lines due to protection system misoperation, based on graph theory. The method is extended from traditional reliability analysis to be applicable to time-series of failure probabilities. This article provides answers to research question 2.

Paper 3 contributes to the prediction of overhead transmission line down times, answering the third research question. This paper structures and decomposes what causes long restoration times due to permanent failures requiring repair following extreme weather. This is a response to the limited work on the restoration time of components for use in power systems vulnerability or resilience analysis. A Bayesian Network (BN) model of transmission line down times is constructed based on expert judgments and historical data. The model can be used to construct down time distributions that are conditioned on time- and location-specific information, both for existing and potential new overhead transmission lines. The BN structure and decomposition of the model visualizes the contributions to long down times.

Identification, visualization and reduction of risk is explored in **Paper 4**, attempting to answer research question 4. The paper discusses different approaches to analyzing extraordinary events. It argues for a distinction between extreme weather scenarios that are constructed to represent an extreme case, and those which follows historical patterns in terms of probability of occurrence. The former can have great exploratory value in finding outages with high impact. The latter can be assigned a probability, which is arguably a necessary condition to perform

Table 1.1: List of publications

Paper 1	[39]	E. S. Kiel and G. H. Kjølle, "Transmission line unavailability due to correlated threat exposure," in 2019 IEEE Milan PowerTech, PowerTech 2019, jun 2019.
Paper 2	[40]	E. S. Kiel and G. H. Kjølle, "Reliability of Supply and the Impact of Weather Exposure and Protection System Failures," Applied Sciences 11, no. 1 (2021): 182.
Paper 3	[41]	E. S. Kiel and G. H. Kjølle, "A Bayesian Network approach to predicting transmission line down times," Proc. 30th Eur. Saf. Reliab. Conf. and the 15th Probabilistic Saf. Assess. Manag. Conf., 2020.
Paper 4	[42]	E. S. Kiel and G. H. Kjølle, "Identification, visualization and reduction of risk related to HILP events in power systems," 2019 54th Int. Univ. Power Eng. Conf. UPEC 2019 - Proc., sept 2019.
Paper A	[26]	I. B. Sperstad and E. S. Kiel, "Development of a qualitative framework for analysing high-impact low-probability events in power systems," in Safety and Reliability - Safe Societies in a Changing World - Proceedings of the 28th International European Safety and Reliability Conference, ESREL 2018, CRC Press, 2018, pp. 1599–1608.

a full risk analysis. A simple metric is constructed to show which lines have historically had the largest impact on expected energy not supplied (ENS). Different methods of risk visualization are discussed, and a probability-consequence diagram including uncertainty bands is suggested.

The work in Paper 4 is then extended to include the cost of ENS as a measure of the criticality for affected end-users due to extraordinary events. Risk visualizations based on uncertainty boxes are further developed in the extended work. The novel risk visualizations are assumed to convey the key information on risk relevant to expected and extraordinary events.

1.4 Thesis structure

The remainder of the thesis is structured as follows. In Chapter 2 the theoretical framework for analyzing extraordinary events is presented. This chapter initially gives an introduction to vulnerability and risk, before introducing important definitions and sources of data used in the thesis. The role of dependent outages is then further explored through two particular contributors to extraordinary

events, extreme weather and protection system misoperation. Lastly, methods of visualizing and communicating risks in the power system domain is presented. Chapter 3 discusses the papers that makes up the thesis, sometimes with added or reduced detail, to highlight or clarify elements in the published papers. The subsection dealing with risk visualization contains an extension of the published work in Paper 4. The contributions to the objective of the thesis and individual research questions are presented in Chapter 4 alongside recommendations for future research.

2 Theoretical foundations

The power system is a critical infrastructure upon which other infrastructures and societal functions rely [43–45]. Small failures of a critical infrastructure can have widespread consequences for other critical infrastructures and consequently for society as a whole. Reliability analysis analysis primarily deals with the expected behavior of the power system; however, rare events can constitute high or unacceptable risks that reliability analysis is not able to communicate. This chapter explores some of the current literature and methods used to analyze and evaluate the risk of extraordinary events in power systems. Common terminology and dependence models especially relevant to extraordinary events is given special attention.

Reliability analysis gives a measure of the system's ability to perform its intended function, and its expected behavior. Newer concepts such as vulnerability and resilience analysis deal with the inability or ability of the system to withstand strains, and the effects of consequent failures. While reliability may adequately capture the expected behavior of the system, it may fail to capture high-consequence scenarios which are included in vulnerability and resilience analysis [7, 8, 46]. Extraordinary, extreme, catastrophic or HILP events are rare, and thus they can have an negligible effect on the expected value of risk, even if the associated consequence is severe. The consequences of these tail-end events may however be deemed unacceptable, and should thus be considered [30, 35].

The concepts of resilience and vulnerability have historically grown out of natural- and social-science research traditions, respectively, and while the former has had a more positivist approach the two fields have grown increasingly similar. Both concepts can be considered as ways of responding to stress and as part of the field of adaptive risk management [47]. Vulnerability may be seen as degree to which the system may react adversely to a threat, while resilience the ability to resist adverse effects [47–49]. There are a large number of approaches and definitions related to resilience and vulnerability applicable to power systems (see e.g. [50–52]), and resilience could be seen as the inverse - or the antonym - of vulnerability [6, 37].

Vulnerability can be understood in a number of different ways depending on the issue at hand, and the methodological approach employed [26, 52]. For the purposes of this thesis, vulnerability is understood as *an expression for the problems a system faces to maintain its function if a threat leads to an unwanted event and the problems the system faces to resume its activities after the event occurred*, where an *unwanted event* is defined as *one or more power system component outages potentially leading to an interruption in the supply of electricity for the end user* [6, 53]. This definition is general, and is applicable both to failures due to external threats and causal mechanisms such as cascading events. The usage of the definition is based on years of developed vulnerability analysis, indicator development and methodologies of analyzing extraordinary events (see e.g. [26, 30, 53–56]), summarized in a comprehensive framework for vulnerability analysis in [6]. This framework is used as a basis for the analysis of risk and uncertainty related to extraordinary events in this thesis.

The remainder of the chapter is structured as follows: Section 2.1 introduces the conceptual bow-tie model of vulnerability in the power system, and clarifies terms and definitions, and their relationship to risk. Section 2.2 presents the Norwegian fault data registration system (FASIT), and definitions related to the registration of faults. Section 2.3 presents common dependencies relevant for the analysis of the vulnerability of the power system. In Section 2.4 quantification and visualization of risk is introduced.

2.1 Vulnerability and risk

Figure 2.1 gives an outline of the vulnerability concept as understood by this thesis. The vulnerability framework upon which this thesis bases itself decomposes vulnerability into several dimensions. On one axis is the power system internal-/external dimension, while another concerns if it is related to the occurrence of an unwanted event or the consequence of the event [6]. A bow-tie diagram depicting the relationship between an unwanted event from cause to consequence, and the associated mitigating barriers (see e.g. [37, p.119]) is superimposed on to the figure to illustrate the risk management process related to a given unwanted event. A distinguishing feature of power system vulnerability is that it is understood as an internal characteristic of the power system: A threat may lead to an unwanted event depending on the *susceptibility* of the system. An unwanted event may similarly lead to different end-user consequences depending on the *coping capacity* of the power system [6].

The relevance of the susceptibility and coping capacity of the system is decided by external factors, through its exposure to threats, and the criticality of the power system consequence. A *threat* is understood as *any indication, circumstance or event with the potential to disrupt or destroy a critical infrastructure or any*

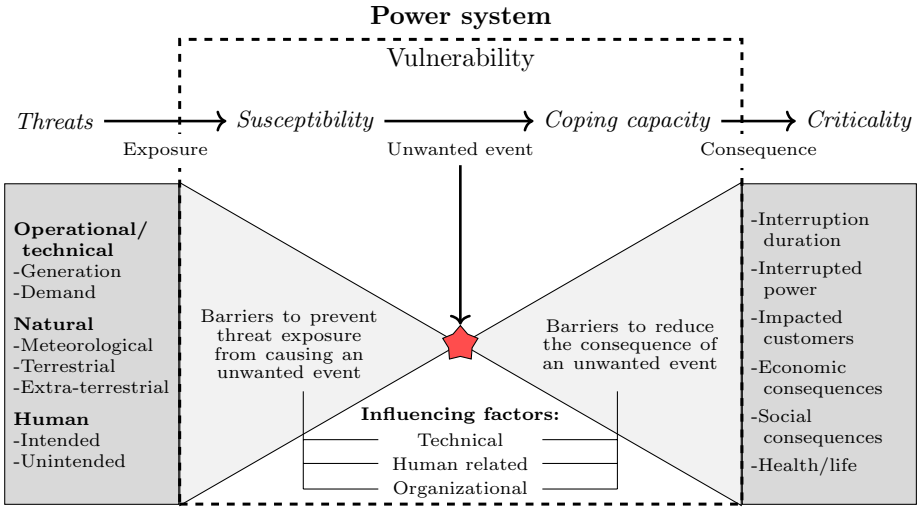

Figure 2.1: Power system vulnerability and associated bow-tie model, adapted from [6].

element thereof [57], and the relevance is decided in accordance to what degree the system is exposed to the threat. Typical threats may be natural hazard events such as severe weather, human threats through intended and unintended actions, or operational/technical decided by the operational stress on the system components. A power system consequence can be measured in several ways that will be discussed later in the thesis, but one possible measure is ENS in terms of MWh. However, the criticality of an extraordinary event reflects the external impact on society due to the power system consequence, depending on the end-user's dependence on the electricity supply. An *extraordinary event* is then understood as a sequence of events that leads to a critical consequence, i.e. a blackout [6].

Barriers can be related the vulnerability of the power system and are influenced by technical, human and organizational factors. Barriers related to susceptibility aims to prevent threat exposure from causing an unwanted event and can be factors such as the technical condition of components, operative competence, and operator awareness. Barriers related to the coping capacity are intended to avoid or reduce the consequence of an unwanted event and may be the availability of spare parts, competence and skill in system restoration, or the availability of contingency plans [37, 53].

The risk associated with a scenario has been defined as a function of its probability and consequence [34] and as such the path from threat to criticality defines the

risk of an extraordinary event. Viewing the power system in isolation gives limited information about the associated risk to society. The power system might be highly vulnerable to a threat that it is never exposed to, and similar consequences can have a widely different criticality for society when the dependence on power of the affected customers is taken into account. The risk of an extraordinary event thus also takes into account power system's external properties, such as threat exposure and criticality for the end-user, which will be further highlighted later in this chapter.

The concept of vulnerability can also be related to resilience. Although the perspective of resilience is not used in this thesis, it is useful to relate the two concepts, as a significant amount of academic work is currently being undertaken on the topic. There is no commonly accepted definition of resilience in the power system domain [8, 58, 59], but a definition of resilience which is analogous to the vulnerability definition used in this thesis is proposed in [6] as *the ability of the system to maintain its function if a threat leads to an unwanted event and the problems the system faces to resume its activities after the event occurred.* The end goals of resilience, *robustness* and *rapidity*, can be analogous to the susceptibility and coping capacity of the system supported by the means of *resourcefulness* and *redundancy* [6, 60, 61]. The conceptual resilience triangle [60, 62] or trapezoid [63] can also be represented with vulnerability specific terms, to a similar effect.

Figure 2.2 shows a timeline where the interaction between threat exposure and susceptibility of the power system develops into an unwanted event. The coping capacity of the system decides the interrupted power and interruption duration, and as a result the consequence of the unwanted event.

As is noted in [26], it is impossible to analyze all relevant aspects related to extraordinary events quantitatively, and it is necessary to decompose and delimit the analysis according to the purpose of the analysis. The purpose of this thesis is to develop methods to understand, quantify and communicate risk related to extraordinary events in the power system. A delimitation of the analyses is therefore decided by the representation of risk: The probability of the unwanted event, and the criticality of the resulting consequences for the end-users.

2.2 Terms, definitions and data

The FASIT (a Fault And Supply Interruption information Tool) reporting tool was developed in the 1990's and implemented in 1995 as a common tool for reliability data collection and reporting for operators in the Norwegian transmission and distribution grid [64]. Over the years it has been further developed, and definitions have been updated as the requirements from the regulatory authorities

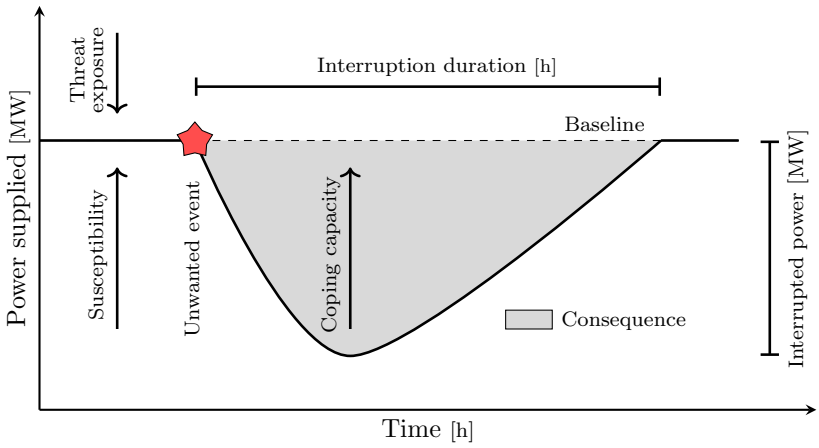

Figure 2.2: Progression of an unwanted event, from threat exposure to consequence.

have evolved. The FASIT system links standardized fault reports with databases containing information on the faulty equipment, and the affected delivery points and customers. A Cost of Energy Not Supplied (CENS) scheme was introduced in 2001 and included in the FASIT system. FASIT has been used by all network companies at all voltage levels, including the Norwegian Transmission System Operator (TSO), Statnett, since 2006. The standardized and mandatory reporting scheme has thus contributed to historical fault statistics which has enabled monitoring of trends over time [64–67]. The FASIT reporting scheme has its own terms and definitions to ensure consistent reporting of faults and interruptions in the Norwegian power system. Some of the definitions in FASIT have been incorporated into the Nordel - and later the ENTSO-E - guidelines for grid disturbance classification [68], and revisions have been made to make the terms and definitions better harmonized with other international standards [66, 69]. Other common sources of relevant English terms and definitions related to the reliability of supply are available from the IEEE [70, 71], IEC [72], ENTSO-E [68] or NERC [73]. The definition sets have grown from their own traditions and is heavily interconnected in terms of terminology. As such there is a need to clarify some key terms that will be used throughout this thesis.

A key term when it comes to the delivery of electrical power is the *delivery point*, or a "point, power transformer or busbar in the grid where the electricity is exchanged". This may be connected to an *end-user* who are defined as "buyers of electrical energy who do not resell all the energy" [68]. A *supply interruption* is understood as a "customer load disconnection from the electric power supply" [72], where the *interruption duration* of such an event is understood as "the time period from the initiation of an interruption until service has been restored to

the affected customers" [71]. *Energy not supplied (ENS)* is understood as "the estimated energy which would have been supplied to end users if no interruption and no transmission restrictions had occurred" [68]. The emphasis of this thesis is on *grid disturbances*, or "outages, forced or unintended disconnection or failed re-connection of breaker as a result of faults in the power grid" [68, 69], and does not include planned outages.

When dealing with extraordinary events, often caused by the physical destruction of infrastructure, it is important to clarify the element of analysis. A *system unit* is understood as "a group of components which fulfils a main function in the power system" and is delimited by circuit breakers, whereas a *component* is "equipment which fulfils a main function in a unit". A component can be further divided into sub-components: isolators, towers, etc., which are considered sub-components of an overhead transmission line [68]. A distinction between a unit and a component is clarified in [71]: A unit is a functional facility which transfers power between designated points, while a component is a specific piece of equipment. Units are often named after the distinguishing component of the unit. The concept of a unit has similar understandings in the different reliability standards, and is sometimes referred to as an *item* [72], or an *element* [73].

A *failure* of a component is understood as a "loss of ability to perform as required" and is considered an event which leads to a *fault* which means an "inability of a component to perform its required function". A "fault that has not become apparent" is considered a *latent* or hidden fault up until the point of fault detection [72]. When registering a fault in FASIT, a "set of circumstances that leads to failure" is specified as the *failure cause*. A distinction is also made between a *primary failure* which is a "failure of an item not caused either directly or indirectly by the failure of another item", and a *secondary failure* which *is* caused by the failure of another item. A *permanent fault* is understood as a fault where *the component or unit is damaged and cannot be restored to service until repair or replacement is completed*, while a *temporary fault* means that "the unit or component is undamaged and is restored to service through manual switching operations without repair being performed, but possibly with on-site inspection", meaning that no other action than a reconnection of circuit breakers, replacement of fuses or signal acknowledgement is required [68]. *Common cause failures* are especially relevant when it comes to harsh weather, and are understood as "failures of multiple items, which would otherwise be considered independent of another, resulting from a single cause" [72].

A component is considered in a *down-state* or *unavailable* while it is "unable to perform as required, due to an internal fault". Faults are related to the concept of an *outage*. This is understood as "[t]he component or unit is not in the in-service state; that is, it is partially or fully isolated from the system" [68], where *in-service* means that the component or unit is "energized and fully connected to the system" [70]. An outage may be due to a failure but this is

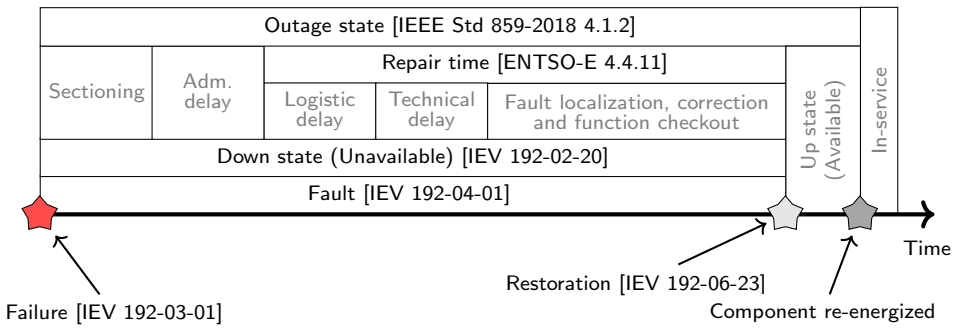

Figure 2.3: Restoration process following a permanent fault of one component, example using key terms. Time not to scale.

not necessarily always the case. An un-faulted, or healthy, component can be in the outage state due to planned maintenance or incorrect operation of protection systems. A latent fault of a protection system can similarly be present without it immediately leading to an outage. The thesis deals with situations where the outage of one or the simultaneous outage of multiple components is considered, however, detailed analysis of fault clearing times is not part of the work. In the case of a permanent fault, the component must be brought back to the in-service state. The understanding of *repair time* used in FASIT (and ENTSO-E) is largely similar to the understanding of *corrective maintenance time* used in IEC [72]; however, they do have points of shared terms with different definitions. The understanding of repair time in this thesis follows the ENTSO-E/FASIT definition.

Figure 2.3 provides an overview of some key terms used in this thesis, illustrated by the process of returning a component to the in-service state following a permanent fault. Text marked in gray is rarely used but is included to clarify what are considered parts of the different terms. The progression of the restoration process following a real event may diverge from this stylized example but it offers an overview of the relationship between the terms used.

An *outage event* involves "the outage occurrence of one or more units or components". Similarly, the "outage occurrence of a single system component", or "the concurrent outage of two or more system components" is termed a *contingency* [72]. As the transmission system is operated according to the N-1 criterion, it is relevant to consider outage events involving two or more component outages, if the goal is to identify end-user consequences.

The notion of a cut-set is often used in reliability analysis. A cut-set can be understood as a "set of basic events whose occurrence (at the same time) ensures that the top event occurs" in a fault-tree. The *top event* in the context of this

thesis is "an event which causes an interruption of service to customers" in terms of interrupted power. A cut-set can be considered *minimal* if "the set cannot be reduced without losing its status as a cut-set" [74, p.103]. A *set* is sometimes used interchangeably with a contingency, and does not necessarily imply that the set causes interrupted power at the end-user.

The power system consists of highly reliable components, and although positive in itself, it can be a challenge to characterize failure behavior using limited statistical failure data [75]. Data availability becomes even more relevant when attempting to investigate multivariate relationships. Subsetting the data based on more than one to two variables can leave few to no observations of events in some categories. Lack of data a particular a challenge when it comes to restoration and repair times in FASIT. Different interpretations and complexity in collection and registration have led these data to be voluntary to report, and thus incomplete [67]. This does however highlight the importance of continued efforts to collect standardized fault reports.

Figure 2.4 shows faults recorded in FASIT for overhead transmission lines, in the period of 2008-2017, separated by cause, voltage level and nature of the fault. It is worth noting that the majority of faults are caused by environmental factors, with wind, lightning and snow/ice being the most frequent contributors. However, only 7% of the registered faults are considered permanent (requiring repair). Despite the contribution of lightning to the frequency of faults, these faults are more often temporary in nature, compared to faults caused by, for example, wind or ice/snow [10]. A list of all fault causes and sub-causes used for classification of faults in Norway can be found in [68, pp. 70–72].

The FASIT database holds a great deal of information that could be used for, for example, failure rate estimation. The methodological options available, however, become limited when data are scarce. A possibility is to "pool" data for similar components, e.g. across voltage levels [75], but this may obscure important differences, both in terms of the susceptibility of the components and how exposed to threats they are. Adjustments of pooled annual failure rates based on inspection data have been proposed in [76]. Bayesian statistics can alleviate some of the challenges of limited data through combining prior domain knowledge with observed data, as is performed for feeder lines in [77]. Historical failure rates and weather data have been used together with a Bayesian updating scheme to estimate line-specific annual failure rates of overhead transmission lines in [78, 79]. This approach incorporates both the threat exposure of the transmission lines through historical weather data, and the susceptibility of the lines through previously observed failures.

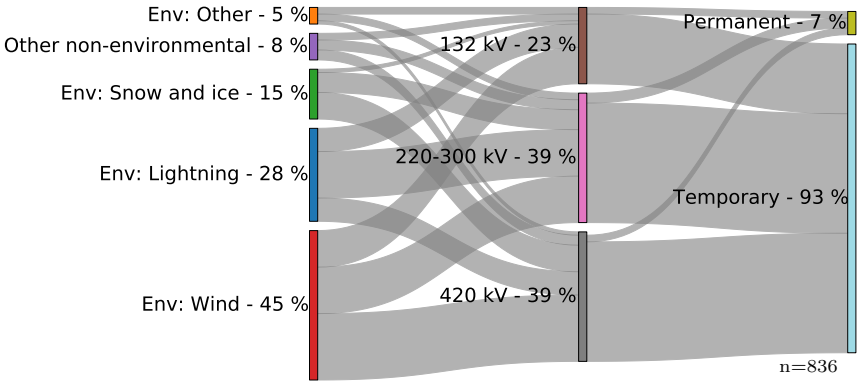

Figure 2.4: Faults registered in FASIT for overhead transmission lines, 2008-2017. By cause, voltage level, and nature of outage.

2.3 Dependence models

Independent multiple outage occurrences rarely occur, as the intersection of independent probabilities of failure for sets of multiple, highly reliable components is small. Related, or dependent, multiple outage occurrences are often the case in large blackout events. There are a number of mechanisms which can cause dependent outage occurrences. In the most recent IEC taxonomy, these are separated into a category of outages due to a common cause, and a category for "other" mechanisms [72]. The term *common mode* outages is not used in this thesis to avoid confusion due to varying, sometimes overlapping, definitions with common cause outages, e.g. [70, IEEE 4.2.2.2.1] [72, IEV 692-05-05]. A *common-cause outage occurrences* is however understood as "a related multiple-outage occurrence with a single external initiating event where the outages involved are not consequences of each other". A categorization of different causes which may result in dependent outage events is presented in [80]. Weather-related outages are a category which may typically cause a common-cause outage occurrence, while, for example, protection system misoperation belongs in the other category.

2.3.1 Correlated weather

Markov models have been a common tool to model dynamic systems, e.g. to incorporate weather effects and protection system failures in power system reliability analysis [81–84]. In more recent works on power system resilience, fragility curves paired with weather data - either historical weather, constructed scenarios, or a combination of the two - have been used to model the impact of severe weather on the resilience of the power system [78, 85].

Figure 2.5 shows a Markov Model with two components (1 and 2), with two condition states (up and down arrows) and two weather states (normal and adverse weather). The model is an illustrative adaptation from [81, 83], and captures any failure bunching between the two components due to adverse weather. The model assumes constant transition rates, where λ denotes the failure rate of the component in normal weather and λ' the failure rate in adverse weather. The transition from adverse to normal weather, and vice versa, is denoted by a_n and n_a respectively. Repair is modeled as only being possible in normal weather, and denoted by μ. In [81] an approximate annual failure rate for the failure of both components is deduced from a three-state weather model, which can be used together with a minimal cut-set approach to reliability evaluation. The model has multiple simplifications - such as assuming an exponential distribution for the transition rates and no repair in adverse weather. Markov models can become very complex as the number of states and transitions increases, and, as is mentioned in [80], it can also be very difficult to parameterize the transition rates in the model. Markov Models to incorporate adverse- and correlated weather are simplifications and yield results suitable from a reliability perspective.

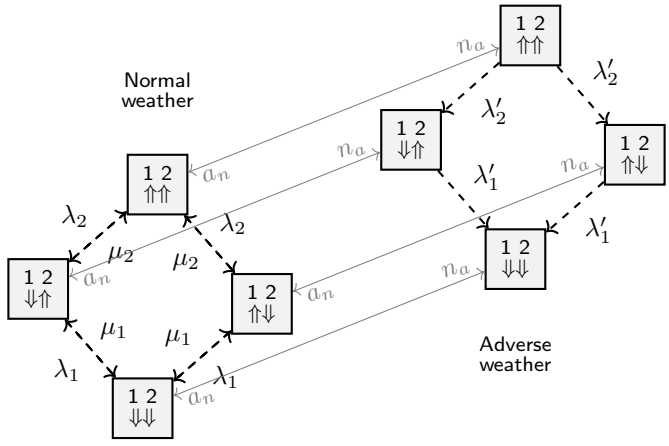

Figure 2.5: Markov chain with two components and two weather states, adapted from [81, 83].

A more recent development in the modeling of severe weather in power systems is the use of fragility curves [78, 85, 86]. Fragility curves describe the conditional probability of failure of a component, subject to a range of possible stresses the system may be exposed to. These fragility curves are often modeled with the cumulative distribution function of a distribution, often the log-normal distribution. Fragility curves can be developed in various ways, such as through expert judgments, empirical observations or structural models, to mention just a few [87]. Figure 2.6 shows an illustration of a fragility curve for a component, exposed to a stress of a certain value, termed an intensity measure (IM). The intensity measure is a function of stress the component faces, such as e.g. wind speed, ground motion, temperature, etc., depending on which threat is being considered. The reliability of the system can then be calculated from the individual component models with their own unique threat exposure. Fragility curves can be paired with historical weather, or generated weather scenarios, to incorporate time and location (and implicitly also weather) dependent failure probability patterns. This is sometimes referred to as the *spatio-temporal correlation* in failure probability between the components [88].

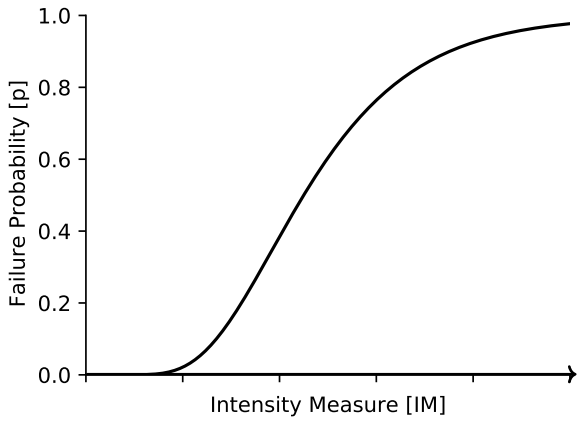

Figure 2.6: Generic fragility curve of a component.

2.3.2 Protection system misoperation

Protection systems are designed to detect and isolate faults and disturbances, and are an important part of the power system. They are also a potential source of dependent failures, which may contribute to the initial stages of a cascade. A failure to isolate faults can have consequences on the power system, and thus protection systems are deployed with backup systems in case the primary protection system fails. Operation of the backup protection system can cause healthy components to be isolated from the system, and it is necessary to weigh the

dependability and security of the protection system in its design [89]. Both dependability and security are facets of the reliability of protection systems, where the former is understood as the degree of certainty of correct operation, and the latter the degree of certainty that it will not operate incorrectly [90, 91]. This is also reflected in the classification of protection systems *misoperations* during faults in the NERC reliability standards [73]:

- **Failure to trip:** *A failure of a Composite Protection System to operate for a Fault condition for which it is designed.*
- **Slow trip:** *A Composite Protection System operation that is slower than required for a Fault condition if the duration of its operating time resulted in the operation of at least one other Element's Composite Protection System.*
- **Unnecessary trip:** *An unnecessary Composite Protection System operation for a Fault condition on another Element.*

It has been observed that failure to trip and unnecessary trips constitute the largest categories of protection system misoperation [91]. Figure 2.7 shows an example power system that is a useful aid for the remainder of the section. The figure illustrates two adjacent transmission lines with a protection system at each end. A failure to trip of the primary protection system following a fault at the source line causes the backup protection system at the target line to react. Similarly, an unnecessary trip would cause the backup protection system at the target line to react to a correctly cleared fault at the source line. In these instances, healthy lines are isolated from the system.

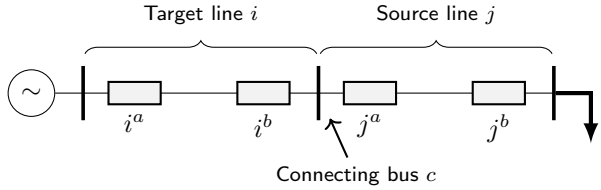

Figure 2.7: Example power system, adapted from [84, 92].

A Markov model was developed for the inclusion of protection system failures and failure to trip in composite generation and transmission system reliability analysis in [82]. However, the model is complex and includes many states, which limits its direct applicability in power systems reliability analysis. This was one of the motivations for creating a Markov model with reduced states, incorporating unnecessary tripping and failure to trip of the protection systems, in [84]. The work initially designed a simplified composite unit model for the availability (up-state) of a component, as seen in Figure 2.8. The figure depicts the up-state of

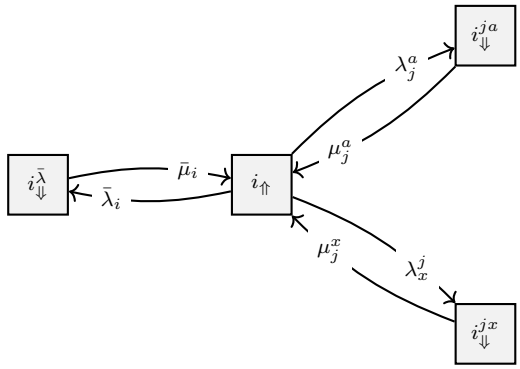

Figure 2.8: Simplified composite unit model for line i, adapted from [84].

a component $i_{\Uparrow}$, a self-induced down-state due to failure of the component or its protection systems $i^{\bar{\lambda}}_{\Downarrow}$, or an induced down-state of the component due to a misoperation of one, $i^{ja}_{\Downarrow}$, or both, $i^{jx}_{\Downarrow}$, protection systems following a fault at the adjacent component j. From this, an analytical systems reliability evaluation was developed. The analytical solution is however only practical for a system with few system states, and an alternative solution using Monte Carlo simulation was simultaneously proposed.

To avoid complex Markov models, approximate equations were designed to incorporate protection system failures and misoperations in a minimal cut-set approach in [27]. The work identifies four unique fault types which have a bearing on the isolation of a given transmission line: Fault type 1 is due to a failure of the transmission line itself. Fault type 2 is the result of spontaneous unwanted operation of the line's own protection systems. Fault type 3 occurs due to a fault at an adjacent line which is not correctly cleared by the primary protection system, causing the backup protection system to isolate both lines. Fault type 4 occurs when an adjacent line experiences a failure which is correctly cleared, but the backup protection system experience an unwanted non-selective tripping and isolates the otherwise healthy line. Together, these fault types comprise the equivalent failure rate of the line. Figure 2.9 illustrates a reliability block diagram of the cut-set of two adjacent transmission lines, x and y. A dependency mode failure rate $\lambda^D_{x,y}$ is calculated to take into account misoperation of the protection systems causing both lines to be isolated due to a failure of only one of the lines. Using approximate methods [93], equivalent failure rates, unavailability and outage durations are calculated for the cut-set. The method depends on the topology of the system, and different equations must be used depending on the adjacency of transmission lines in the cut-set.

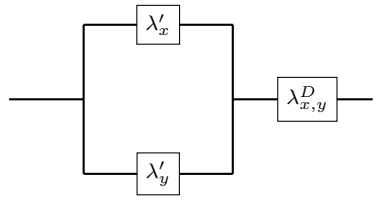

Figure 2.9: Reliability block diagram of cut-set including protection system misoperation, adapted from [94].

2.4 Quantification and communication of risk

There are multiple definitions and understandings of risk [36,95]. A basis for this thesis understanding of risk, is the definition put forward by Kaplan and Garrick as risk as a function of the consequence and probability of a scenario [34].

It can be difficult to determine the severity of a power system blackout. There are considerations such as power interrupted, but also the conditions under which the blackout occurs, the duration of the event, people affected and so on. There are also relative considerations for the system operator, such as the size of the power system in both electrical and geographical terms, and consumer dependence on power. This is suggested to be reduced into the axes of power interrupted and outage duration in [30], and is reflected in Figure 2.10. The rationale is that many of the more detailed considerations are related to the these two overarching factors, e.g. number of customers affected through interrupted power or the experienced severity of those affected through the duration of the event, although the categorizations for what is critical are up to the system operator to decide. It is pointed out that particularly long duration blackouts may be critical if they pass a certain duration especially during winter, which is reflected in the kink in the border between the classifications near the axes. The product of the axes could be represented as a single point value in the form of Energy Not Supplied (ENS) in terms of $[MW \cdot h]$. Although ENS is a useful measure of consequence, it does not directly translate into criticality for society. Nonetheless, a considerable volume of work was been conducted on the cost of energy not supplied (CENS) that is a useful added layer to ENS in terms of criticality for end-users affected by a power interruption.

CENS is used to consider the socioeconomic impact of reliability in the power system. For the purposes of this thesis, CENS is used interchangeably with the concept of value of lost load (VOLL), following the understanding in [96]. An aim is to balance the cost of reliability with the cost of power interruptions. The cost of power interruptions to customers is however not readily available information and different approaches have been developed to estimate these costs. Direct

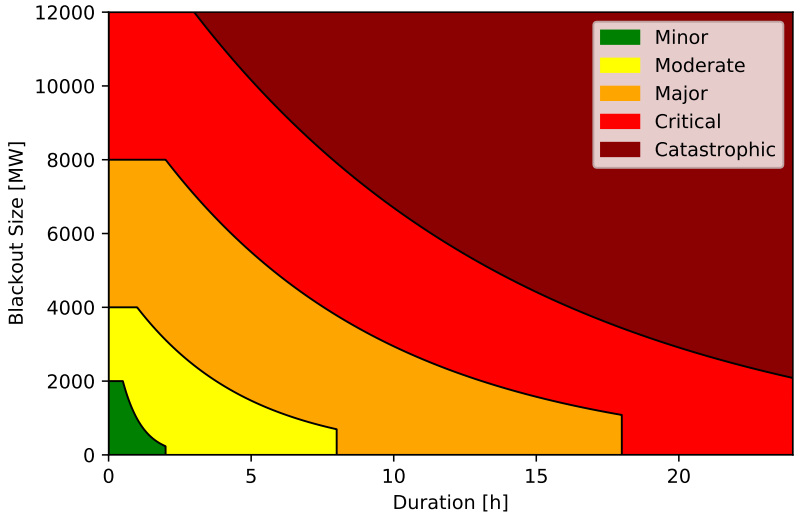

Figure 2.10: Consequence classification of blackouts, illustration adapted from [30].

approaches includes studies of the economic consequences of previous blackouts, surveys or interviews with end-users to assess the willingness to pay/avoid blackouts, where the respondent is asked to assess the damage cost related to different scenarios. Indirect approaches are typically based on the production factor, where the cost is related to the drop in production due to the loss of an input factor. Different methods of calculating the CENS also incorporate various factors such as customer types, time of interruption, interruption duration, weather or if the customers have been notified of the interruption in advance [31, 33, 96, 97].

Network operators in Norway have an regulated revenue cap, to ensure good socioeconomic performance in a monopolistic market. More importantly, CENS to customers is deducted from the allowed annual revenues, incentivizing network operators to maintain their assets and make the necessary new investments to avoid power outages in a socioeconomic manner [98]. The calculated CENS takes into account which customer groups are affected, when the interruption happens, and the duration of the interruption, and is applicable for all disconnects in installations above 1 kV. A normalized CENS for each customer group is calculated at a reference time based on survey information, before it is adjusted according to when the interruption occurs. The survey mostly combines elements of the direct worth and willingness to pay approaches to estimate customer costs related to power interruptions. The CENS model takes into account (net) private customer costs. These include monetary costs, which are relatively easy to measure in terms of money such as lost production, destroyed equipment or goods, and

any added operating costs. It also takes into account non-monetary costs, e.g. inconvenience and loss of free time. Net costs to the rest of society for actors that are not themselves directly affected by the interruption are not included in the CENS [32, 99, 100]. Figure 2.11 shows the CENS cost rates at a reference time (as of 2020 [101]) as a function of different interruption durations for different customer groups. Although CENS only captures a proportion of the criticality of an extraordinary event, it nonetheless incorporates much more information about the criticality of the event from the customer perspective than pure ENS.

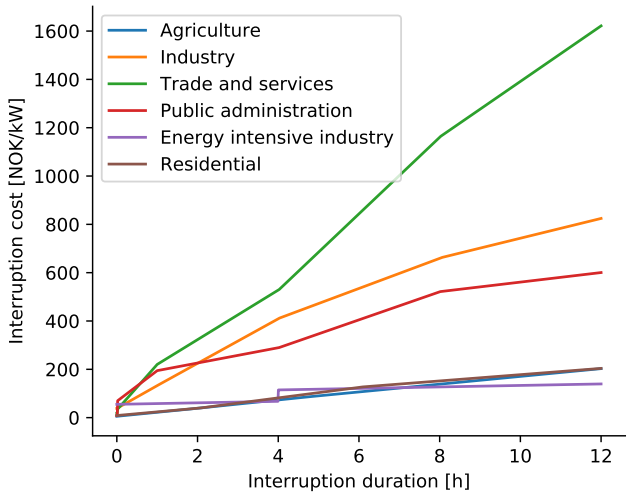

Figure 2.11: Customer damage functions at reference time[1]. Norwegian Kroner (2017 values) per kW [101].

This does however only classify the consequence side of the risk. A convenient and understandable method of presenting risk is the risk matrix. Risk matrices, as a tables representing categories of likelihood (or probability) of a scenario and the associated consequence, have been widely used in risk management. The tool enables the quick and easily compiled ranking and comparisons of risks for attention, and the graphical representation aids decision making regarding risk. Their use has however been heavily criticized for numerous reasons [102]. Few risk categories, or identical ratings to very different risks are some commonly objections, to mention just a few. Especially relevant to this thesis, however, is the limited ability to reflect uncertainty in input and output variables [102–104]. Some of these shortcomings are illustrated in Figure 2.12 displaying a risk matrix where three (numbered) risks are included. Each dot in the relevant square represents the judgment of the expected risk due to the associated scenario, placed according to continuous scales. To exemplify, the judgment of risks 1

[1]The reference time varies among customer groups but all reference times are on weekdays in January between 06:00 and 17:00 [101].

and 3 is notably different on the continuous scales but both are considered low risk in a discrete categorization. Risk 2 is considered medium in the discrete categorization, yet the risk - as the product of the probability and consequence on the continuous scale - is lower than that of risk 3. There is also no clarity in the uncertainties related to the categorization of the risks, and extreme outcomes or frequencies may be consumed into the expected value.

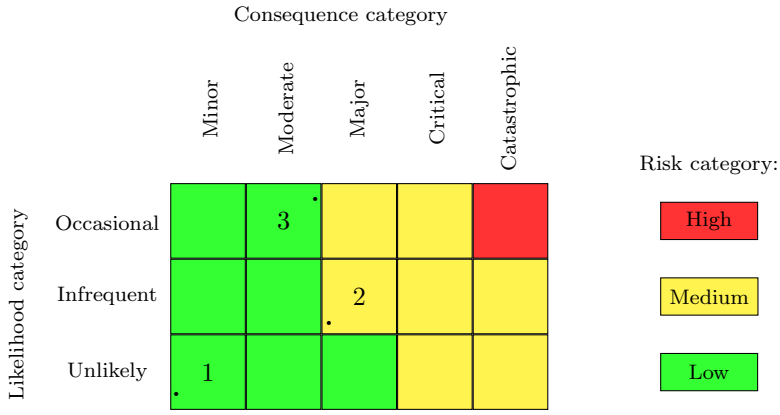

Figure 2.12: Risk matrix. Adapted from [30, 105].

A common division in the classification of uncertainty is between aleatory and epistemic uncertainty. The former is sometimes referred to as inherent- or irreducible uncertainty, and is caused by natural variation such as varying weather conditions. The latter is tied to a lack of knowledge, or ignorance, and can be reduced through the acquisition of new knowledge [37, p. 501]. The choice of classification may be considered philosophical (is there aleatory uncertainty at all if knowledge exist which can reduce it?), but from a modeling perspective it is an important distinction which reflects the modeling choices that are made [106]. More specifically, the choice reflects which components of the model are considered completely random (aleatory), and which components are attempted to be modeled in detail to reduce variation (epistemic). It is also important to convey that processes which could be considered epistemic uncertainty in reality, may be treated as aleatory uncertainty in the model due to considerations such as complexity, computational requirements or accuracy requirements. This conveys which uncertainties are actually reduced in the analysis, and yields transparency for the decision maker [106].

In power systems, the probability and consequence of a scenario can change throughout the year together with the weather and operational states. Annual indices reflect an expected value of the probability and consequence of a scenario throughout the year, often combined into an aggregated measure of risk, such as an annual expected ENS. Aggregating such events into an expected value

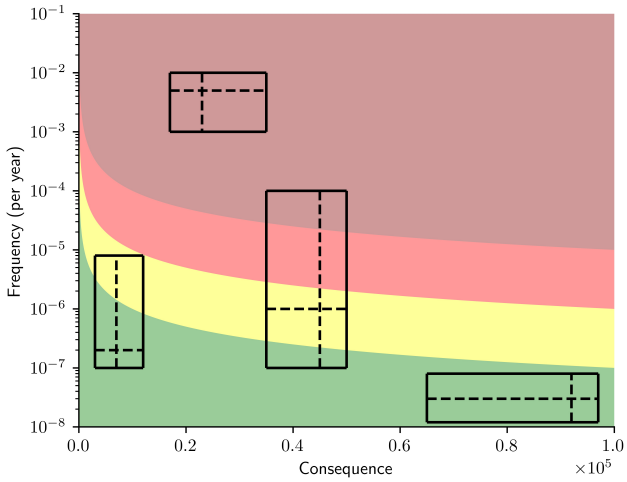

Figure 2.13: Risk diagram with uncertainty boxes.

can hide large observational outliers, such as a few rare events with very high consequences, if the relative contribution of other events with low - or no - consequences dominates the expected value. To avoid such events being hidden, it is important to quantify and visualize the more extreme possibilities in both the probability and consequence axis.

Continuous scale risk diagrams incorporating measures of uncertainty have been suggested to alleviate some of the challenges related to risk matrices [105, 107]. Uncertainty bands for the consequence dimension, incorporating epistemic uncertainty have been suggested in [108]. Uncertainty boxes, covering both the probability and consequence dimension are suggested in [105]. Uncertainties related to the natural variation of weather, the actual fragility of the component, the operating state of the system or affected customer groups can yield very different risks in different periods of time. Figure 2.13 shows a continuous scale risk diagram with uncertainty boxes. Each box represents the uncertainty of a given scenario, where the middle cross gives the expected value of the risk. This representation of risk incorporates uncertainty which should also be conveyed to the decision maker.

2.5 Summary

This section has introduced the concept of power system vulnerability and how it relates to extraordinary events, from threats to criticality of interrupted power

for end users. Key terms and definitions were introduced alongside the FASIT reporting scheme.

Methods of incorporating failure bunching effects and spatio-temporal correlation in failure probabilities were introduced, to support the investigation of how time-varying failure rates affect the rate of unwanted events. Models to include protection system failures and misoperation were presented to show how an initiating event can cause a further weakening of the system through dependent events, potentially leading to a cascade. Protection system misoperations are conditional on an initial failure and could have a interaction effect with failure bunching, further heightening the risk of extraordinary events in adverse weather, which will be explored further in answering research question 2.

The risks related to extraordinary events are related to the frequency or probability of a scenario, and the consequences of the scenario. The consequence of the scenario is often related to theENS to the customers, as a function of the interruption duration and magnitude. Availability and generalizability of statistical data to aid in characterizing failure behavior were discussed, alongside possible mitigating strategies. Lack of data is especially relevant for repair and restoration times in the Norwegian FASIT database. Coupled with the importance of the interruption duration in establishing the consequence of an extraordinary event, it is a valuable contribution to better understand and model long restoration times caused by permanent failures requiring repair.

Interruption duration is also important when it comes to the criticality of the consequence for the affected end-users. One way of incorporating criticality into the risk picture is to rely on previously developed methods of estimating a cost of ENS for the end-users. Different risk-visualizations are explored, primarily focusing on risk diagrams including uncertainty bands or uncertainty boxes. This form of risk visualization incorporates information beyond the expected risk through conveying uncertainties in the probability and consequence axes.

3 Contributions

The objective of this thesis is to develop methodologies for understanding and communicating uncertainties and risks related to extraordinary events. Four research questions have been defined to narrow down the topic. The research questions can be broadly categorized into four different themes: 1) Spatio-temporal correlation in failure frequency and subsequent unavailability of components, i.e. due to harsh weather. 2) Initial stages of propagating events through protection system misoperation. 3) Long infrastructure restoration times due to physical damage following natural hazard events. 4) Risk identification and visualization.

This chapter presents the contributions to answering the research questions formulated in this thesis. Section 3.1 provides an implementation of the methods developed in [78] with minor modifications which is used as a basis for many of the methods presented later in the thesis. Section 3.2 contributes to answering research question 1 through developing a method for calculating time-series of component unavailability due to time-varying threats such as, for example, wind or lightning. Section 3.3 combines the effects of spatio-temporal correlation with dependent failures due to protection system misoperation, thus contributing to answering research question 2. A Bayesian Network model is developed to predict transmission line down times due to permanent failures requiring repairs in Section 3.4. The model decomposes transmission line down time into smaller, constituent parts, and thus sheds light on research question 3. Methods of communicating risk and uncertainty related to extraordinary events in power systems are discussed and presented Section 3.5.

3.1 Time-series of failure probability

Time-series of hourly failure probabilities can be calculated in a number of ways, depending on data availability and need for accuracy. For weather-related phenomena, the combined use of historical failure data and weather conditions as seen in [78, 79] can be of great help in capturing historical susceptibility to given threats, as well as failure bunching effects. Time-series of hourly wind-dependent failure probabilities are generated according to the method presented in [78], with minor modifications in this section.

Unique annual failure rates for overhead transmission lines are calculated by a Bayesian updating procedure taking into account historical failures. Fragility curves are then fitted to a measure of weather exposure for each line segment of the line. This is combined with line segment information and historical wind speeds to construct time-series of historical failure probability due to wind. An underlying assumption behind the Bayesian updating scheme is that we have some general knowledge about the failure rate of certain component types. However, some transmission lines may be less robust and over time experience more failures than others. This new information can be incorporated into the previous knowledge through Bayesian inference. This is done by combining a prior assumption about the failure rate of comparable transmission lines, observing the likelihood of historical events for the specific line, and constructing a posterior distribution of the annual failure rate where information from both sources is incorporated. Details on the Bayesian updating scheme presented in the following section can be found in [78] and [109, p. 44].

To find the likelihood of the data the annual failure rate is modelled with a Poisson-distribution, where y is the number of failures per year and λ the parameter value. The probability density function (PDF) is given by (3.1).

$$p(y|\lambda) = \frac{\lambda^y e^{-\lambda}}{y!} \tag{3.1}$$

Given a vector $y = \{y_1, y_2, ..., y_n\}$ of observed annual failures over n years, the likelihood of the data is found in (3.2).

$$\begin{aligned} l(y|\lambda) &= \prod_{i=1}^{n} \frac{\lambda^y e^{-\lambda}}{y_i!} \\ &\propto y^{\sum y_i} e^{-n\lambda} \end{aligned} \tag{3.2}$$

The conjugate prior of the Poisson distribution is the gamma distribution, with

parameter values α and β (3.3). A gamma distribution with $\alpha = 1$, in practice an exponential distribution, with rate $\beta = 1/\lambda$ is opted for, following the original work. A historical failure rate for comparable lines has been found to be, 0.78 per 100 km, of which 90% are temporary and out of these 19% due to wind [78], and is near identical to what has been found in the source material for this thesis. To reflect permanent failures, a prior wind dependent failure rate of $\lambda = 0.78 \cdot 0.1 \cdot 0.19 \approx 0.015$ is chosen.

$$\begin{aligned} p(\lambda) &= \frac{\beta^{\alpha}\lambda^{\alpha-1}e^{-\lambda\beta}}{\Gamma(\alpha)} \\ &\propto \lambda^{\alpha-1}e^{-\lambda\beta} \end{aligned} \tag{3.3}$$

This is then inputted into the Bayes formula to find the posterior distribution in (3.4). The result is a gamma distribution with updated parameters $\alpha' = \alpha + \sum y_i$ and $\beta' = \beta + n$. The posterior gamma distribution has an expected value given by $E(X) = \frac{\alpha'}{\beta'}$, which is the updated failure rate, λ'.

$$\begin{aligned} p(\lambda|y) &= \frac{l(y|\lambda)p(\lambda)}{p(y)} \\ &\propto \lambda^{\alpha+\sum y_i-1}e^{-\lambda(\beta+n)} \end{aligned} \tag{3.4}$$

A fragility curve is then fitted to a measure of wind exposure for each line segment to distribute the failures in time, before the probability of failure for each line is calculated. The aim of the fitting process is to find the parameters of a line-specific fragility curve which yields an expected annual failure rate of the line which is equal to that found in the Bayesian updating process. The calculated annual failure rate after curve fitting is held equal to the annual failure rate found by Bayesian updating in the previous step to maintain consistency.

An overhead transmission line l is divided into multiple line segments s, separated by transmission towers. For each line segment, an intensity measure (IM) is calculated. The IM gives a measure of the wind exposure of the different line segments, dependent on the line length d and wind speed w cubed at time t (3.5). The weather data used to calculate wind exposure of line segments are historical hourly wind speeds in a 1-kilometer grid using re-analysis data from [110]. Line segment length data are found by splitting transmission lines by tower positions, as seen in Fig. 3.1.

$$IM_{l,s}^{t} = d_{l,s} \cdot (w_{l,s}^{t})^{3} \tag{3.5}$$

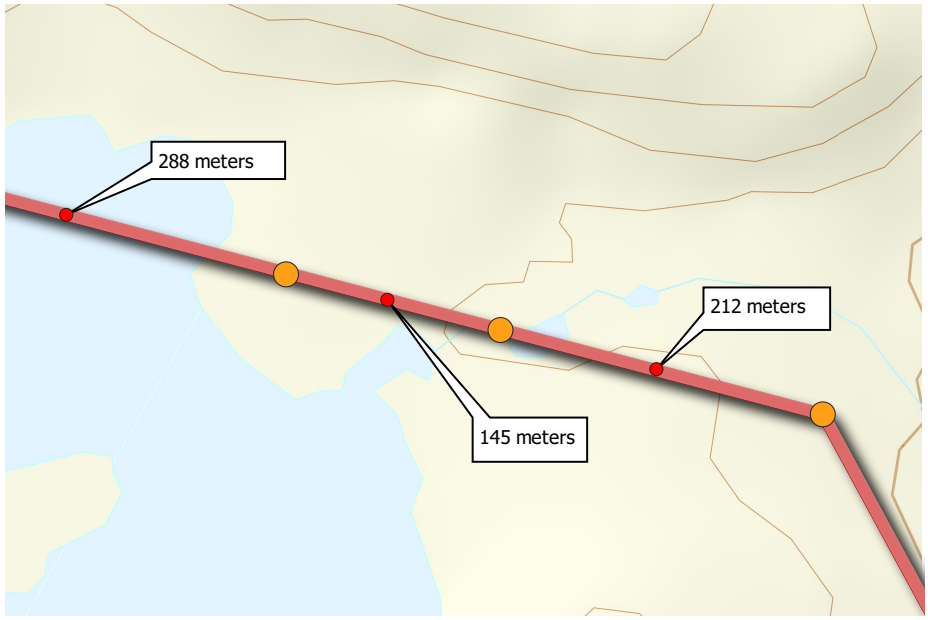

Figure 3.1: Line segment lengths. Main transmission line in red, towers as yellow points. Illustrative example using data from [111, 112].

The distribution of *IM* for all line segments in a single line is then fitted with a fragility curve shaped by the lognormal cumulative distribution function (3.6). The fragility curve gives the probability of failure for the line segments at different values of *IM*. It is assumed that the fragility curve is the same for all times, and for all line segments within each line. Hence there is only one set of parameters μ and σ for each line, valid at all times.

$$p_{l,s}^{t} = F(IM_{l,s}^{t}; \mu_l, \sigma_l) = \frac{1}{2} + \frac{1}{2} erf\left[\frac{ln(IM_{l,s}^{t}) - \mu_l}{\sqrt{2}\sigma_l}\right] \quad \text{where: } IM_{l,s}^{t}, \mu_l, \sigma_l > 0 \tag{3.6}$$

The aim of the fitting process is to find the parameters of a line-specific fragility curve which yields an expected annual failure rate *for the line as a whole* equal to that found in the Bayesian updating process. To achieve this, a set of historical failures and a time-series of wind belonging to the same period for $k = [0, T]$ years are considered. The fragility curve is fitted at the line segment level but during the optimization process the result is constrained to the annual failure rate of the line. This is done by considering the probability of failure for a line l as the series system of its line segments (3.7). The annual failure rate of the

line found during the optimization process can be calculated from the resulting time-series of failure probabilities (3.8).

$$p_l^t = 1 - \prod_{s=1}^{m}(1 - p_{l,s}^t) \tag{3.7}$$

$$\hat{\lambda}_l = \frac{1}{k}\sum_{t=0}^{T} p_l^t \tag{3.8}$$

The Brier Score (3.9) is used as a loss function in the fitting process and is the squared difference between the estimated probability and the actual occurrence of the event. Observed failure of a line at a given time, o_l^t, is compared to the calculated probability of failure of the line at the same point in time. Using the previous equations, the loss function can be expressed in detail (3.10). This formulation of the optimization is slightly different from that found in [78].

$$BS = \frac{1}{N}\sum_{t=1}^{N}(p_l^t - o_l^t)^2 \tag{3.9}$$

$$g(IM_{l,s}^t; \mu_l, \sigma_l) = \frac{1}{N}\sum_{t=1}^{N}\left[\left[1 - \prod_{s=1}^{m}(1 - F(IM_{l,s}^t; \mu_l, \sigma_l))\right] - o_l^t\right]^2 \tag{3.10}$$

Using the historical *IM* measure for the different line segments of the line, the parameter values can be found. The minimization of the loss is held under the constraint that the sum of the annual failure rate estimated from the fragility curve fitting is held equal to the Bayesian updated failure rate (3.11).

$$\mu_l, \sigma_l = \underset{s.t.\ \hat{\lambda}_l = \lambda_l'}{\arg\min}\ g(IM_{l,s}^t; \mu_l, \sigma_l) \tag{3.11}$$

The curve fitting of the fragility curve to the historical *IM* measures of the lines can be computationally heavy. To save on computations, low-wind values could be removed from the curve-fitting procedure. Typically, it is possible to set a lower wind limit at 15 m/s. The historical percentage of failures occurring below 15 m/s wind speeds is around 20% [67]. For this work, all wind speeds are considered, as there is no requirement for repeated and fast calculation of the fragility curves. An *illustrative* example of a fitted fragility curve can be seen in Fig. 3.2. The figure shows how the line-specific fragility curve, defined by μ_l and σ_l yields a probability of failure at different *IM* values. The gray histogram

shows a distribution of historical *IM* values for the line segments. A sample of hourly failure probabilities due to wind exposure for one line ($\lambda' \approx 0.3$) can be seen in Fig. 3.3.

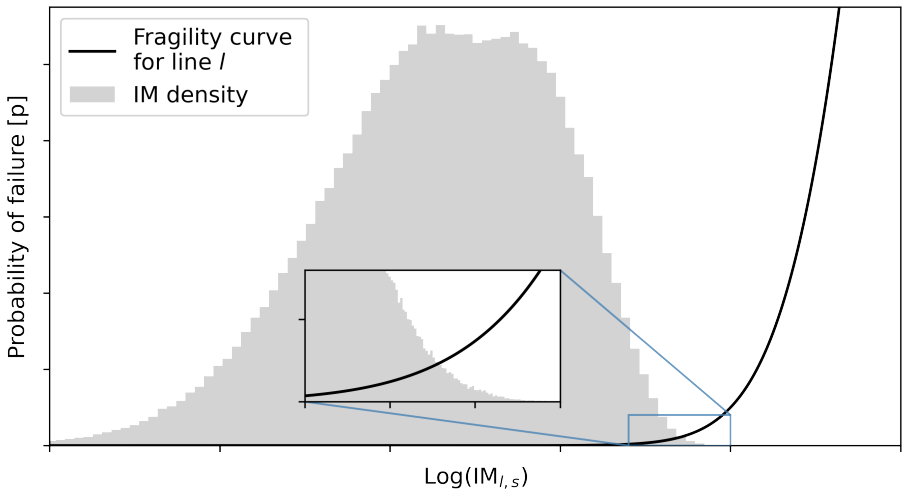

Figure 3.2: Illustrative example of line-specific fragility curve with superimposed histogram of hourly line segment *IM* observations.

Using historical wind data for real transmission lines captures correlations in failure probability between them. This is typically the case where transmission lines in the same geographical area are exposed to the same weather at the same time, which can cause failure bunching effects. The correlation in failure probability between 9 overhead transmission lines is presented in Figure 3.4 using the method presented in this section and Norwegian weather data from [110]. Data for lines 1 to 8 were collected from the same geographical area, while line 9 belongs to a widely different geographical area with different weather, as reflected in the correlation matrix. Lines 4 and 5 are located parallel to each other, and are thus exposed to the same weather. This is one example of how the method incorporates weather zones into the time-series of failure probability.

The method developed in [78] and implemented here is a useful basis for further work. It incorporates historical weather into time-series of failure probability, thus taking into account the spatio-temporal correlation in failure probability between lines. It also provides a method to include information about the transmission lines' susceptibility to wind into the model, even when faced with scarce data. These are both important aspects to consider when it comes to the vulnerability of the system when the unwanted event is the simultaneous outage of more than one transmission line. This is therefore used as a basis for further work in this thesis.

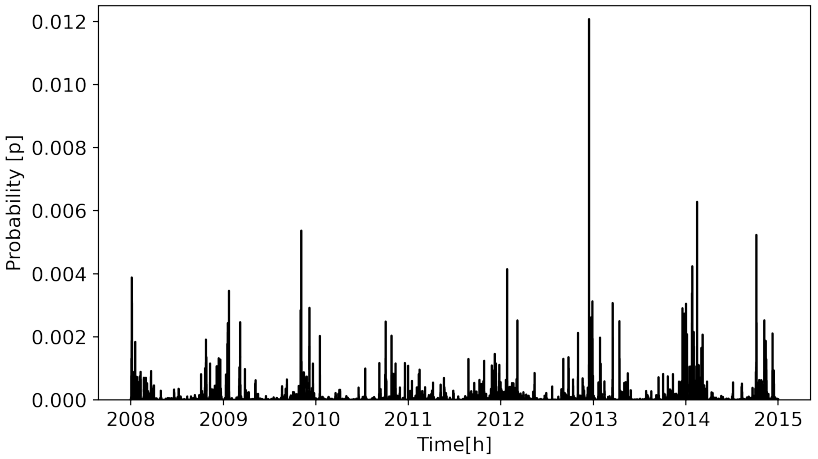

Figure 3.3: Illustrative example of time-series of calculated hourly failure probabilities for an overhead transmission line.

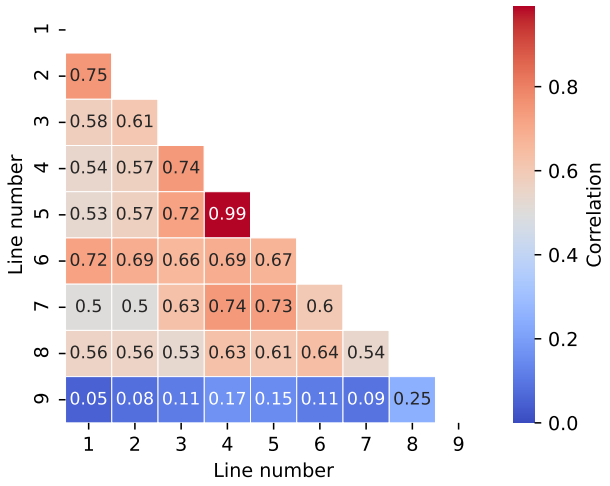

Figure 3.4: Correlation matrix. Wind-dependent failure probability for 9 overhead transmission lines.

3.2 Unavailability

The following section is based on the work published in Paper 1 [39] and develops a method for calculating transmission line unavailability due to correlated threat exposure, contributing to answering research question 1. Transmission systems are largely developed and operated in accordance with the N-1 criterion, and the simultaneous outage of multiple components is thus of special interest when considering extraordinary events. Spatio-temporal correlation in the failure of components can cause blackouts to occur more often than anticipated. Additionally, events caused by natural hazards are associated with longer outage durations due to mechanical damage or limitation to accessibility for repairs. This subchapter demonstrates how time-series of component unavailability due to external threats can be calculated based on predefined outage distributions and time-series of failure probability. The resulting time-series of unavailability can be used to predict the expected occurrence of contingencies.

The method includes three main steps: Time-series of failure probability for components in the system are constructed using the method outlined in 3.1. Outage duration distributions are found from historical data. These are then combined by an algorithm to form time-series of probability that the components are unavailable.

Initially, data on outage durations for transmission lines are fitted to a log-normal distribution represented by a probability density function (PDF) in (3.12), where r denotes the outage duration.

$$f(r) = \frac{1}{r\sigma\sqrt{2\pi}} e^{-\frac{(ln(r)-\mu)^2}{2\sigma^2}} \tag{3.12}$$

The expected value and variance, respectively, from the historical data are summarized for the random variable of outage durations R in (3.13) and (3.14), where n is the total number of observations and r_i are individual data points.

$$E(R) = \frac{1}{n}\sum_{i=1}^{n} r_i \tag{3.13}$$

$$Var(R) = \frac{\sum_{i=1}^{n}(r_i - E(R))^2}{n-1} \tag{3.14}$$

Using the Method of Moments (MoM), parameter estimates for the log-normal distribution $LN \sim (\mu, \sigma)$ is calculated in (3.15) and (3.16). Other parameter fitting alternatives are available, such as the maximum likelihood estimation (MLE),

although MoM is used to maintain the mean of the distribution with the observed mean in the data.

$$\mu = ln\left[\frac{E(R)^2}{\sqrt{Var(R) + E(R)^2}}\right] \tag{3.15}$$

$$\sigma = \sqrt{ln\Big[1 + \frac{Var(R)}{E(R)^2}\Big]} \tag{3.16}$$

To find the probability that the component is in a failed state x hours after a failure event, the survival function $S(x)$ is used. The survival function is the complement of the cumulative distribution function (CDF), denoted $F(x)$, and can be expressed by (3.17).

$$S(x) = 1 - F(x) = 1 - \int_0^x f(r)dr \tag{3.17}$$

The true outage duration function is a continuous distribution, while the time-series resolution is in one-hour intervals. The analysis represents the probability of a component being unavailable in a given hour, thus a mean value needs to be calculated for the given time interval. To achieve this the trapezoidal rule is used, (3.18), where P is the number of intervals used in the calculation of the mean value in the given hour, $(t-1, t)$.

$$\int_{t-1}^{t} S(x)dx \approx \sum_{a=1}^{P} \frac{S(x_{a-1}) + S(x_a)}{2} \Delta x_a \tag{3.18}$$

A simpler and computationally lighter alternative to using the trapezoidal rule is to select an offset, $o \in R(0, 1)$, for the survival function, which is assumed to represent the mean of the survival function within hourly intervals sufficiently well (3.19).

$$\int_{t-1}^{t} S(x)dx \approx S(x - o) \tag{3.19}$$

If the survival function was a linear function, this would be the middle of the interval $(t-1, t)$. The choice of solution depends on the error tolerance, computational capacity and the shape of the distribution considered. An illustrative example of the different approaches, using FASIT data, can be found in Figure 3.5. The figure shows a sample survival function, an offset solution where

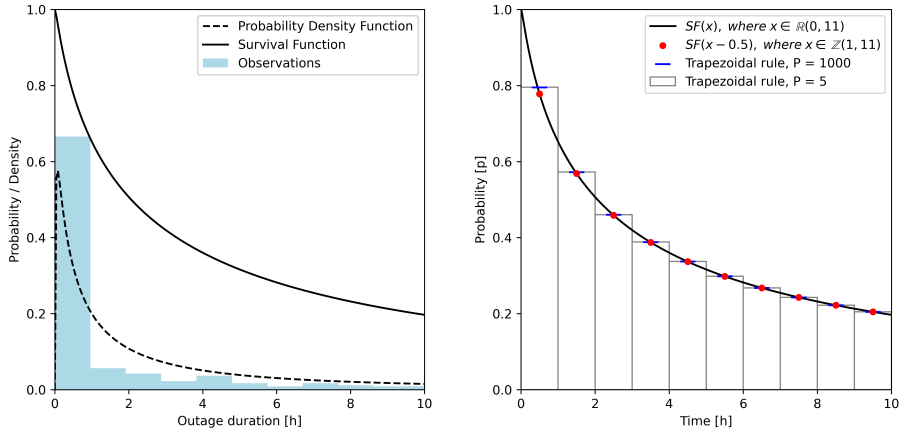

(a) Observed outage duration of power lines (132kV-420kV), 2006-2016

(b) Survival function and representative point approximations.

Figure 3.5: Survival function fitting (a) and approximation (b).

$o = -0.5$ for the mean value of the interval, the approximated mean calculated by the trapezoidal rule with $P = 5$ and $P = 1000$. The latter serves as a baseline for comparison between the solutions.

The tail-end of the outage duration distribution is cut off in the algorithmic approach. The cut-off limit is a consideration between necessary accuracy and computational cost. The impact of the adjustment is to keep the results consistent, where the sum of outage durations is kept the same as without a cut-off, but at a cost to the shape of the distribution (inflated values before the cut-off). The alternative expectation formula is used to make the adjustments (see e.g. [113]), which states that the integral from zero to infinity of the survival function for a continuous non-negative random variable equals the expected value of the distribution (3.20). Hence, an inflation factor k can be calculated (3.21).

$$E(R) = \int_0^{\inf} [S(x)]dx \tag{3.20}$$

$$k = \frac{E(R)}{\int_0^{1000} [1 - F(x)]dx} \tag{3.21}$$

Combining failure probabilities with outage duration curves, we obtain a measure of the probability that the line is unavailable at a given time. This is illustrated in pseudo-code in Algorithm 1. The algorithm traverses the time-series of failure

probabilities and appends any additional outages a number of time-steps ahead in time, taking into account any previous unavailability at the potential time of failure.

Algorithm 1 Algorithm for calculating unavailability

Input: time-series of t failure probabilities
Output: time-series of t unavailability probabilities
Initialization:
$p_t \leftarrow$ failure probability at time t
$S(x) \leftarrow$ outage survival function at time x since failure
$u_t \leftarrow$ unavailability probability at time t
cutoff $\leftarrow$ limit to forward propagating time-steps
$k \leftarrow$ inflation factor due to cut-off
LOOP Process:
1: **for** all increasing time steps t **do**
2: **for** x in $range(0, cut\text{-}off)$ **do**
3: $u_{t+x} += p_t \cdot (1 - u_t) \cdot S(x) \cdot k$
4: **end for**
5: **end for**
6: **return** u_t

Figure 3.6 shows the algorithm applied to a 150-hour time window. Each line represents the added probability of the line being unavailable due to a failure at a given time-step. The surface of the graph is the cumulative probability of unavailability for the line due to all previous failures within the cut-off window. The probability of a set of components, CS, being unavailable at the same time, t, is the calculation of the joint independent probability of unavailability for the components in the set: $P(U^t_{cs}) = \prod_{i \in CS} P(U^t_i)$.

The method contributes to identifying the risk of extraordinary events in several ways. By incorporating the historical weather patterns into the unavailability of lines, the spatio-temporal correlation in threat exposure is included. The output of the method can be paired with a time-dependent consequence analysis, and in this way give a more complete view of the historical risk of extraordinary events in the system. It is also possible to identify lines which have a high impact on a given consequence metric, such as ENS, informing decisions regarding which hardening measures to implement.

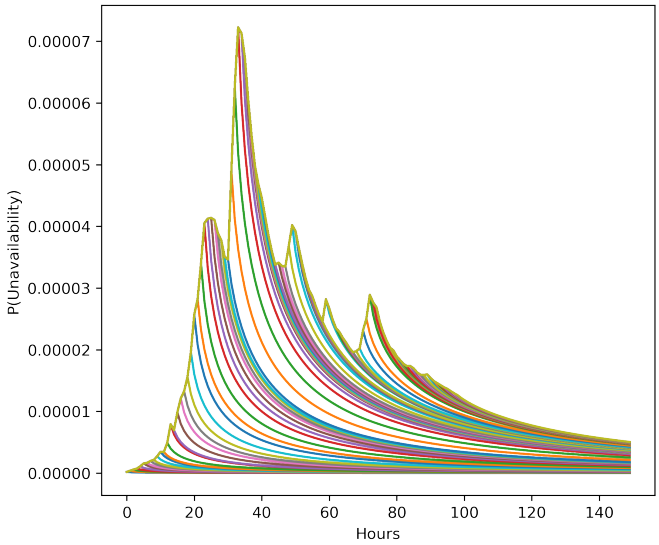

Figure 3.6: Illustration of unavailability algorithm applied with a 150-hour time-series of failure probability. Each colored line represents how the failure probability at one time-step adds to the probability of unavailability for the transmission line at the current- and later time-steps. The surface of the plot show the calculated unavailability of the transmission line once the algorithm is completed.

3.3 Dependent failures: Protection systems

The following section is based on the work published in Paper 2 [40] and presents a compact and generalized method for including protection system failures and misoperation in power system reliability analysis which can be combined with time-series of failure probability due to adverse weather. This is a contribution to answering research question 2. Extreme weather is known to cause failure bunching in the electrical transmission system. However, protection systems can also contribute to the worsening of the system state through spontaneous, missing or unwanted operation of the protection system. The latter two types of failures only occur when an initial failure has happened, and thus are more likely to take place when the probability of failure of transmission lines is high, such as in an extreme weather scenario. This causes an exacerbation of failure bunching effects, increasing the risk of extraordinary events. It is thus useful to combine the effects of extreme weather exposure and protection system reliability.

The following is a compact generalization of including protection system failures in reliability analysis using approximate methods. It extends the solution to be applicable to time-series of failure probability. This section only includes some conceptual clarifications and the general idea underlying Paper 2 [40], while the full set of equations can be found in the original work. The starting point of the work is the failure of overhead transmission lines, and subsequent protection system misoperations causing adjacent lines to be isolated from the system.

In [27] four fault types (FTs) are identified, two of which are related to the dependent isolation of healthy lines due to protection system misoperations following an initial failure: Fault type 1 (FT1) is the failure rate of the transmission line. Fault type 2 (FT2) represents failures due to the spontaneous unwanted operation of a line's own protection system, and is not a dependent failure in this sense. Fault type 3 (FT3) occurs when there is a failure on a neighboring line that is not correctly cleared due to missing operation of the neighboring line's protection system, and thus causes the line in focus to be isolated from the system. Fault Type 4 (FT4) is a result of a fault on the neighboring line that is correctly cleared by the neighboring line's protection system but causes an unwanted non-selective tripping of the line in focus.

Propagating events makes it necessary to consider the adjacency between components. Traditionally, a power system can be considered a graph G where each bus belongs to a vertex set V, and each transmission line belongs to an edge set E, where each edge element $l = \{u, v\}$ represents a transmission line between bus u and v (3.22) – (3.24). The method presented makes use of the fact that this graph in its traditional power system representation can be reformed to take into account paths of propagation between components.

$$G = (V, E) \tag{3.22}$$

$$V = \{b_1, b_2, \ldots, b_n\} \tag{3.23}$$

$$E = \{l_1, l_2, \ldots, l_m\} = \big\{\{u_1, v_1\}, \{u_2, v_2\}, \ldots, \{u_m, v_m\}\big\} \tag{3.24}$$

Two different categorizations can be considered: The target line, i, for which an event may propagate to, and the source line j at which the propagating failure from line j to i is initiated. In the method, two lines must be connected through a shared bus, c, for propagation to be considered. Sometimes it is necessary to refer to a line without referencing if it is a source or a target line, in which case it is denoted with the subscript l and corresponds to an element in the edge set. The lines are associated with a failure rate λ_l. Each line is associated with two protection systems P_l^s on each end, with the set $s = \{a, b\}$ denoting which of the two protection systems it is referencing. See Figure 3.7.

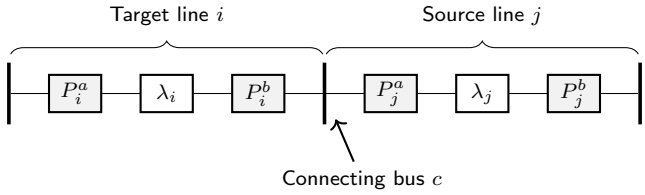

Figure 3.7: Two adjacent transmission lines, *i,j* [40].

For a line, the bus connected on the a-side protection system side is denoted u, and v is connected on the b-side. The protection systems are associated with three parameters: 1) a specific annual failure rate $p_l^{s,\lambda}$, 2) a conditional probability of missing operation $p_l^{s,m}$, and 3) a conditional probability of unwanted non-selective tripping at the target line upon a correctly cleared failure at an adjacent source line $p_l^{s,u}$. Unwanted non-selective tripping can be considered side-independent, and denoted $p_l^u = P(p_l^{a,u} \cup p_l^{b,u})$. The primary concern of the approach is conditional probabilities, and how a failure or protection system response at one transmission line can cause an adjacent line to be isolated from the system.

To achieve this, an adjacency matrix is constructed for each side of the source line. An adjacency matrix indicates connections between vertices in the initial graph, and represents the system in a form where the vertices are transmission lines, and the edges are directed paths of failure propagation between the lines. The side of the protection system is taken into account by making two adjacency matrices. The approach is presented in (3.25), to form the two adjacency matrices

A^{s}. The idea is that if the a-side protection system of the source line j shares a bus u_i or v_i with the target line i, then the corresponding element $a^a_{i,j} = 1$, otherwise 0. Matrices are typeset in uppercase regular font, vectors are typeset in lowercase bold italics, while scalar values such as specific elements of vectors or matrices are typeset with italic fonts.

$$\mathrm{A}^{\mathrm{s}} = \left[a^s_{i,j}\right] = \begin{bmatrix} a_{1,1} & \dots & a_{1,l} \\ \vdots & \ddots & \vdots \\ a_{l,l} & \dots & a_{l,l} \end{bmatrix} \tag{3.25}$$

where:

$$a^a_{i,j} = \begin{cases} 1 & \text{if } u_j \in \{u_i, v_i\} \\ 0 & \text{Otherwise} \end{cases}$$

$$a^b_{i,j} = \begin{cases} 1 & \text{if } v_j \in \{u_i, v_i\} \\ 0 & \text{Otherwise} \end{cases}$$

$$s \in \{a, b\}$$
$$i \in \{1, ..., l\}$$
$$j \in \{1, ..., l\}$$

Figure 3.8 shows a 4-bus system represented as a graph, with vertices representing busbars and edges representing transmission lines. Figure 3.9 shows the transformed graph after applying (3.25), where a failure and/or missing function of the protection system at the source line j can cause the adjacent line to be isolated from the system.

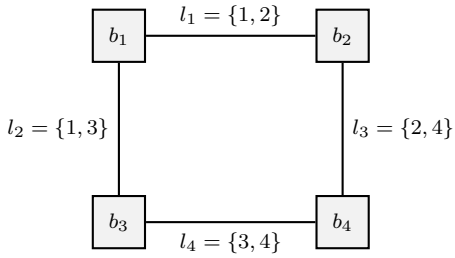

Figure 3.8: Busbars as vertices, edges as transmission lines [40].

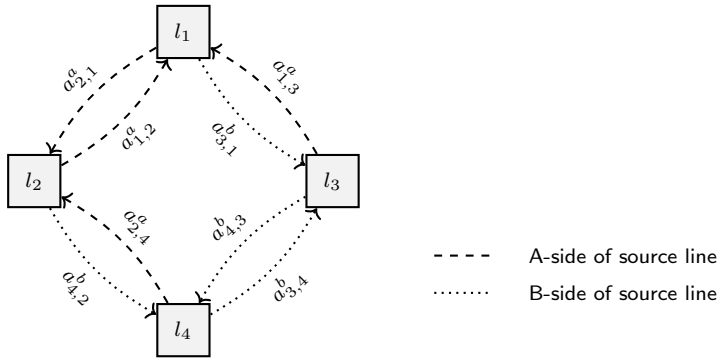

Figure 3.9: Transmission lines as vertices, edges as propagation paths [40].

$$\mathrm{A^a} = \begin{bmatrix} 0 & 1 & 1 & 0 \\ 1 & 0 & 0 & 1 \\ 0 & 0 & 0 & 0 \\ 0 & 0 & 0 & 0 \end{bmatrix} \quad , \quad \mathrm{A^b} = \begin{bmatrix} 0 & 0 & 0 & 0 \\ 0 & 0 & 0 & 0 \\ 1 & 0 & 0 & 1 \\ 0 & 1 & 1 & 0 \end{bmatrix} \tag{3.26}$$

The adjacency matrices can be further modified to incorporate the conditional probability that a failure at a source line will isolate the target line. The resulting probability matrices (PT) are the basis for further calculations of the identified fault types. FT3 is related to a failure on an adjacent line, which is not correctly cleared by the adjacent line's protection system. The probability of missing operation of the protection system on the s side for a given line is represented by the column vector $p_l^{s,m}$. A matrix containing the probability that a failure propagates from the source line j to the target line i through the FT3 mechanism is created, named $PT3$, by multiplying the adjacency matrix with the diagonal of a vector containing the probability that the line's protection system misoperates (3.27). The probability of misoperation is considered equal for all protection systems in the example, at 0.0205. Multiplying the probability matrix PT3 with a vector containing the (ordered) annual failure rates of the lines, $\lambda = \{2, 3, 4, 5\}$, gives a vector of FT3 contributions from adjacent lines for each target line (3.29).

$$\mathrm{PT3} = \sum_s \left[\mathrm{A^s} \cdot \mathrm{diag}(\boldsymbol{p^{s,m}}) \right] \tag{3.27}$$

$$\begin{aligned}\mathrm{PT3} &= \begin{bmatrix}0&1&1&0\\1&0&0&1\\0&0&0&0\\0&0&0&0\end{bmatrix} \cdot diag \begin{bmatrix}0.0205\\0.0205\\0.0205\\0.0205\end{bmatrix} + \begin{bmatrix}0&0&0&0\\0&0&0&0\\1&0&0&1\\0&1&1&0\end{bmatrix} \cdot diag \begin{bmatrix}0.0205\\0.0205\\0.0205\\0.0205\end{bmatrix} \\ &= \begin{bmatrix}0&0.0205&0.0205&0\\0.0205&0&0&0.0205\\0.0205&0&0&0.0205\\0&0.0205&0.0205&0\end{bmatrix}\end{aligned} \tag{3.28}$$

$$\begin{aligned}\boldsymbol{ft3} &= \mathrm{PT3} \cdot \boldsymbol{\lambda} \\ &= \begin{bmatrix}0&0.0205&0.0205&0\\0.0205&0&0&0.0205\\0.0205&0&0&0.0205\\0&0.0205&0.0205&0\end{bmatrix} \cdot \begin{bmatrix}2\\3\\4\\5\end{bmatrix} = \begin{bmatrix}0.1435\\0.1435\\0.1435\\0.1435\end{bmatrix}\end{aligned} \tag{3.29}$$

Similarly, FT4 is the result of a working protection system response at the source line following a failure but unwanted non-selective tripping at the target line (3.30).

$$\mathrm{PT4} = \sum_{s} \left[\left[\mathrm{A^s} \cdot \mathrm{diag}(1 - \boldsymbol{p^{s,m}}) \right]^T \cdot \mathrm{diag}(\boldsymbol{p^u}) \right]^T \tag{3.30}$$

The topology of the system is then incorporated into the failure probability matrices, which can be used with equations in a general form to solve reliability evaluations using either approximate methods, or where time-series of failure probability are used as input.

3.3.1 Incorporating protection system failures using approximate methods

Initially, an equivalent failure rate, λ' is calculated for each line (3.32). This is done by summing the failure rate of target line i (FT1), its protection systems (FT2), isolation of healthy lines due to missing protection system response at a neighboring source line j (FT3) or unwanted non-selective tripping of the target line's protection system following a failure at an adjacent line (FT4) (3.31).

$$\boldsymbol{ft1_i = \lambda_l} \; ; \; \boldsymbol{ft2_i} = \sum_{\boldsymbol{s}} \boldsymbol{p_l^{\lambda,s}} \; ; \; \boldsymbol{ft3_i} = \text{PT3} \cdot \boldsymbol{\lambda_l} \; ; \; \boldsymbol{ft4_i} = \text{PT4} \cdot \boldsymbol{\lambda_l} \tag{3.31}$$

$$\boldsymbol{\lambda' = ft1 + ft2 + ft3 + ft4} \tag{3.32}$$

From this, equivalent unavailability and outage durations for all target lines are found in (3.33)-(3.34), where the vectors of fault type contributions are paired with vectors of the associated repair or switching times using element-wise Hadamard operations. As opposed to the other fault types, FT3 is dependent on the switching time at the source line, j, rather than the target line i. To include this, the contribution of the unavailability from the source to target line is carried through the probability matrix for FT3.

$$\boldsymbol{U' = ft1 \circ r^{FT1} + ft2 \circ r^{FT2}} + \text{PT3} \cdot [\boldsymbol{\lambda \circ r^{FT3}}] + \boldsymbol{ft4 \circ r^{FT4}} \tag{3.33}$$

$$\boldsymbol{r' = U' \oslash \lambda'} \tag{3.34}$$

Second order cut-sets involving the two lines x and y can be calculated from this in a general form, using the adjacency matrix to avoid distinctions in equations between lines in different topologies. This involves two considerations: If two lines in a cut-set are adjacent and experience a FT3 or FT4 where the source and target line are in the cut-set, there is a dependency between them. Everything else should be treated as independent events. This is done by first finding dependent failures which occur in the cut-set: for each line in the cut-set an adjustment to the independent failure rate - i.e. the dependent failures stemming from a given line in the cut-set - is calculated for each line. This is exemplified for line x in (3.35), where λ_x^a is the adjustment to the failure rate of line x due to a dependent failure initiated by a failure at line y . This is carried through into an adjustment to the unavailability of the line due to independent events in (3.36), and a new outage duration in (3.37). If the lines in the cut-set are not adjacent, these relevant elements of the probability matrices will be zero, and there are zero adjustments.

$$\lambda_x^a = (pt3_{x,y} + pt4_{x,y}) \cdot ft1_y \tag{3.35}$$

$$U_x^a = \left(pt3_{x,y} \cdot r_y^{FT3} + pt4_{x,y} \cdot r_x^{FT4}\right) \cdot ft1_y \tag{3.36}$$

$$r_x^n = (U'_x - U_x^a)/(\lambda'_x - \lambda_x^a) \tag{3.37}$$

The adjustments due to dependent events are then represented as a dependency mode failure rate in (3.38), with an associated outage duration in (3.39).

$$\lambda^D_{\{x,y\}} = \lambda_x^a + \lambda_y^a \tag{3.38}$$

$$r^D_{\{x,y\}} = \begin{cases} (U_x^a + U_y^a)/\lambda^D_{\{x,y\}} & \text{if } \lambda^D_{\{x,y\}} > 0 \\ 0 & \text{Otherwise} \end{cases} \tag{3.39}$$

The equivalent annual failure rate, expected annual unavailability and expected restoration time for the cut-set including any potential dependent failures are then calculated in (3.40)-(3.42).

$$\lambda'_{\{x,y\}} = \frac{(\lambda'_x - \lambda_x^a)\left(\lambda'_y - \lambda_y^a\right)\left(r_x^n + r_y^n\right)}{8760} + \lambda^D_{\{x,y\}} \tag{3.40}$$

$$U'_{\{x,y\}} = \frac{(\lambda'_x - \lambda_x^a)\left(\lambda'_y - \lambda_y^a\right)\left(r_x^n \cdot r_y^n\right)}{8760} + \lambda^D_{\{x,y\}} \cdot r^D_{\{x,y\}} \tag{3.41}$$

$$r'_{\{x,y\}} = \frac{U'_{\{x,y\}}}{\lambda'_{\{x,y\}}} \tag{3.42}$$

3.3.2 Incorporating time-varying failure probability due to weather

Time-series of failure probabilities may be used to incorporate time-varying failure probabilities, e.g. due to wind, lightning, etc. Primarily, the challenge is to create time-series adjustments for the dependent failures stemming from FT3 and FT4, as well as a time-series for the dependency mode failure rate. Calculation of the unavailability due to the failures is performed using the method outlined in Section 3.2. Failure rates are now considered with a time dimension, and when referring to the time-series of failure probability for a single line, the column vector is denoted $\lambda_{:,l}$. The fault types for a single target line i are given in (3.44)-(3.48).

$$\lambda^{\mathrm{s}} = \left[\lambda^{s}_{t,l}\right] = \begin{bmatrix} \lambda_{1,1} & \dots & \lambda_{1,l} \\ \vdots & \ddots & \vdots \\ \lambda_{t,1} & \dots & \lambda_{t,l} \end{bmatrix} \tag{3.43}$$

$$\mathrm{FT1}_{:,\mathrm{i}} = \lambda_{:,\mathrm{l}} \tag{3.44}$$

$$\mathrm{FT2}_{:,\mathrm{i}} = [ft2_{t,i}], \text{ where } ft2_{t,i} = \frac{\sum_s p_l^{\lambda,s}}{8760} \tag{3.45}$$

$$\mathrm{FT3}_{:,\mathrm{i}} = \sum_j [\lambda_{:,\mathrm{j}} \cdot pt3_{i,j}] \tag{3.46}$$

$$\mathrm{FT4}_{:,\mathrm{i}} = \sum_j [\lambda_{:,\mathrm{j}} \cdot pt4_{i,j}] \tag{3.47}$$

$$\lambda'_{:,\mathrm{i}} = \mathrm{FT1}_{:,\mathrm{i}} + \mathrm{FT2}_{:,\mathrm{i}} + \mathrm{FT3}_{:,\mathrm{i}} + \mathrm{FT4}_{:,\mathrm{i}} \tag{3.48}$$

When calculating the unavailability and failure probability of second order cut-sets it is necessary to adjust FT3 and FT4 to account for adjacency as was performed in the approximate equations, for both lines x and y, as seen in (3.49)-(3.50). A time-series of dependency mode failure probability for the two lines in conjunction is calculated in (3.51). Again, the adjustments and dependency mode failure rate are equal to zero if the lines are not adjacent.

$$\mathrm{FT3}'_{:,\mathrm{x}} = \mathrm{FT3}_{:,\mathrm{x}} - \mathrm{FT1}_{:,\mathrm{y}} \cdot pt3_{x,y} \tag{3.49}$$

$$\mathrm{FT4}'_{:,\mathrm{x}} = \mathrm{FT4}_{:,\mathrm{x}} - \mathrm{FT1}_{:,\mathrm{y}} \cdot pt4_{x,y} \tag{3.50}$$

$$\begin{aligned} \lambda^{\mathrm{D}}_{:,\{\mathrm{x,y}\}} = {} & \mathrm{FT1}_{:,\mathrm{y}} \cdot pt3_{x,y} + \mathrm{FT1}_{:,\mathrm{y}} \cdot pt4_{x,y} \\ & + \mathrm{FT1}_{:,\mathrm{x}} \cdot pt3_{y,x} + \mathrm{FT1}_{:,\mathrm{x}} \cdot pt4_{y,x} \end{aligned} \tag{3.51}$$

$$\mathrm{U}'_{:,\{\mathrm{x,y}\}} = \mathrm{U}'_{:,\mathrm{x}} \circ \mathrm{U}'_{:,\mathrm{y}} + \mathrm{U}^{\mathrm{D}}_{:,\{\mathrm{x,y}\}} \tag{3.52}$$

$$\lambda'_{:,\{\mathrm{x,y}\}} = \mathrm{U}'_{:,\mathrm{x}} \circ \lambda'_{:,\mathrm{y}} + \mathrm{U}'_{:,\mathrm{y}} \circ \lambda'_{:,\mathrm{x}} + \lambda^{\mathrm{D}}_{:,\{\mathrm{x,y}\}} \tag{3.53}$$

Using the method outlined in section 3.2, time-series of unavailability of the cut-sets can be calculated as shown in (3.52) and (3.53). An application of the method considering a cut-set involving two adjacent lines is exemplified in

Figure 3.10. The top graph shows the equivalent failure rates for the individual components as seen in isolation. The middle graph shows the failure rate of the cut-set including and excluding protection system failures and misoperation. The bottom graph shows the unavailability of the cut-set under the same two conditions. It is illustrative that the failure probability of the cut-set is near four-fold at the tenth hour if protection system misoperation is included.

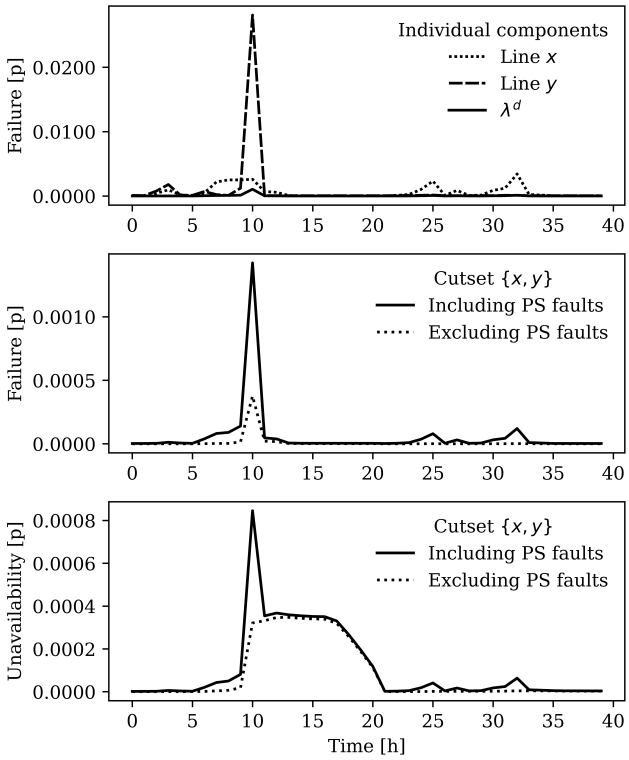

Figure 3.10: Failure probability of components of a cut-set, dependency mode failure probability, and failure probability and unavailability of cut-set [40].

Propagating events can contribute to the occurrence of extraordinary events. The method outlined in this section is a compact and generalized method for including protection system failures and misoperation in power system reliability analysis which can be combined with time-series of failure probability due to adverse weather. Protection system misoperation follows an initial failure, and propagating failures cluster around periods of high failure probability from other causes. This can further increase risks associated with failure bunching effects, as the probability of an unwanted event may be underestimated if protection system misoperation is not included in the analysis. The method presented incorporates the topology of the system, and the use of adjacency matrices to

include dependent failures is a useful tool to do this.

3.4 Restoration times due to permanent faults

The following section is based on the work published in Paper 3 [41] and explores a Bayesian Network approach to predicting transmission line down times, contributing to answering research question 3. While there has been a substantial amount of work on the failure probability of transmission lines in severe weather, more detailed work on the restoration time has been limited. The latter is of high importance as extreme weather can cause considerable damage to power system infrastructure and delayed access to the failure site, subsequently leading to increased down times and long-lasting power supply interruptions. Limited historical data of varying levels of quality challenges the ability to generalize fixed statistical down time distributions to different transmission lines under different conditions. An alternative to relying on (often lacking) historical data is to build a logical model. The proposed method is to use a Bayesian Network (BN) model to systematically predict transmission line down times.

There are a variety of reasons as to why a component or unit is isolated from the system. To narrow down the scope of the analysis, the target variable is considered to be transmission line down time due to permanent forced outages requiring physical repair or replacement of equipment. The aim is to make a predictive model that can act as a support in the analysis of extreme events, particularly long outage durations due to physical damage to the infrastructure. The model designed to incorporate time-dependent information - when the failure occurs -, line-specific information - such as accessibility to line segments - and type of threat which causes the failure. Initially, a conceptual model of the restoration process following a failure is drafted, before it is subsequently reduced into a more sparse BN model.

The conceptual model of transmission line down times was developed in cooperation with experts from the Norwegian TSO. The model is based on the logic and terminology used in the Norwegian FASIT reporting scheme [64], and serves as an overarching guide to which variables and causal mechanisms should be considered. After populating the conceptual model, the potential benefits and capability of accurate modeling of the different elements was considered. In Figure 3.11 the conceptual model is presented, with arrows indicating causal relationships. Dashed lines and gray boxes indicates variables and relationships which were omitted in the final BN.

A benefit of BNs is that they can take information from different sources. In this particular case, three sources exists: Expert judgment through a structured elicitation process, historical fault data, and assumptions about the duration of the weather event. Expert judgments were elicited through structured interviews following the SHELF [114] protocol to minimize bias. Distributions for variables related to the work-process, i.e. delays and repair time, were also elicited. Tri-

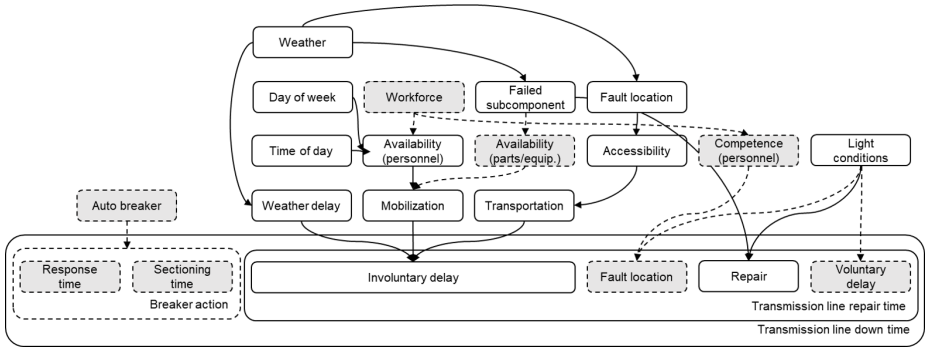

Figure 3.11: Conceptual model of transmission line down time [41].

angular distributions were selected as there was high uncertainty in the expert responses. The elicited distributions can be found in Table 3.1.

Table 3.1: Elicited triangular distributions, in hours [41].

Variable	Min	Mode	Max
Hours delay			
Working hours	1.5	3	6
Night	4	6	8
Evening	4	10	20
Day delay			
Weekend	4.5	11	15
Accessibility			
High	0.5	2	4
Medium high	0.5	3	5
Medium	1	4	6
Medium low	2	6	10
Low	5	10	15
Repair time			
Tower	84	190	350
Insulator	9	18	36
Phase line	16	68	123
Top line	15	43	60
Other	4.5	8	16
Daylight delay			
Darkness	5.5	10	12

Data from the FASIT system were used as a source of historical failures, and to model the relationship between which subcomponents of the transmission line were more likely to fail due to different threats. There are few observations of permanent failures in the data and a Bayesian updating scheme is performed for these categorical data (see e.g. [109, p.69]). A multinomial likelihood with a Dirichlet prior leads to a Dirichlet posterior with updated parameters (3.54), where k is the number of categories, α a vector of parameters for each category, and y is a vector of the number of observations within each category. An unin-

formative Dirichlet prior of $\alpha = 1$ is chosen due to limited previous knowledge.

$$f(\theta|y) \propto \prod_{j=1}^{k} \theta_j^{\alpha'_j - 1}$$
$$\alpha'_j = \alpha_j + y_j \tag{3.54}$$

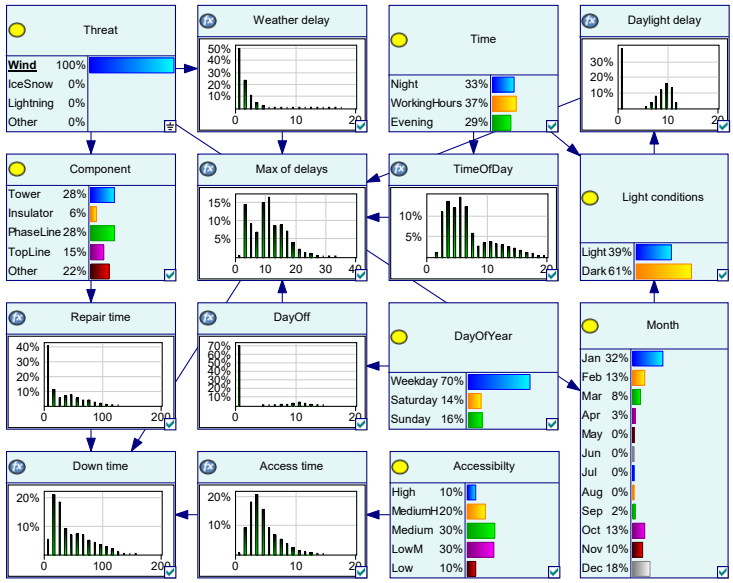

Figure 3.12: BN model of transmission line down time, conditioned on wind as the external threat. Down-time duration in hours [41].

The BN structure is used to predict down time durations for specific lines at different times by updating variables or conditioning on when or where the failure is more likely to occur. This is seen in Figure 3.12, where variables are represented as boxes, and conditional dependence is represented as directed edges. Time-dependent information (month, time of day, and whether it is a weekday) can be combined with line-specific information, such as accessibility categories of the various line segments of the line. Time-series of log-normal distribution parameters for the outage duration are created. The resulting time-series can be used to calculate the probability of unavailability for transmission lines, using time-varying failure probabilities and outage durations.

The available data on permanent failures - especially when narrowed down by specific cause, i.e. threat - are scarce and have high uncertainty. Reporting of repair times is not mandatory due to the uncertainty related to interpretation

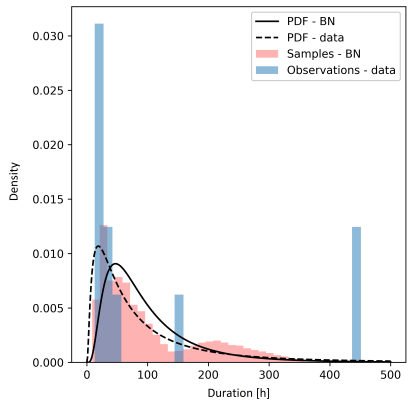

Figure 3.13: Comparison between the predicted distribution of down-times due to wind using the BN approach, and actual observed down-times (n=11) in the Norwegian transmission system.

and registration in the FASIT database, and thus does not necessarily represent a true value of the distribution. A comparison of the results from the BN approach and historical observations of permanent failures due to wind for overhead transmission lines as registered in the FASIT database can be seen in Figure 3.13. The pink histogram represents samples generated by the BN, while the blue histogram represents data of actual observed down-times. The solid line represents a fitted log-normal probability density function (PDF) for the BN sample, while the dashed line represents the log-normal PDF of the observed down-times. To ensure a comparable data-to-method sample, the historical observations have been filtered with a lower bound of 5 hours to ensure that the material does not include restoration processes not performed at the fault-site, i.e. switching of breakers.

Having a good understanding of down times due to physical destruction of infrastructure is an important part of understanding the consequence dimension of the risk related to extraordinary events. Historical data are scarce, with unclear quality and generalizability. The approach decomposes the contributing factors to down times following permanent faults into a conceptual model, which is then used to construct a BN. Using a BN allows us to incorporate relevant information from various sources in the task of predicting transmission line down times. The BN structure also allows conditioning on input variables, such as when the failure occurs, which threat caused it, or the accessibility of the affected transmission line. The presented BN approach to predicting transmission line down times can serve as an alternative to using historical data.

3.5 Visualization and communication

The following section is in part based on the work published in Paper 4 [42] and explores methods for communicating and visualizing risks related to extraordinary events, contributing to answering research question 4. A challenge with extraordinary events is that they belong to tail-end probabilities, and are not communicated clearly through the methods established in traditional reliability analysis. Their low probability may cause consequences to become negligible additions to the expected value. To visualize this, a risk matrix can be used with categorical variables describing the probability and consequences in predetermined intervals.

However, placing a scenario in risk matrices is not straightforward. The span of probabilities and consequences can be wide and uncertain, and the risk is not necessarily appropriately captured as a single value in a single risk category. Different methods have been suggested to alleviate some of the challenges associated with risk matrices. One method for handling this inherent uncertainty is to introduce a degree of belief into the estimate, introducing a third axis. Another is to introduce uncertainty bands along the already established dimensions of probability and consequence. The uncertainty bands are connected to an expected value of probability and consequence as a center-point, and illustrates the maximum and minimum values along the different axes [105, 107].

For the purposes of illustrating blackouts due to natural hazard events, the compression of high probabilities of failures within a short span of time in periods with high consequences is especially relevant. Most of the time, the probability of contingencies occurring due to a weather-related event is near zero. Illustrating time-series with many probability-consequence pairs related to the same scenario through their mean value may therefore be misleading. Introducing uncertainty bands, or the related uncertainty boxes, gives a measure of the outer edges of the information, i.e. high-risk periods.

Paper 4 presents different risk visualizations supported by a case study with varying load and failure probabilities. The purpose was to show how aggregate values can hide potentially extreme scenarios, especially if the load and failure probabilities are correlated. This was exemplified by the hourly probability that a cut-set was unavailable, and the associated interrupted power if the cut-set was indeed unavailable at that hour.

Figure 3.14 shows an example of the construction of a risk diagram including uncertainty bands for a given cut-set, as presented in Paper 4. Red scatters represents observations of hourly probability-consequence pairs. The purple circle represents the expected values of the contingency, while the black lines represents uncertainty bands along the different axes. Note that the expected value of the

probability is near zero, while the expected interrupted power is approximately 32 MW. The scaling of the axes makes it difficult to distinguish the probability of the cut-set being unavailable, hence a log-scale is a good alternative representation. The key question is if the combination of a center-point and uncertainty bands adequately communicates the important uncertainty in the components of risk inherent in the real data (red scatters). Cluttering in the graph may become a challenge when several cut-sets are considered in the same graph. This could have a negative effect on the ability to judge risk for the recipient [115, 116]. It is therefore also useful to consider what information is necessary for the recipient to take informed decisions.

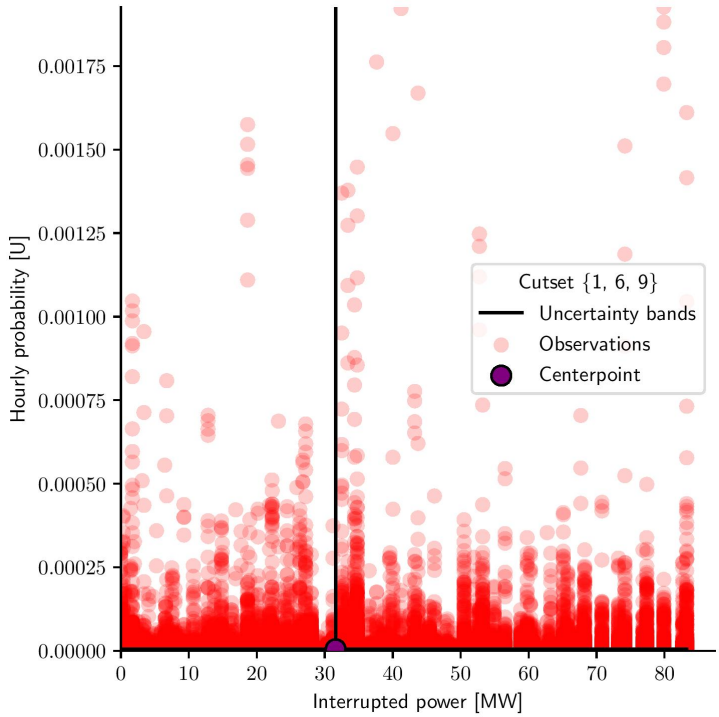

Figure 3.14: Risk diagram including uncertainty bands, for the unavailability of a cut-set. Recreated from [42].

Arguably it could be said that the expected value holds important information about the expected risk, as do the high-end of the uncertainty band of the hourly probability (there are periods of very elevated probability that this cut-set is unavailable). The uncertainty band representing interrupted power on the right hand side of the center-point communicate that the interrupted power can be almost three times higher than the expected value. The uncertainty bands on the left- and lower side of the center-point do however hold limited useful information:

The lower end of the probability is often near zero, and the interrupted power may similarly be zero in some cases. The expected value and the maximum value in combination sufficiently convey the most important aspects of the risk to a decision maker. Omitting the minimum side of the uncertainty bands would also contribute to sparsity, and remove cluttering if multiple cut-sets are compared on the same graph.

3.5.1 Continuation of the risk visualization

The work in Paper 4 incorporated time-varying failure probabilities and loads, and visualization of the risk associated with a cut-set as a function of the probability of unavailability, and the interrupted power at the corresponding time of unavailability. The use of uncertainty bands to reveal uncertainty related to extraordinary events was also explored. Although interesting in itself, a more common representation is risk as a function of the probability that the scenario occurs, and the associated consequences in terms of energy not supplied (ENS). The following subsection is an extension of the work presented in Paper 4, where the cost of energy not supplied (CENS) is incorporated in the consequence/criticality dimension, taking into account the criticality of the event for the affected end-users. Risk visualizations are further developed to limit the amount of information to what is most relevant in the graphic representation of risk. The extended work is exemplified with a case study.

Case study

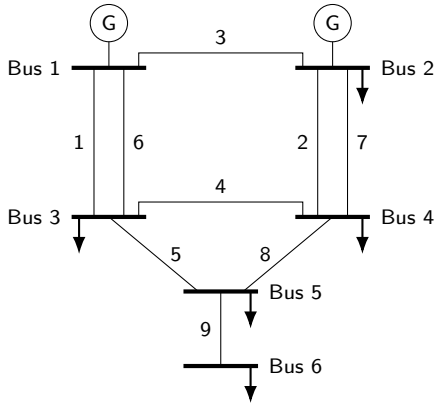

Figure 3.15: The Roy Billinton Test System (RBTS) [117].

The case study illustrates the risk associated with wind-dependent failures, causing permanent outages and thus potentially severe consequences. The basis of

the case study is the topology from the Roy Billinton Test System [117], seen in Figure 3.15. To generate a realistic case, time-series of historical failure probabilities due to wind for nine overhead transmission lines in the Norwegian grid was created using the method in [39], based on [78]. The failure probability due to wind is weighted so that the annual failure rate of the transmission lines match the Permanent Outage Rate (POR) in the RBTS test system, and the share of failures due to wind observed in the historical data for 300-220kV overhead transmission lines in Norway in the period 2009-2018 [10]. In (3.55) $p(\lambda_{i,:})$ is a generated time-series of failure probability for line i, $y = 9$ is the number of years in the time-series, POR is the Permanent Outage Rate as is presented in the RBTS case-study [117], and $w = 0.31$ is the share of failures due to wind.

$$\sum_{t} p(\lambda_{i,t}) = y \cdot POR_i \cdot w \tag{3.55}$$

The load demand of the system in the case study is based on the actual consumption in Norway from the period of 2006-2014, gathered from the Norwegian TSO, Statnett [118]. Using real system load data combined with actual weather conditions at the same time gives a more realistic picture of the risk the system has been exposed to. Figure 3.16 shows the time-series of historical load demand, where the load demand is presented as the share of maximum load for the system over the 9-year period, and a time-series reflecting the probability of at least one component in the system failing due to a permanent wind-dependent outage. The Spearman's rank correlation between the load and failure probability is $\rho = 0.20$, indicating a positive correlation. This relationship between wind-dependent outages and load in the Norwegian transmission system becomes even more clear for the the time-series of unavailability with a $\rho = 0.47$. This shows a potential positive correlation between the probability and consequence associated with an unwanted event scenario.

A distribution of the outage duration for each overhead transmission line was generated using the method outlined in [41], with one log-normal distribution representing the outage duration for the line throughout the entire year. It is assumed that the outage duration of the transmission line is equal to the component down time. These distributions are used together with the time-series of failure probability to generate time-series of the probability that the transmission line is unavailable due to a permanent wind-related outages using the method in [39]. The unavailability of higher order sets is the (independent) intersection of the components of the set being unavailable at the same time.

The failure probability of the higher order sets is the probability of any combination of failures and simultaneous transmission line unavailability that causes the set to occur at that time. To generate the equations, consider a set S where each component i can either be unavailable ($s_{i,j} = p(u_i)$) or fail ($s_{i,j} = p(\lambda_i)$)

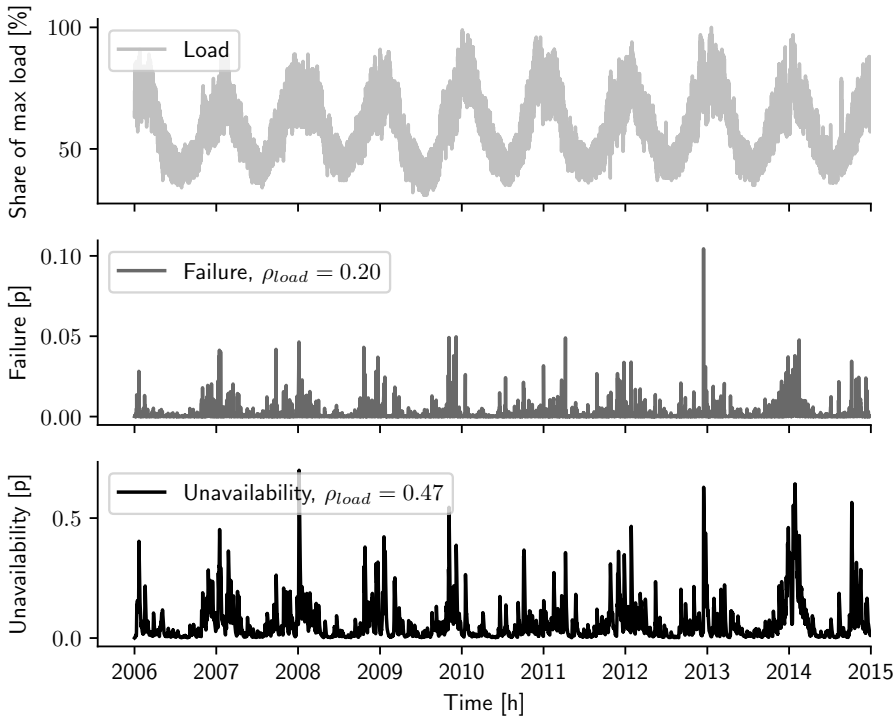

Figure 3.16: Key variables in the case study: Hourly time-series of share of maximum load demand for the system (top panel), hourly probability of one or more transmission lines experiencing a failure (mid panel), hourly probability of one or more transmission lines in the system being unavailable (bottom panel). Spearman's correlation coefficient, ρ, is calculated between the time-series of hourly maximum load demand and the two other time series.

in a given set state j. For a set of n components, there are $k = 2^n$ combinations of possible set states. For all states, the probability that the set occurs is the product of all possible combinations of failures and unavailability, minus the probability that all components in the set are unavailable due to previous failures (3.56). This is exemplified for a set of two transmission lines in (3.57).

$$p(\lambda_{\{i,\dots,n\}}) = \sum_{j}^{k} \prod_{i}^{n} s_{i,j} - \prod_{i}^{n} u_i \tag{3.56}$$

$$p(\lambda_{\{1,2\}}) = p(\lambda_1) \cdot p(u_2) + p(u_1) \cdot p(\lambda_2) + p(\lambda_1) \cdot p(\lambda_2) \tag{3.57}$$

An extreme scenario outage event is created. The scenario assumes that at the process of restoring the transmission lines to service has not been initiated for any of the lines in the set when the set occurs. The outage duration of the set is assumed to be equal to the time it takes for the first component of the set to be restored to service. This is found analytically from the cumulative distribution function (CDF) of the outage distribution for sets including only one transmission line. The outage duration distribution for sets with more than one line is found by sampling ($n = 100000$) individual component outage occurrences. The extreme outage event scenario assumes that the outage duration of the set is equal to the 90^{th} percentile of the distribution. An illustrative example of the process of creating an outage distribution for a set including two components is found in Figure 3.17. The figure shows the probability that the individual transmission lines have been repaired in the top two panels, and the probability that both lines are unavailable in the bottom panel. The CDF is plotted alongside the sample distribution. The CDF of the minimum of the distributions for a set S with $n > 1$ can be found by evaluating the set's constituent CDF's at the same values, $F(x)_S = 1 - \prod_i^n (1 - F(x)_i)$, see e.g. [119].

The time-series of power consumption in Figure 3.16 is divided into 100 equal-sized bins, representing a percentage of the peak load in the RBTS. This is used together with an AC Optimal Power Flow (OPF) with generation rescheduling and load shedding to calculate the potential interrupted power at the different load points due to a contingency, as specified in [120,121]. The analysis considers contingencies up to the 3^{rd} order. This yields time-series of interrupted power at the 6 buses for each contingency.

To incorporate the criticality of ENS for the customer, each bus of the RBTS is associated with a customer type, as found in [122], classified by the Norwegian CENS arrangement [101]. The CENS arrangement is a measure of the socioeconomic costs of interrupted power dependent the time of the interruption, the interruption duration and the affected end-users. Besides reflecting a stipulated cost to the customer, CENS also has a direct impact on the grid operator, mak-

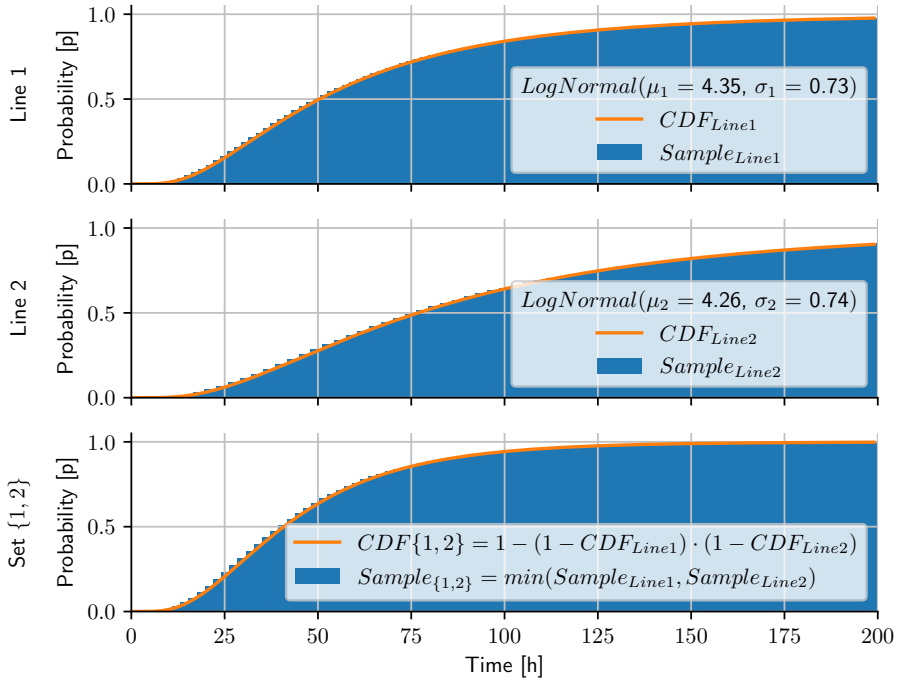

Figure 3.17: Construction of outage duration distributions for sets of transmission line(s). Cumulative distributions representing the predicted outage duration of two overhead transmission lines (top and mid panel), and the outage duration distribution of the set containing the two lines in a generated extreme scenario outage event (bottom panel). The blue histograms in each panel represent the random sample of outage durations following the analytical rule represented by the orange line.

ing it an important measure of criticality for both the operator and the affected customers.

Table 3.2: Customer types and customer cost functions at buses used in case study[2].

Bus	Type	Cost function at reference time [NOK/kW]
2	Industry	$c(r)_{Ref,2} = 660.9 + 41 \cdot (r - 4)$
3	Energy-intensive industry	$c(r)_{Ref,3} = 102.3 + 3.1 \cdot r$
4	Residential	$c(r)_{Ref,4} = 444.5 + 13.3 \cdot (r - 24)$
5	Public service	$c(r)_{Ref,5} = 521.5 + 19.8 \cdot (r - 8)$
6	Agriculture	$c(r)_{Ref,6} = 74.2 + 16.1 \cdot (r - 4)$

The Norwegian CENS arrangement is the result of surveys conducted, stipulating the cost of outages of different durations at a reference time, as seen in Table 3.2. The stipulated cost at the reference time is then subjected to correction factors taking into account the month, day and hour the outage occurs. The cost of interrupted power (NOK/kW) for an end-user interruption at time t with a duration r, using appropriate correction factors f for month, day and hour is calculated in (3.58). The correction factors can be found in Appendix C.

$$c(r)_t = c(r)_{Ref} \cdot f_{month} \cdot f_{day} \cdot f_{hour} \tag{3.58}$$

Annual indices for the individual transmission lines can be found in Table 3.3. The annual failure rate, λ, is calculated as the sum of failure probability in the time-series divided by number of years of observations, as is the annual unavailability, U. Approximate equations (see e.g. [93]) assume that new outages in the set happens at a fixed rate during the outage of the previous component(s). This does not hold true when there are correlated failure probabilities. The mean outage duration is thus found either from the outage distribution of the individual line, or as $r = U/\lambda$ for higher order sets.

Equation (3.59) shows the calculation of the *potential* CENS of a set $\{x, y\}$ *if* the set occurs at a specific time, t. Interrupted power calculated from the time-varying load demand is used rather than the interrupted power at a reference time. This ensures that the calculated CENS and the time-series of failure probability reflects the historical conditions in load and threat exposure. The interrupted power is multiplied with the associated cost function and summed across all buses, b. This gives a measure of the potential economic impact of the outage at each time-step. The annual *expected* CENS is calculated in (3.60). The annual

[2]Customer types at buses following [122]. Customer cost functions at reference time for outage durations above 8 hours for all customer types except the "residential" category which uses outage durations between 24 and 74 hours, from [101].

Table 3.3: Annual indices for the transmission lines.

Line	$\lambda[f/y]$	$r[h]$	$U[h/y]$
1	0.463	61.8	28.6
2	1.544	92.0	142.0
3	1.235	88.4	109.2
4	0.309	108.6	33.5
5	0.309	102.3	31.6
6	0.463	97.4	45.1
7	1.544	74.8	115.5
8	0.309	106.4	32.8
9	0.309	99.6	30.7

expected CENS is the sum of hourly potential CENS weighted by the probability of the outage occurrence, divided by the number of years the time-series covers.

$$CENS_{\{x,y\},t} = \sum_{b} [P_{\{x,y\},interr,b,t} \cdot c(r_{\{x,y\}})_{b,t}] \tag{3.59}$$

$$E(CENS_{\{x,y\}}) = \frac{\sum_t \lambda_{\{x,y\},t} \cdot CENS_{\{x,y\},t}}{y} \tag{3.60}$$

Results

Figure 3.18 shows the ranked distribution of the 15 cut-sets with the highest expected ENS given that an outage occurs, paired with the associated expected CENS. Only cut-sets containing more than one component are considered, to highlight the impact of multiple overlapping outages. Annual expected CENS for the same cut-sets follows much of the same distribution as for the ENS but there are some instances where the divergence between the consequence and the criticality. This illustrates some of the impact of taking the criticality for the customer into account when performing the risk assessment. This discrepancy is especially apparent for cut-set $\{1, 6\}$. This particular cut-set (as does the cut-sets it is a subset of: $\{1, 2, 6\}$ and $\{1, 3, 6\}$) has two features that can explain this discrepancy. The occurrence of this cut-set causes interrupted power in most system load scenarios. The interrupted power due to the cut-set also primarily affects the loads at bus 3 (energy intensive industry) and 6 (agriculture), which have a low CENS for long outage durations compared to other customer types. This combined causes a high ENS on one side, and a low CENS compared to similar ENS affecting other customer types on the other. Although the expected

values are a good measure of the reliability of the system, these can conceal periods with high potential consequences and associated risk.

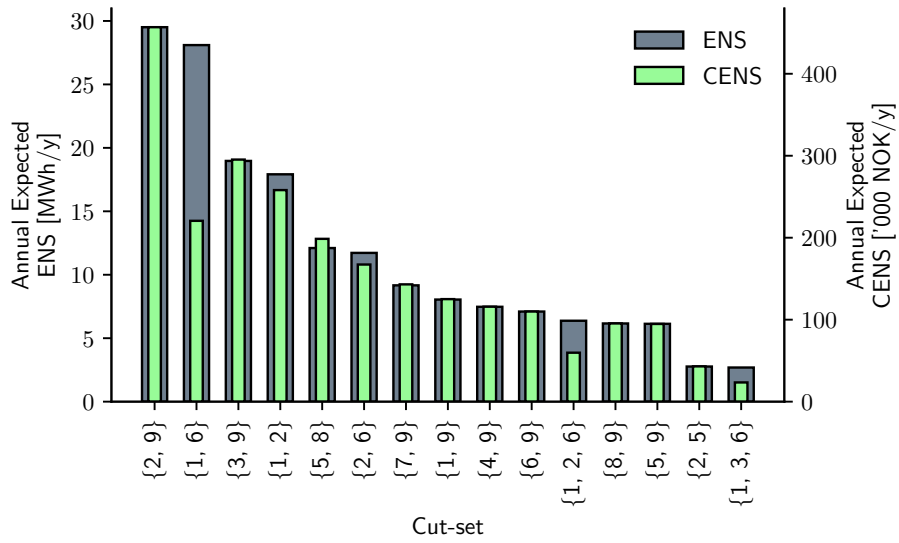

Figure 3.18: Paired histograms of expected ENS and CENS for the 15 cut-sets with the highest expected ENS values. Grey bars illustrate the Annual Expected ENS of the cut-set which can be seen on the left hand side y-axis, while the green bars represent the associated CENS for the same cut-set (as seen on the right hand side y-axis).

Figure 3.19 shows different representations of the hourly risk associated with cut-set $\{5, 8\}$ over the span of the case study. As noted in [6, 30], what is acceptable risk is inherently a political question, and ultimately up to the transmission system operator to decide. On the graph, linear risk limits have been superimposed to illustrate how the expected risk can be considered medium, or even close to low, while the an extreme event may be well into the critical territory. Dashed horizontal lines are added in sub-figures (a), (b) and (c) to show the limits of the highest and lowest probability of the outage occurrence of the scenario. The dashed vertical line in (a) shows the minimum criticality of an event of an expected duration. The dashed vertical line in (b) shows the maximum criticality of a constructed extreme event scenario. Together these lines makes up the outer borders of the uncertainty box in sub-figure (c), where dashed lines cross the expected hourly probability and criticality of the scenario, intersecting in the expected hourly risk of the scenario marked by a red dot. The latter can be multiplied by the number of hours in the year to find the expected annual CENS of the scenario.

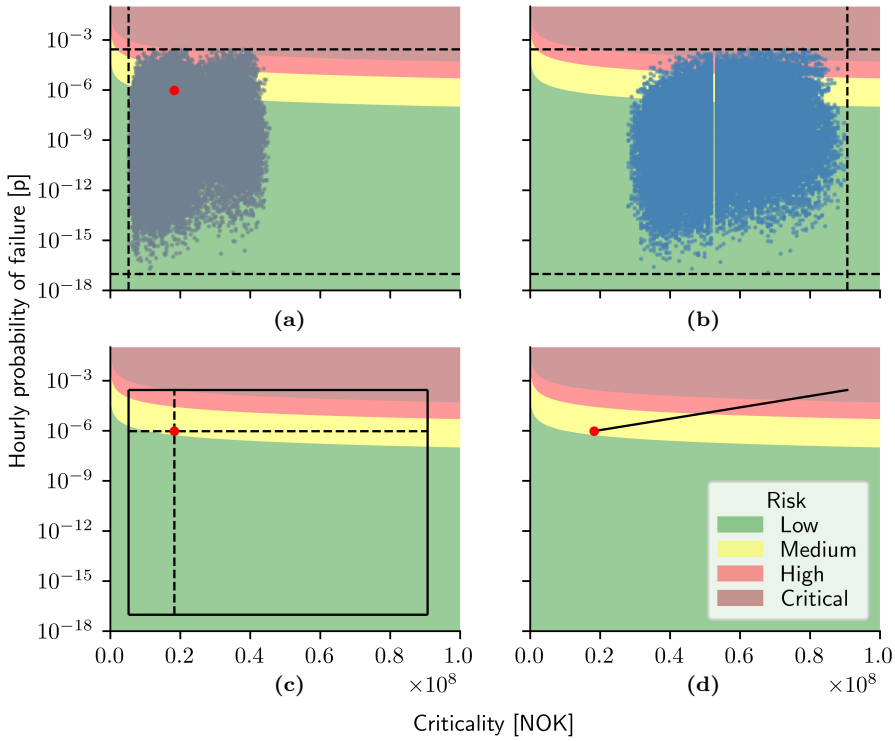

Figure 3.19: Stepwise construction of risk diagram with uncertainty boxes for a cut-set in the case study and a reduced "dot-and-line" representation of the risk. *(a)* Scatter-plot representing the pairwise hourly observations of failure probability and criticality of an event with an expected duration (grey scatters), red dot representing the expected risk across observations. Dashed lines represents the upper and lower bounds of failure probability (vertical), and the lower bound of criticality (horizontal). *(b)* Scatter-plot representing the pairwise hourly failure probability and criticality of an extreme scenario (blue scatter), with vertical dashed line showing the upper bound of criticality. *(c)* Uncertainty-box representing the risk associated with the cut-set, using information from sub-figure (a) and (b). *(d)* A reduced "dot-and-line" representation of the upper right quadrant of the uncertainty box in (c).

The lower and left quadrants of the uncertainty box in Figure 3.19 (c) hold limited information relevant to the risk of extraordinary events beyond the expected values. In many cases both the minimum probability and criticality are zero, and the overall risk relevant to reliability analysis is contained within the expected value. The upper-right quadrant holds the relevant information about the tail end risk associated with the extreme scenario. In Figure 3.19 (d) the diagonal from the expected values to the maximum values are drawn to represent the information contained in the upper-right quadrant of the uncertainty box. This "dot-and-line" representation reduces the amount of clutter but still conveys the key information contained in the graph. It also compresses the necessary span of the axes which aids when comparing multiple contingencies. The most relevant information related to the risk of extraordinary events is however still contained in the graph.

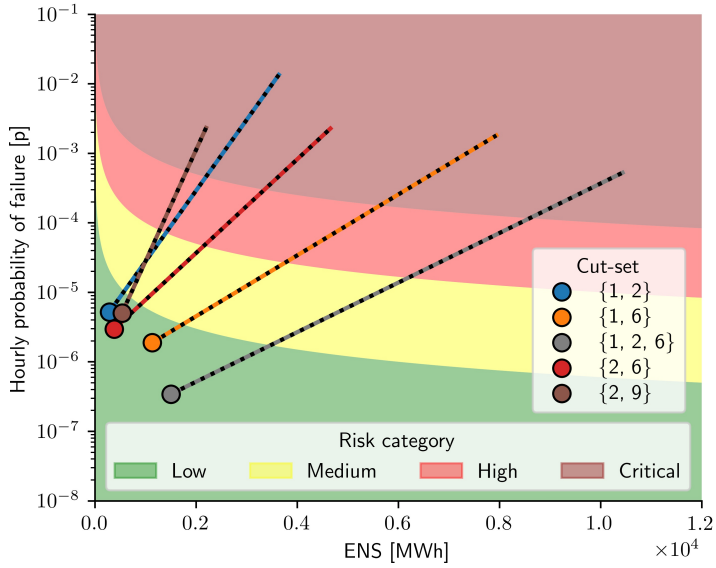

Figure 3.20: Risk diagram using a "dot-and-line" representation: Probability and consequence (ENS).

Figure 3.20 shows a risk graph using the dot-and-line representation for the 5 sets of transmission line outages in the case study with the highest identified hourly risk in the extreme scenario as a function of failure probability and ENS. The cut-sets are listed in order from highest to lowest risk in the extreme scenario. Using this representation, the ordering of the cut-sets is different from what is found in Figure 3.18. Cut-set $\{1, 2, 6\}$ in particular was ranked as the 11^{th} when considering expected ENS but when considering the risk in the extreme scenario it is considered the 3^{rd}. The cut-set also has a much higher potential ENS due to an extreme scenario than any of the other cut-sets in the graph. This potential of an

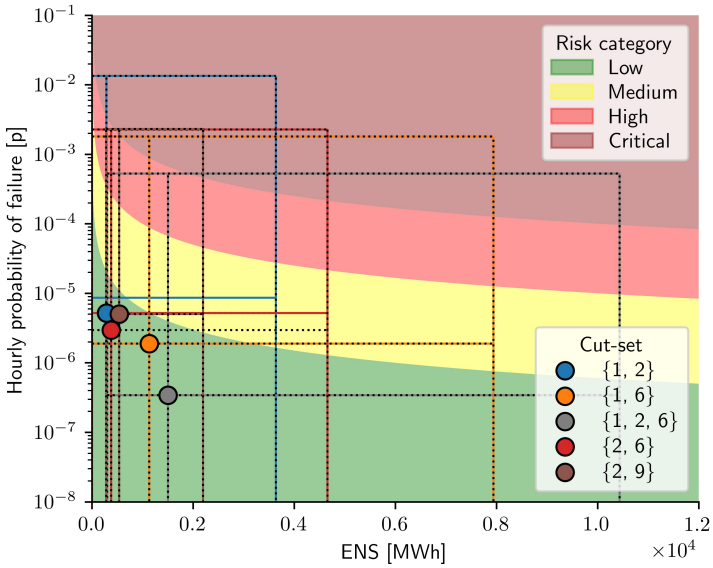

Figure 3.21: Risk diagram using uncertainty boxes: Probability and consequence (ENS).

extraordinary event was not readily communicated by Figure 3.18 or the expected value. The proposed graph readily communicates key information regarding the risk associated with a scenario and the potential for an extraordinary event.

Figure 3.21 shows the same risks scenarios as 3.20 visualized using the full uncertainty boxes. The y-axis is cut off at 10^{-8} but the lower bounds extends further. This representation of multiple cut-sets in a single graph contains more information but is difficult to decipher. Much of the information contained in the graph is not strictly relevant to extraordinary events and the inclusion of this information hampers the easy identification of scenarios that could potentially lead to extraordinary events. The proposed "dot-and-line" representation contributes to sparsity and clarity when communicating the important information related to expected and extraordinary events, compared to a graph using the full uncertainty boxes. This makes it easier to compare multiple cut-sets in the same graph.

Figure 3.22 shows a similar graph, where the five contingencies with the highest risk as a function of failure probability and CENS in the extreme scenario are included in the graph. Cut-set $\{1, 2, 6\}$ is no longer included in the list of cut-sets due to a lower criticality associated with an extreme scenario, despite its high potential ENS. Differences in customer groups affected by the power interruption should the cut-set occur also change the ranking of other cut-sets. The CENS

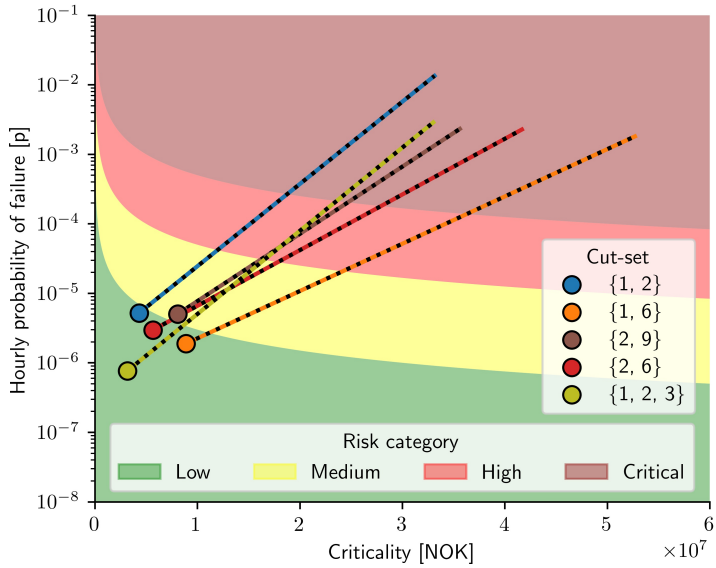

Figure 3.22: Risk diagram using a "dot-and-line" representation: Probability and criticality (CENS).

measure of criticality incorporates some of the impact ENS has external to the power system. The criticality of an extraordinary event should inform the grid operator's prioritization of mitigating efforts.

Conclusion

There are multiple novelties in the contribution. The CENS is included as a measure of criticality for the affected end-users. This can yield substantially different results when analyzing some cut-sets due to differences in affected customer groups. Risk, as a function of probability and criticality can also inform the grid operators' prioritization of mitigating or grid hardening efforts, also in the case of extraordinary events. A method of visualizing risk of extraordinary events in power systems is developed.

The "dot-and-line" risk visualization is developed to include relevant uncertainties in the probability and consequence/criticality axes. The visualization is a reduction of the uncertainty boxes that has previously been suggested as a method for incorporating tail-end events into risk visualizations. This is justified in that only one quadrant of the uncertainty boxes holds information relevant to expected and extraordinary events, and it is sufficiently represented by the expected value and the most extreme event. This reduces cluttering when multiple cut-sets are visualized simultaneously.

4 Conclusion and further work

The objective of the thesis was to *develop methodologies for understanding and communicating uncertainties and risks related to extraordinary events.* Four research questions were developed to contribute in reaching the objective:

How do time-varying failure rates affect the rate of unwanted events? This The method of calculating time-series of unavailability of components in Paper 1 is novel in itself, and gives a clear output that can be visually inspected. It is a possible alternative method for incorporating correlated threat exposure due to, for instance, harsh weather, compared to existing methods such as multi-state weather models that can become highly complex and difficult to parameterize. The method combines the previous work on time-varying failure probabilities in [78] with an iterative algorithm that combines the failure probability and outage duration of single components. The probability and consequences of a contingency which includes multiple components can easily be calculated as combinations of its constituent parts. The results of the method aids in identifying components and sets of components that can be considered parts of high-risk contingencies. This information can thus be used for targeted grid hardening efforts.

How do interactions between failure bunching phenomena and protection system failures contribute to unwanted events? The method developed in Paper 2 combines two forms of dependencies: correlated threat exposure between components causing failure bunching due to weather, and dependent outages caused by protection systems misoperations. The combination of these two forms of dependencies is a novelty in itself. The method extends the work in [27], and, by taking a graph-theoretical approach, the topology of the system is incorporated into the reliability equations. The use of probability matrices to include protection system misoperation in reliability evaluations is then made applicable to time-series of component failures. The use of the developed probability matrices could be a useful tool to incorporate protection system misoperation into other forms of analysis, such as those relying on Monte Carlo methods.

What are the contributions to long restoration times caused by natural hazard events? Long restoration times due to permanent failures caused by natural hazard events is one of the major challenges when it comes to extraordinary events. However, the transmission system is highly reliable and there is limited historical data available to create generalized fixed down-time distributions for different components with varying degrees of accessibility. Paper 3 proposes a solution to this challenge by decomposing the down-time duration of overhead transmission lines into constituent parts which are analyzed individually, before it is put together to predict transmission line down time distributions. This is done by combining limited statistical data and expert judgments in a logical model using a Bayesian Network. The decomposition of the problem and reliance on different sources of information to parameterize the model is a novelty in itself. The model can be updated based on threat-, time- and location-dependent information, thus making it a versatile tool that can contribute to improved modeling of component down times. The framework developed in the paper has multiple potential further developments: The conceptual model can serve as a basis for further development and refinement of the overarching model, and new data sources incorporated using the methods in the paper can improve the parametrization of the model(s).

How can the risk of extraordinary events be communicated and visualized? A contribution to answering this research question was presented in Paper 4 and further developed in Section 3.5 of this thesis. There are several contributions to this field of research in the work: The inclusion of criticality for the end-users in the calculation of the risk related of extraordinary events is one. Criticality in terms of CENS due to outage occurrences is based on stipulated costs to the end-users which experiences an interruption, and is reflected through an economic impact for the system operator. It is thus a measure of criticality that clearly covers the interests of both the end-user and the system operator, and contributes to a socioeconomically sound operation of the power system. CENS, unlike many other measures of criticality, has a clear quantitative interpretation which makes it ideal for representation in a continuous scale risk diagram. Risk diagrams including uncertainty boxes are considered, and further developed in this work. A reduced "dot-and-line" representation of the traditional uncertainty boxes is proposed, as it is assumed to contain important information regarding probability and consequence of risk related to extraordinary events. This is a further novelty in the work presented. Visualization of tail-end risk in a clear and concise manner is an area that could benefit from continued research. The incorporation of criticality in the risk diagram could also potentially spur the inclusion of measures of criticality other than CENS using similar methods. Looking beyond monetary values as a measure of criticality would be a welcome addition to this branch of power systems risk analysis.

Bibliography

[1] U.S.–Canada Power System Outage Task Force, "Final report on the August 14, 2003 Blackout in the United States and Canada: Causes and recommendations," U.S. Environmental Protection Agency, Washington, D.C., Tech. Rep., 2004. [Online]. Available: https://www3.epa.gov/region1/npdes/merrimackstation/pdfs/ar/AR-1165.pdf

[2] G. Andersson, P. Donalek, R. Farmer, N. Hatziargyriou, I. Kamwa, P. Kundur, N. Martins, J. Paserba, P. Pourbeik, J. Sanchez-Gasca, R. Schulz, A. Stankovic, C. Taylor, and V. Vittal, "Causes of the 2003 Major Grid Blackouts in North America and Europe, and Recommended Means to Improve System Dynamic Performance," *IEEE Transactions on Power Systems*, vol. 20, no. 4, pp. 1922–1928, nov 2005. [Online]. Available: http://ieeexplore.ieee.org/document/1525122/

[3] G. H. Kjølle, M. Tapper, and K. Hanninen, "Major storms - main causes, consequences and crisis management," in *22nd International Conference and Exhibition on Electricity Distribution (CIRED 2013)*. Institution of Engineering and Technology, 2013, pp. 0658–0658. [Online]. Available: https://digital-library.theiet.org/content/conferences/10.1049/cp.2013.0863

[4] AEMC, "Mechanisms to enhance resilience in the power system - Review of the South Australian black system event, Final report," Australian Energy Market Commission, Tech. Rep., 2019. [Online]. Available: https://www.aemc.gov.au/sites/default/files/documents/aemc_-_sa_black_system_review_-_final_report.pdf

[5] R. Yan, N.-A. Masood, T. Kumar Saha, F. Bai, and H. Gu, "The Anatomy of the 2016 South Australia Blackout: A Catastrophic Event in a High Renewable Network," *IEEE Transactions on Power Systems*, vol. 33, no. 5, pp. 5374–5388, sep 2018. [Online]. Available: https://ieeexplore.ieee.org/document/8327538/

[6] I. B. Sperstad, G. H. Kjølle, and O. Gjerde, "A comprehensive framework for vulnerability analysis of extraordinary events in power

systems," *Reliability Engineering & System Safety*, vol. 196, p. 106788, apr 2020. [Online]. Available: https://linkinghub.elsevier.com/retrieve/pii/S0951832019307008

[7] E. Ciapessoni, D. Cirio, A. Pitto, M. Panteli, M. V. Harte, and C. Mak, "Defining Power System Resilience," *Electra*, vol. October, no. 306, pp. 32–34, 2019.

[8] A. Stankovic, "The Definition and Quantification of Resilience," IEEE PES Industry Technical Support Task Force, Tech. Rep. PES-TR65, apr 2018.

[9] R. Moreno, M. Panteli, P. Mancarella, H. Rudnick, T. Lagos, A. Navarro, F. Ordonez, and J. C. Araneda, "From Reliability to Resilience: Planning the Grid Against the Extremes," *IEEE Power and Energy Magazine*, vol. 18, no. 4, pp. 41–53, jul 2020. [Online]. Available: https://ieeexplore.ieee.org/document/9120304/

[10] Statnett - Feilanalyse, "Årsstatistikk 2018. Driftsforstyrrelser og feil i 33-420 kV-nettet [In Norwegian]," Statnett SF, Oslo, Norway, Tech. Rep., 2019. [Online]. Available: https://www.statnett.no/contentassets/5fb5605039314f498ed16f8561695a0c/arsstatistikk-2018-33-420-kv.pdf

[11] Y. Zhou, A. Pahwa, and S. S. Yang, "Modeling weather-related failures of overhead distribution lines," *IEEE Transactions on Power Systems*, vol. 21, no. 4, pp. 1683–1690, nov 2006.

[12] E. Bompard, T. Huang, Y. Wu, and M. Cremenescu, "Classification and trend analysis of threats origins to the security of power systems," *International Journal of Electrical Power & Energy Systems*, vol. 50, no. 1, pp. 50–64, sep 2013.

[13] P. Hines, J. Apt, and S. Talukdar, "Large blackouts in North America: Historical trends and policy implications," *Energy Policy*, vol. 37, no. 12, pp. 5249–5259, dec 2009.

[14] Peng Wang and R. Billinton, "Reliability cost/worth assessment of distribution systems incorporating time-varying weather conditions and restoration resources," *IEEE Transactions on Power Delivery*, vol. 17, no. 1, pp. 260–265, 2002.

[15] H. Guo, C. Zheng, H. H. C. Iu, and T. Fernando, "A critical review of cascading failure analysis and modeling of power system," *Renewable and Sustainable Energy Reviews*, vol. 80, pp. 9–22, 2017.

[16] E. Hillberg, "Perception, Prediction and Prevention of Extraordinary Events in the Power System," Doctoral Theses, Norwegian University of Science and Technology, Trondheim, Norway, 2016.

[17] R. Billinton, G. Singh, and J. Acharya, "Failure Bunching Phenomena in Electric Power Transmission Systems," *Proceedings of the Institution of Mechanical Engineers, Part O: Journal of Risk and Reliability*, vol. 220, no. 1, pp. 1–7, 2006.

[18] Y. Wang, C. Chen, J. Wang, and R. Baldick, "Research on Resilience of Power Systems under Natural Disasters - A Review," *IEEE Transactions on Power Systems*, vol. 31, no. 2, pp. 1604–1613, 2016.

[19] S. E. Chang, T. L. McDaniels, J. Mikawoz, and K. Peterson, "Infrastructure failure interdependencies in extreme events: power outage consequences in the 1998 Ice Storm," *Natural Hazards*, vol. 41, no. 2, pp. 337–358, Apr. 2007. [Online]. Available: http://link.springer.com/10.1007/s11069-006-9039-4

[20] H. Haes Alhelou, M. Hamedani-Golshan, T. Njenda, and P. Siano, "A Survey on Power System Blackout and Cascading Events: Research Motivations and Challenges," *Energies*, vol. 12, no. 4, p. 682, Feb. 2019. [Online]. Available: http://www.mdpi.com/1996-1073/12/4/682

[21] I. Dobson and D. E. Newman, "Cascading blackout overall structure and some implications for sampling and mitigation," *International Journal of Electrical Power and Energy Systems*, vol. 86, pp. 29–32, 2017.

[22] P. Pourbeik, P. S. Kundur, and C. W. Taylor, "The anatomy of a power grid blackout," *IEEE Power and Energy Magazine*, vol. 4, no. 5, pp. 22–29, sep 2006.

[23] M. Vaiman, K. Bell, Y. Chen, B. Chowdhury, I. Dobson, P. Hines, M. Papic, S. Miller, and P. Zhang, "Risk assessment of cascading outages: Methodologies and challenges," *IEEE Transactions on Power Systems*, vol. 27, no. 2, pp. 631–641, 2012.

[24] A. G. Phadke, "Hidden failures in electric power systems," *International Journal of Critical Infrastructures*, vol. 1, no. 1, pp. 64–75, 2004.

[25] H. M. Merrill, M. A. Hossain, and M. Bodson, "Nipping Blackouts in the Bud: Introducing a Novel Cascading Failure Network," *IEEE Power and Energy Magazine*, vol. 18, no. 4, pp. 64–75, jul 2020. [Online]. Available: https://ieeexplore.ieee.org/document/9120298/

[26] I. B. Sperstad and E. S. Kiel, "Development of a qualitative framework for analysing high-impact low-probability events in power systems," in *Safety and Reliability - Safe Societies in a Changing World - Proceedings of the 28th International European Safety and Reliability Conference, ESREL 2018*. CRC Press, 2018, pp. 1599–1608.

[27] V. V. Vadlamudi, O. Gjerde, and G. Kjølle, "Dependability and security-based failure considerations in protection system reliability studies," in

2013 4th IEEE/PES Innovative Smart Grid Technologies Europe, ISGT Europe 2013. Denmark: IEEE, 2013.

[28] Department of Business, Energy Emergencies Executive Committee, "GB power system disruption on 9 August 2019," Secretary of State for Business, Energy and Industrial Strategy, Tech. Rep. Energy Emergencies Executive Committee (E3C): Final report, Aug. 2019. [Online]. Available: https://assets.publishing.service.gov.uk/government/uploads/system/uploads/attachment_data/file/855767/e3c-gb-power-disruption-9-august-2019-final-report.pdf

[29] J. Bialek, "What does the GB power outage on 9 August 2019 tell us about the current state of decarbonised power systems?" *Energy Policy*, vol. 146, p. 111821, Nov. 2020. [Online]. Available: https://linkinghub.elsevier.com/retrieve/pii/S0301421520305395

[30] G. Doorman, K. Uhlen, G. H. Kjølle, and E. Huse, "Vulnerability Analysis of the Nordic Power System," *IEEE Transactions on Power Systems*, vol. 21, no. 1, pp. 402–410, feb 2006. [Online]. Available: http://ieeexplore.ieee.org/document/1583739/

[31] M. Ovaere, E. Heylen, S. Proost, G. Deconinck, and D. Van Hertem, "How detailed value of lost load data impact power system reliability decisions," *Energy Policy*, vol. 132, pp. 1064–1075, Sep. 2019. [Online]. Available: https://linkinghub.elsevier.com/retrieve/pii/S0301421519304288

[32] G. Kjølle, K. Samdal, B. Singh, and O. Kvitastein, "Customer Costs Related to Interruptions and Voltage Problems: Methodology and Results," *IEEE Transactions on Power Systems*, vol. 23, no. 3, pp. 1030–1038, Aug. 2008. [Online]. Available: http://ieeexplore.ieee.org/document/4511482/

[33] T. Schröder and W. Kuckshinrichs, "Value of Lost Load: An Efficient Economic Indicator for Power Supply Security? A Literature Review," *Frontiers in Energy Research*, vol. 3, Dec. 2015. [Online]. Available: http://journal.frontiersin.org/Article/10.3389/fenrg.2015.00055/abstract

[34] S. Kaplan and B. J. Garrick, "On The Quantitative Definition of Risk," *Risk Analysis*, vol. 1, no. 1, pp. 11–27, 1981.

[35] Y. Y. Haimes, "Risk of extreme events and the fallacy of the expected value," *Control and Cybernetics*, vol. 22, no. 4, pp. 7–31, 1993.

[36] T. Aven, "On how to define, understand and describe risk," *Reliability Engineering & System Safety*, vol. 95, no. 6, pp. 623–631, jun 2010. [Online]. Available: https://linkinghub.elsevier.com/retrieve/pii/S095183201000027X

[37] M. Rausand, *Risk assessment: theory, methods, and applications*. John Wiley & Sons, 2013.

[38] R. Billinton and D. Huang, "Aleatory and Epistemic Uncertainty Considerations in Power System Reliability Evaluation," *Proceedings of the 10th International Conference on Probablistic Methods Applied to Power Systems*, pp. 1–8, 2008.

[39] E. S. Kiel and G. H. Kjølle, "Transmission line unavailability due to correlated threat exposure," in *2019 IEEE Milan PowerTech, PowerTech 2019*. Italy: IEEE, jun 2019.

[40] ——, "Reliability of supply and the impact of weather exposure and protection system failures," *Applied Sciences*, vol. 11, no. 1, p. 182, 2021.

[41] ——, "A Bayesian Network approach to predicting transmission line down times," *Proceedings of the 30th European Safety and Reliability Conference andt he 15th Probabilistic Safety Assessment and Management Conference*, 2020.

[42] ——, "Identification, visualization and reduction of risk related to HILP events in power systems," *2019 54th International Universities Power Engineering Conference, UPEC 2019 - Proceedings*, 2019.

[43] M. Ouyang, "Review on modeling and simulation of interdependent critical infrastructure systems," *Reliability Engineering & System Safety*, vol. 121, pp. 43 – 60, 2014. [Online]. Available: http://www.sciencedirect.com/science/article/pii/S0951832013002056

[44] A. A. Ghorbani and E. Bagheri, "The state of the art in critical infrastructure protection: a framework for convergence," *International Journal of Critical Infrastructures*, vol. 4, no. 3, pp. 215–244, 2008.

[45] M. Iturriza, L. Labaka, J. M. Sarriegi, and J. Hernantes, "Modelling methodologies for analysing critical infrastructures," *Journal of Simulation*, vol. 12, no. 2, pp. 128–143, 2018. [Online]. Available: https://doi.org/10.1080/17477778.2017.1418640

[46] J. Johansson, H. Hassel, and E. Zio, "Reliability and vulnerability analyses of critical infrastructures: Comparing two approaches in the context of power systems," *Reliability Engineering and System Safety*, vol. 120, pp. 27–38, 2013.

[47] R. W. Scholz, Y. B. Blumer, and F. S. Brand, "Risk, vulnerability, robustness, and resilience from a decision-theoretic perspective," *Journal of Risk Research*, vol. 15, no. 3, pp. 313–330, 2012.

[48] F. Miller, H. Osbahr, E. Boyd, F. Thomalla, S. Bharwani, G. Ziervogel, B. Walker, J. Birkmann, S. Van der Leeuw, J. Rockström *et al.*, "Resilience and vulnerability: complementary or conflicting concepts?" *Ecology and Society*, vol. 15, no. 3, 2010.

[49] V. Proag, "The concept of vulnerability and resilience," *Procedia Economics and Finance*, vol. 18, pp. 369–376, 2014.

[50] S. Hosseini, K. Barker, and J. E. Ramirez-Marquez, "A review of definitions and measures of system resilience," *Reliability Engineering and System Safety*, vol. 145, pp. 47–61, 2016.

[51] P. Gasser, P. Lustenberger, M. Cinelli, W. Kim, M. Spada, P. Burgherr, S. Hirschberg, B. Stojadinovic, and T. Y. Sun, "A review on resilience assessment of energy systems," *Sustainable and Resilient Infrastructure*, pp. 1–27, 2019.

[52] A. Abedi, L. Gaudard, and F. Romerio, "Review of major approaches to analyze vulnerability in power system," *Reliability Engineering & System Safety*, vol. 183, pp. 153–172, mar 2019. [Online]. Available: https://linkinghub.elsevier.com/retrieve/pii/S0951832018303041

[53] G. H. Kjølle and O. Gjerde, "Vulnerability analysis related to extraordinary events in power systems," in *2015 IEEE Eindhoven PowerTech, PowerTech 2015*. Eindhoven, Netherlands: IEEE, 2015, pp. 1–6.

[54] M. Hofmann, G. H. Kjølle, and O. Gjerde, "Vulnerability indicators for electric power grids," SINTEF Energy Research, Tech. Rep. TR A7276, 2013.

[55] G. H. Kjølle, O. Gjerde, and A. Nybø, "A Framework For Handling High Impact Low Probability (HILP) Events," in *CIRED Workshop*, Lyon, 2010, p. Paper 0094.

[56] G. H. Kjølle, I. B. Utne, and O. Gjerde, "Risk analysis of critical infrastructures emphasizing electricity supply and interdependencies," *Reliability Engineering and System Safety*, vol. 105, pp. 80–89, 2012.

[57] Commission of the European Communities, "Green Paper on a European Programme for Critical Infrastructure Protection," European Union, Brussels, Tech. Rep. COM(2005) 576 final, nov 2005.

[58] N. Bhusal, M. Abdelmalak, M. Kamruzzaman, and M. Benidris, "Power System Resilience: Current Practices, Challenges, and Future Directions," *IEEE Access*, vol. 8, pp. 18 064–18 086, 2020. [Online]. Available: https://ieeexplore.ieee.org/document/8966351/

[59] M. A. Mohamed, T. Chen, W. Su, and T. Jin, "Proactive Resilience of Power Systems Against Natural Disasters: A Literature Review," *IEEE Access*, vol. 7, pp. 163 778–163 795, 2019. [Online]. Available: https://ieeexplore.ieee.org/document/8894433/

[60] M. Bruneau, S. E. Chang, R. T. Eguchi, G. C. Lee, T. D. O'Rourke, A. M. Reinhorn, M. Shinozuka, K. Tierney, W. A. Wallace, and D. Von Winterfeldt, "A Framework to Quantitatively Assess and Enhance the Seismic Resilience of Communities," *Earthquake Spectra*, vol. 19, no. 4, pp. 733–752, nov 2003.

[61] T. McDaniels, S. Chang, D. Cole, J. Mikawoz, and H. Longstaff, "Fostering resilience to extreme events within infrastructure systems: Characterizing decision contexts for mitigation and adaptation," *Global Environmental Change*, vol. 18, no. 2, pp. 310–318, may 2008. [Online]. Available: https://linkinghub.elsevier.com/retrieve/pii/S0959378008000174

[62] K. Tierney and M. Bruneau, "Conceptualizing and Measuring Resilience: A Key to Disaster Loss Reduction," *TR News*, vol. 250, 2007.

[63] M. Panteli, P. Mancarella, D. N. Trakas, E. Kyriakides, and N. D. Hatziargyriou, "Metrics and Quantification of Operational and Infrastructure Resilience in Power Systems," *IEEE Transactions on Power Systems*, vol. 32, no. 6, pp. 4732–4742, nov 2017.

[64] J. Heggset, G. H. Kjølle, and K. Sagen, "FASIT - a tool for collection, calculation and reporting of reliability data," in *IET Conference Publications*, no. 550 CP. Prague, Czech Republic: IET, 2009, p. 716.

[65] J. Heggset and G. H. Kjølle, "Experiences with the fasit reliability data collection system," in *2000 IEEE Power Engineering Society Winter Meeting. Conference Proceedings (Cat. No.00CH37077)*, vol. 1, 2000, pp. 546–551.

[66] J. Heggset, K. Johannessen, A. O. Eggen, and K. Sagen, "National reporting of faults and interruptions using cim and mades/ecp," in *CIRED 2019 - 25th International Conference on Electricity Distribution*, 2019.

[67] J. Heggset, "Norwegian disturbance management system and database: PS2/Q2.6," in *CIGRE Session 46*, vol. 2016-Augus, Paris, 2016.

[68] ENTSO-E, *Guidelines for the classification of grid disturbances above 100 kV*. ENTSO-E Regional Group Nordic (RGN), apr 2017. [Online]. Available: https://eepublicdownloads.entsoe.eu/clean-documents/Publications/SOC/Nordic/HVAC_guidelines_2017_04_13.pdf

[69] FASIT, "Definisjoner knyttet til feil og avbrudd i det elektriske kraftsystemet [In Norwegian]," p. 22, 2019. [Online]. Available: https://www.statnett.no/globalassets/for-aktorer-i-kraftsystemet/systemansvaret/leveringskvalitet/definisjoner-knyttet-til-feil-og-avbrudd-i-det-elektriske-kraftsystemet_final.pdf?csf=1&web=1&e=VZFmbk

[70] IEEE, *859-2018 IEEE Standard Terms for Reporting and Analyzing Outage Occurrences and Outage States of Electrical Transmission Facilities - Redline*. S.l.: IEEE, 2019. [Online]. Available: https://ieeexplore.ieee.org/servlet/opac?punumber=8748235

[71] ——, "1366-2012 - IEEE Guide for Electric Power Distribution Reliability Indices," 2012.

[72] The International Electrotechnical Commission, "International Electrotechnical Vocabulary." [Online]. Available: http://www.electropedia.org/

[73] NERC, "Glossary of Terms," p. 47, 2020. [Online]. Available: https://www.nerc.com/pa/Stand/GlossaryofTerms/Glossary_of_Terms.pdf

[74] M. Rausand and A. Høyland, *System Reliability Theory: Models, Statistical Methods, and Applications*, 2nd ed. John Wiley & Sons, 2004.

[75] R. Rocchetta, E. Zio, and E. Patelli, "A power-flow emulator approach for resilience assessment of repairable power grids subject to weather-induced failures and data deficiency," *Applied Energy*, vol. 210, pp. 339–350, 2018.

[76] R. E. Brown, G. Frimpong, and H. L. Willis, "Failure rate modeling using equipment inspection data," *IEEE Transactions on Power Systems*, vol. 19, no. 2, pp. 782–787, 2004.

[77] A. Moradkhani, M. R. Haghifam, and M. Mohammadzadeh, "Failure rate estimation of overhead electric distribution lines considering data deficiency and population variability," *International Transactions on Electrical Energy Systems*, vol. 25, no. 8, pp. 1452–1465, 2015.

[78] Ø. R. Solheim, T. Trötscher, and G. H. Kjølle, "Wind dependent failure rates for overhead transmission lines using reanalysis data and a Bayesian updating scheme," in *2016 International Conference on Probabilistic Methods Applied to Power Systems (PMAPS)*. IEEE, oct 2016, pp. 1–7. [Online]. Available: https://ieeexplore.ieee.org/document/7764104/

[79] Ø. R. Solheim and T. Trötscher, "Modelling transmission line failures due to lightning using reanalysis data and a Bayesian updating scheme," in *2018 International Conference on Probabilistic Methods Applied to Power Systems, PMAPS 2018 - Proceedings*. Boise, ID: IEEE, 2018.

[80] M. Papic, S. Agarwal, R. N. Allan, R. Billinton, C. J. Dent, S. Ekisheva, D. Gent, K. Jiang, W. Li, J. Mitra, A. Pitto, A. Schneider, C. Singh, V. V. Vadlamudi, and M. Varghese, "Research on Common-Mode and Dependent (CMD) Outage Events in Power Systems: A Review," *IEEE Transactions on Power Systems*, vol. 32, no. 2, pp. 1528–1536, 2017.

[81] R. Billinton and G. Singh, "Application of adverse and extreme adverse weather: Modelling in transmission and distribution system reliability evaluation," in *IEE Proceedings: Generation, Transmission and Distribution*, vol. 153, no. 1, Sevilla, 2006, pp. 115–120.

[82] R. Billinton and J. Tatla, "Composite generation and transmission system adequacy evaluation including protection system failure modes," *IEEE Transactions on Power Apparatus and Systems*, vol. PAS-102, no. 6, pp. 1823–1830, 1983.

[83] R. Billinton, "Basic models and methodologies for common mode and dependent transmission outage events," in *2012 IEEE Power and Energy Society General Meeting*. IEEE, jul 2012.

[84] K. Jiang and C. Singh, "New models and concepts for power system reliability evaluation including protection system failures," *IEEE Transactions on Power Systems*, vol. 26, no. 4, pp. 1845–1855, nov 2011.

[85] M. Panteli and P. Mancarella, "Modeling and evaluating the resilience of critical electrical power infrastructure to extreme weather events," *IEEE Systems Journal*, vol. 11, no. 3, pp. 1733–1742, 2017.

[86] C. Chen, J. Wang, and D. Ton, "Modernizing Distribution System Restoration to Achieve Grid Resiliency Against Extreme Weather Events: An Integrated Solution," *Proceedings of the IEEE*, vol. 105, no. 7, pp. 1267–1288, jul 2017. [Online]. Available: http://ieeexplore.ieee.org/document/7915694/

[87] M. T. Schultz, B. P. Gouldby, J. Simm *et al.*, "Beyond the factor of safety developing fragility curves to characterize system reliability," *Geotechnical and Structures Laboratory*, 2010.

[88] M. Panteli and P. Mancarella, "Influence of extreme weather and climate change on the resilience of power systems: Impacts and possible mitigation strategies," *Electric Power Systems Research*, vol. 127, pp. 259–270, 2015.

[89] J. Sykes, V. Madani, J. Burger, M. Adamiak, and W. Premerlani, "Reliabilty of protection systems (what are the real concerns)," in *2010 63rd Annual Conference for Protective Relay Engineers*, 2010, pp. 1–16.

[90] IEEE, "Ieee standard definitions for power switchgear," *IEEE Std C37.100-1992*, pp. 1–82, 1992.

[91] J. J. Bian, A. D. Slone, and P. J. Tatro, "Protection system misoperation analysis," in *2014 IEEE PES General Meeting — Conference & Exposition*. IEEE, jul 2014, pp. 1–5. [Online]. Available: http://ieeexplore.ieee.org/document/6939488/

[92] E. S. Kiel and G. H. Kjølle, "The impact of protection system failures and weather exposure on power system reliability," in *2019 IEEE International Conference on Environment and Electrical Engineering and 2019 IEEE Industrial and Commercial Power Systems Europe (EEEIC / I&CPS Europe)*. IEEE, jun 2019.

[93] R. Billinton and R. N. Allan, *Reliability Evaluation of Power Systems*. New York, NY, USA: Plenum Press, 1996.

[94] V. V. Vadlamudi, O. Gjerde, and G. Kjolle, "Impact of protection system reliability on power system reliability: A new minimal cutset approach," in *2014 International Conference on Probabilistic Methods Applied to Power Systems, PMAPS 2014 - Proceedings*. Durham: IEEE, 2014.

[95] C. E. Althaus, "A disciplinary perspective on the epistemological status of risk," *Risk Analysis: An International Journal*, vol. 25, no. 3, pp. 567–588, 2005.

[96] GARPUR, "State of the art on reliability assessment in power systems including socioeconomic impact (Garpur D1.1)," SINTEF Energy Research, Tech. Rep., Mar. 2014. [Online]. Available: https://www.sintef.no/globalassets/project/garpur/deliverables/garpur-d1.1-state-of-the-art-on-reliability-assessment-in-power-systems.pdf

[97] M. de Nooij, R. Lieshout, and C. Koopmans, "Optimal blackouts: Empirical results on reducing the social cost of electricity outages through efficient regional rationing," *Energy Economics*, vol. 31, no. 3, pp. 342–347, May 2009. [Online]. Available: https://linkinghub.elsevier.com/retrieve/pii/S0140988308001692

[98] The Norwegian Water Resources and Energy Directorate, "Economic regulation," 2020. [Online]. Available: https://www.nve.no/norwegian-energy-regulatory-authority/economic-regulation/

[99] G. H. Kjølle, "KILE-satsene og hva de dekker [In Norwegian, translated title: CENS rates and what they cover]." SINTEF Energy Research, Trondheim, Norway, Tech. Rep., 2011. [Online]. Available: https://www.sintef.no/globalassets/project/kile/prosjektnotat_kile-satser_v4_2011-01-20.pdf

[100] G. H. Kjølle and H. Vefsnmo, "Customer Interruption Costs in Quality of Supply Regulation: Methods for Cost Estimation and Data Challenges," in *Proceedings CIRED 2015*, Lyon, France, Jun. 2015.

[101] The Royal Norwegian Ministry of Petroleum and Energy, "Forskrift om økonomisk og teknisk rapportering, inntektsramme for nettvirksomheten og tariffer. §9. [English translation: Regulation of economic and technical reporting, revenue cap for network operators, and tariffs. §9],"

2020. [Online]. Available: https://lovdata.no/dokument/SF/forskrift/1999-03-11-302/KAPITTEL_4-3#KAPITTEL_4-3

[102] L. Cox, "What's Wrong with Risk Matrices?" *Risk Analysis*, vol. 28, no. 2, pp. 497–512, apr 2008. [Online]. Available: http://doi.wiley.com/10.1111/j.1539-6924.2008.01030.x

[103] B. Ale, P. Burnap, and D. Slater, "On the origin of PCDS – (Probability consequence diagrams)," *Safety Science*, vol. 72, pp. 229–239, feb 2015. [Online]. Available: https://linkinghub.elsevier.com/retrieve/pii/S0925753514002136

[104] C. Peace, "The risk matrix: uncertain results?" *Policy and Practice in Health and Safety*, vol. 15, no. 2, pp. 131–144, 2017. [Online]. Available: https://doi.org/10.1080/14773996.2017.1348571

[105] N. J. Duijm, "Recommendations on the use and design of risk matrices," *Safety Science*, vol. 76, pp. 21–31, 2015.

[106] A. D. Kiureghian and O. Ditlevsen, "Aleatory or epistemic? does it matter?" *Structural Safety*, vol. 31, no. 2, pp. 105 – 112, 2009, risk Acceptance and Risk Communication. [Online]. Available: http://www.sciencedirect.com/science/article/pii/S0167473008000556

[107] F. Goerlandt and G. Reniers, "On the assessment of uncertainty in risk diagrams," *Safety Science*, vol. 84, pp. 67–77, apr 2016.

[108] T. Aven, "Practical implications of the new risk perspectives," *Reliability Engineering and System Safety*, vol. 115, pp. 136–145, 2013.

[109] T. Fearn, A. Gelman, J. B. Carlin, H. S. Stern, and D. B. Rubin, *Bayesian Data Analysis.*, 3rd ed., ser. Chapman & {Hall}/{CRC} texts in statistical science. Boca Raton: CRC Press, 1996, vol. 52, no. 3.

[110] K. Vindteknikk, "Long-term data series, WRF ERA-Interim." [Online]. Available: http://www.vindteknikk.com/services/analyses/wind-power/pre-construction/long-term-series-2

[111] NVE, "Map Services," 2020. [Online]. Available: https://www.nve.no/map-services/

[112] Kartverket, "Topografisk Norgeskart," 2020. [Online]. Available: https://register.geonorge.no/inspire-statusregister/topografisk-norgeskart/f004268c-d4a1-4801-91cb-daa46236fab7

[113] S. Chakraborti, F. Jardim, and E. Epprecht, "Higher-Order Moments Using the Survival Function: The Alternative Expectation Formula," *American Statistician*, vol. 73, no. 2, pp. 191–194, 2019.

[114] A. O'Hagan, "Expert Knowledge Elicitation: Subjective but Scientific," *American Statistician*, vol. 73, no. sup1, pp. 69–81, 2019.

[115] S. Ognjanovic, M. Thüring, R. O. Murphy, and C. Hölscher, "Display clutter and its effects on visual attention distribution and financial risk judgment," *Applied Ergonomics*, vol. 80, pp. 168–174, Oct. 2019. [Online]. Available: https://linkinghub.elsevier.com/retrieve/pii/S0003687019300924

[116] D. Spiegelhalter, M. Pearson, and I. Short, "Visualizing Uncertainty About the Future," *Science*, vol. 333, no. 6048, pp. 1393–1400, Sep. 2011. [Online]. Available: https://www.sciencemag.org/lookup/doi/10.1126/science.1191181

[117] R. Billinton, S. Kumar, N. Chowdhury, K. Chu, K. Debnath, L. Goel, E. Khan, P. Kos, G. Nourbakhsh, and J. Oteng-Adjei, "A reliability test system for educational purposes - basic data," *IEEE Transactions on Power Systems*, vol. 4, no. 3, pp. 1238–1244, aug 1989.

[118] Statnett, "Data From The Power System: Production and Consumption," 2020. [Online]. Available: https://www.statnett.no/en/for-stakeholders-in-the-power-industry/data-from-the-power-system/{#}production-and-consumption

[119] M. Shaked, "On the Distribution of the Minimum and of the Maximum of a Random Number of I.I.D. Random Variables," in *A Modern Course on Statistical Distributions in Scientific Work*. Dordrecht: Springer Netherlands, 1975, pp. 363–380. [Online]. Available: http://link.springer.com/10.1007/978-94-010-1842-5_29

[120] G. H. Kjølle, I. B. Sperstad, and S. H. Jakobsen, "Interruption costs and time dependencies in quality of supply regulation," in *2014 International Conference on Probabilistic Methods Applied to Power Systems, PMAPS 2014 - Conference Proceedings*. Durham: IEEE, 2014, pp. 1–6.

[121] W. Wangdee and R. Billinton, "Impact of load shedding philosophies on bulk electric system reliability analysis using sequential Monte Carlo simulation," *Electric Power Components and Systems*, vol. 34, no. 3, pp. 355–368, 2006.

[122] I. B. Sperstad, S. H. Jakobsen, and O. Gjerde, "Modelling of corrective actions in power system reliability analysis," in *2015 IEEE Eindhoven PowerTech*. IEEE, jun 2015.

[123] O. P. Veloza and F. Santamaria, "Analysis of major blackouts from 2003 to 2015: Classification of incidents and review of main causes," *Electricity Journal*, vol. 29, no. 7, pp. 42–49, sep 2016.

[124] CERC, "Report on the Grid Disturbance on 30th July 2012 and Grid Disturbance on 31st July 2012." Central Electricity Regulatory Commission, Tech. Rep., Aug. 2012. [Online]. Available: http://www.cercind.gov.in/2012/orders/Final_Report_Grid_Disturbance.pdf

[125] J. Araneda, H. Rudnick, S. Mocarquer, and P. Miquel, "Lessons from the 2010 Chilean earthquake and its impact on electricity supply," in *2010 International Conference on Power System Technology*. Zhejiang, Zhejiang, China: IEEE, Oct. 2010, pp. 1–7. [Online]. Available: http://ieeexplore.ieee.org/document/5666023/

[126] S. Giovinazzi, T. Wilson, C. Davis, D. Bristow, M. Gallagher, A. Schofield, M. Villemure, J. Eidinger, and A. Tang, "Lifelines performance and management following the 22 February 2011 Christchurch earthquake, New Zealand," *Bulletin of the New Zealand Society for Earthquake Engineering*, vol. 44, no. 4, pp. 402–417, Dec. 2011. [Online]. Available: https://bulletin.nzsee.org.nz/index.php/bnzsee/article/view/232

[127] ENTSO-E, "Report on Blackout in Turkey on 32st March 2015," ENTSO-E: Project Group Turkey, Tech. Rep., Sep. 2015. [Online]. Available: https://eepublicdownloads.entsoe.eu/clean-documents/SOC%20documents/Regional_Groups_Continental_Europe/20150921_Black_Out_Report_v10_w.pdf

[128] TenneT, "Enabling the change: Integrated Annual Report 2015," TenneT, Netherlands, Annual report, Mar. 2016. [Online]. Available: https://www.tennet.eu/fileadmin/user_upload/Company/Investor_Relations/Annual_Report/TenneT-AR15_UK.pdf

[129] A. Nordrum, "Transmission Failure Causes Nationwide Blackout in Argentina," *IEEE Spectrum: Technology, Engineering, and Science News*, 2019. [Online]. Available: https://spectrum.ieee.org/energywise/energy/the-smarter-grid/transmission-failure-causes-nationwide-blackout-in-argentina

[130] U.S. Energy Information Administration, "Extreme winter weather is disrupting energy supply and demand, particularly in Texas," *Today in Energy*, Feb. 2021. [Online]. Available: https://www.eia.gov/todayinenergy/detail.php?id=46836

[131] G. H. Kjølle, O. Gjerde, and M. Hofmann, "Vulnerability and security in a changing power system," SINTEF Energy Research, Trondheim, Norway, Technical Report TR A7278, Jul. 2013. [Online]. Available: https://sintef.brage.unit.no/sintef-xmlui/bitstream/handle/11250/2598690/TR%2bA7278.pdf?sequence=2&isAllowed=y

[132] E. Allen, G. Andersson, A. Berizzi, S. Boroczky, C. Canizares, Q. Chen, S. Corsi, J. Dagle, A. Danell, I. Dobson, R. Farmer, P. Gomes, N. Hatziargyriou, J. F. Hauer, S. Imai, C. Jiang, P. Kundur, S. Larsson, J. D. McCalley, and W. Wong, *Blackout Experiences and Lessons, Best Practices for System Dynamic Performance, and the Role of New Technologies.* IEEE, 2007.

[133] S. Larsson and A. Danell, "The black-out in southern Sweden and eastern Denmark, September 23, 2003." in *2006 IEEE PES Power Systems Conference and Exposition.* IEEE, 2006, pp. 309–313. [Online]. Available: http://ieeexplore.ieee.org/document/4075763/

[134] Eurelectric, "Impacts of Severe Storms on Electric Grids," EURELECTRIC - Task Force on Power Outages, Brussels, Belgium, Tech. Rep. Ref : 2006-181-0001, Jan. 2006. [Online]. Available: https://web.archive.org/web/20130921054333/http://www.globalregulatorynetwork.org/Resources/ImpactsofSevereStorms.pdf

[135] J. Barkans and D. Zalostiba, "Blackout Prevention and Power System Self-Restoration," in *EUROCON 2007 - The International Conference on "Computer as a Tool".* Warsaw, Poland: IEEE, 2007, pp. 1547–1554. [Online]. Available: http://ieeexplore.ieee.org/document/4400262/

[136] D. Johnson, "The triangular distribution as a proxy for the beta distribution in risk analysis," *Journal of the Royal Statistical Society Series D: The Statistician*, vol. 46, no. 3, pp. 387–398, sep 1997.

Publications

Paper I

Cite as:
E. S. Kiel, G. H. Kjølle
"Transmission line unavailability due to correlated threat exposure"
2019 IEEE Milan PowerTech conference proceedings, jun 2019
DOI: 10.1109/PTC.2019.8810845
URL: `https://doi.org/10.1109/PTC.2019.8810845`

Co-author declaration:
The publication was conceptualized by the candidate, who was the main contributor to the literary review, methodology, writing of associated computer programs and visualizations, as well as the analysis of the results. This was done with contributions from the second author in the form of supervision, discussions and input on prepared material. The candidate produced an original draft, and incorporated review comments and editing.

Transmission line unavailability due to correlated threat exposure

Erlend Sandø Kiel
Department of Electric Power Engineering
NTNU - Norwegian University of Science and Technology
Trondheim, Norway
erlend.kiel@ntnu.no

Gerd Hovin Kjølle
Department of Electric Power Engineering
SINTEF Energy Research/NTNU
Trondheim, Norway

***Abstract*—Blackouts in the power system are rare events that can have large consequences for society. Successful preparation and prevention of such events calls for models capable of predicting their occurrence. The simultaneous outage of multiple components is of special interest in an N-1 secure transmission grid. Spatio-temporal correlation in probability of failure for components can cause blackouts to occur more often than anticipated. This paper demonstrates a new method of calculating time-series of component unavailability due to external threats based on historical data. The time-series of unavailability can be used to predict the expected occurrence of contingencies throughout the year. A test case is presented where an hourly time series of wind dependent failure probabilities and historical outage durations of transmission lines are combined to illustrate the proposed method. The results show that the simultaneous unavailability of multiple transmission lines may be significantly larger than estimated using traditional reliability analysis.**

***Index Terms*—Power system reliability, resilience, risk analysis.**

I. Introduction

The electrical power system is a highly complex, critical infrastructure on which society depends. Blackouts are rare but with potentially severe consequences, and due to these properties they are sometimes referred to as High Impact Low Probability (HILP) events. In an N-1 secure transmission grid multiple contingencies, or failure of multiple components, must occur in overlapping time-frames to cause blackouts. Harsh weather, such as wind, lightning and icing are some of the most common causes of transmission line failures and subsequent blackouts [1], [2]. Such events often occur in short and intense periods of weather exposure such as severe storms [3]. The overlap in time and place of failures due to correlated threats is of high importance. The timing of when a contingency occurs can also affect the associated consequences. Thus, it is necessary to develop models that capture spatio-temporal correlation in threat exposure.

Capturing HILP events using traditional power system reliability methods can be difficult. The emerging field of power systems resilience methodology goes beyond traditional reliability assessments and aim to capture such low probability events [3]. Although there are no commonly accepted definition of resilience in the power systems domain, a proposed definition is found in [4] as "the ability to withstand and reduce the magnitude and/or duration of disruptive events, which includes the capability to anticipate, absorb, adapt to, and/or rapidly recover from such an event". In [5], it is argued that "a main difference between a reliable power grid and a resilient power grid is that, in the latter, low probability-high consequence events (e.g. extreme weather events) are specifically considered and handled, with the ability to learn from past occurrences".

The two main paths to capture spatio-temporal correlaction in threat exposure has either been to use Monte Carlo simulation techniques or contingency enumeration approaches, considering multiple weather states [6], [7]. It has been considered that for single contingency events, contingency enumeration may be best suited, however for more complex systems and higher order contingencies Monte Carlo simulation techniques may produce better results [8]–[10].

This paper proposes a method of calculating time-series of unavailability probability of transmission lines based on historical data, and can serve as an alternative to Sequential Monte Carlo simulations. The probability of higher order contingencies can be calculated from the time-series unavailability of single components. The method answers two of the set of risk-triplets put forwards by Kaplan [11], namely what can happen (the scenario) and how likely is it that this scenario happens (likelihood). However, by also knowing the 'when' of the scenario, it is possible to make some inferences of the last of the triplets: the consequence of the scenario.

The main contribution of this article is to calculate time-series of probability of contingencies occurring due to threats that are spatio-temporally correlated. It is also a benefit that each primary parameter in the analysis - the failure rate and outage duration - can be analyzed separately before being combined into an expected unavailability of components. The production of historical time series of unavailability makes it possible to couple the analysis with other time-dependent information, for example measures of consequence of a given contingency in a specific period of time. The method is transparent and the resulting data can form the basis for

The research leading to these results has received funding through the project "Analysis of extraordinary events in power systems" (HILP) (Grant No. 255226), co-funded by the Research Council of Norway, Statnett and Fingrid.

further analysis, or serve as a benchmark when developing other methods for predicting HILP events. The method is exemplified for transmission lines using wind dependent failure- and outage durations, as they are well known to contribute to failure bunching effects in the power system [10], [12]. Results from the analysis can be used, for example, to prioritize maintenance and repair, strengthening of system components, rerouting or undergrounding transmission lines, or improvement of emergency and preparedness plans [10].

The rest of the paper is structured as follows: Section II defines central terms and introduces the practical implementation of the method such as the inclusion of failure rates, outage duration curves and the calculation of unavailability of transmission lines. In Section III, a sample case study on a 4-bus test system is presented to show the relevance of the method, before the paper is concluded in Section IV.

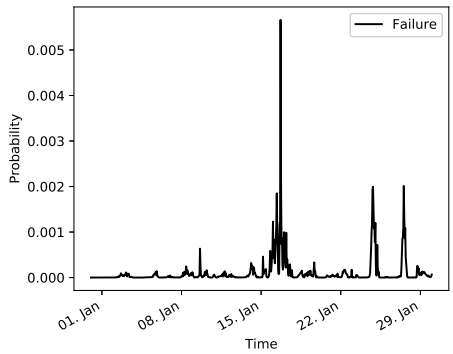

Fig. 1. Hourly probability of line failure. Sample.

II. Method

The proposed method calculates the expected instantaneous unavailability of transmission lines. The method is exemplified using unplanned transmission line outages due to wind, although the approach can be applied to other components that are subject to spatio-temporally correlated threats. Instantaneous unavailability can be defined as the "probability that an item is not in a state to perform as required at a given instant" [13], where "a given instant" is here understood as the time-scale granularity of the analysis, which is set to one hour in this example. Instantaneous unavailability will from now on simply be referred to as unavailability.

The method consists of three different steps. Initially, a time series of failure probabilities of transmission lines due to wind exposure is either created or served as an input into the analysis. Probability distributions of outage durations are then parameterized using historical data. These outage distributions are then combined with failure probabilities to create a measure of unavailability of transmission lines.

A. Failure probabilities

Time series of hourly failure probabilities can be calculated in a number of ways, depending on data availability and need for accuracy. For weather related phenomena, the combined use of historical failure data and weather conditions as seen in [14], [15] can be of great help to capture historical susceptibility to given threats, as well as failure bunching effects.

Time-series of hourly wind dependent failure probabilities are generated according to the method of [14], with Bayesian updating of failure rates and fragility curve estimation based on historical failure and wind exposure. Initially, unique annual failure rates for each line is calculated by doing a Bayesian updating using the historical average failure rate due to wind of all comparable lines in the system, and actual failures due to wind for individual lines in a given time-span. A fragility curve is then fitted to a wind exposure measure for each line segment to distribute the failures in time, before the probability of failure for each line is calculated as a series system of failure probability of its line segments. The calculated annual failure rate after curve fitting is held equal to the annual failure rate found by Bayesian updating in the previous step to maintain consistency. The weather data used to calculate wind exposure of line segments is historical hourly wind speeds in a 1 kilometer grid based on [16]. A more detailed description of how to construct the time-series of failure probabilities can be found in [14].

In this paper a slight alteration of the original method is done. The fragility curve is not cut off at a lower wind-speed limit. The relatively low probability of failure at the low end of the fragility curve matches well with the historical percentage of failures occurring below 15 m/s wind-speeds at about 20 percent [17], which is the justification of this alteration. A sample of the calculated hourly failure probabilities due to wind exposure for one line can be seen in Fig. 1, showing the hourly probability of failure for a transmission line due to wind exposure.

B. Outage duration

Events caused by natural hazards are also associated with longer outage durations due to mechanical damage or limitation to accessibility for repairs [1], [18]. The aim of the following subsection is to create an outage duration curve that represents the probability of a component still being out of operation a given number of hours following a failure caused by wind exposure.

Outage duration curves is constructed using data from the Norwegian fault and disturbance database, FASIT [17], [19]. The database contains information on historical failures of components, delivery point interruptions, and restoration and repair times. Outage duration is here understood as the time from a failure occurs until the component is again ready for operation and covers both temporary and permanent failures.

The outage durations due to wind exposure from the FASIT data show a right skewed distribution of outage durations as shown in the histogram in Fig. 2. Other sources of outage and repair statistics show similar patterns [20], [21]. The two-parameter log-normal distribution is a good choice to represent

the data, which is in line with what was found by [20]. The log-normal distribution is given by (1), where $f(r)$ is the probability density function (PDF) of the distribution of outage durations of r hours.

$$f(r) = \frac{1}{r\sigma\sqrt{2\pi}} e^{-\frac{(ln(r)-\mu)^2}{2\sigma^2}} \tag{1}$$

The moments found from the FASIT data are then used to fit a log-normal PDF of outage duration by modifying the equations for the mean and variance. The method of moments approach is used to ensure that the mean and variance found in the data is maintained. The mean (2) and variance (3) of the outage duration data is used to fit the parameters of the log-normal distribution in (4) and (5). D represents the random variable of outage duration, while d_i represents the unique outage duration observations in hours.

$$E(D) = \frac{1}{n}\sum_{i=1}^{n} d_i \tag{2}$$

$$Var(D) = \frac{\sum_{i=1}^{n}(d_i - E(D))^2}{n-1} \tag{3}$$

$$\mu = ln\left[\frac{E(D)^2}{\sqrt{Var(D)+E(D)^2}}\right] \tag{4}$$

$$\sigma = \sqrt{ln\left[1+\frac{Var(D)}{E(D)^2}\right]} \tag{5}$$

Furthermore, we want to know the probability that a component has not been restored by a given time, x. This can be found through the survival function (SF) of the distribution. The survival function $S(x)$ is the complement of the cumulative distribution function (CDF) denoted $F(x)$, and can be expressed as in (6).

$$S(x) = 1 - F(x) = 1 - \int_0^x f(r)dr \tag{6}$$

The function now describes the probability that a component is in a failed state for a given number of hours after a failure event. The original outage duration data and the fitted distribution can be seen in Fig. 2. However, the outage duration function is a continuous distribution while the time-series is in one-hour intervals. To account for this, the approximate mean value of each time-step is calculated using the trapezoidal rule.

C. Unavailability probability

When failure probabilities are combined with outage duration probabilities, we get a measure of probability of the line being unavailable at a given time. Unavailability is calculated algorithmically by looping through failure probability time-series and applying the outage probability functions. The logic behind the approach is best illustrated in pseudo-code, seen in Algorithm 1. After looping through all time-steps, an approximation of the expected unavailability of the transmission line at a given time is achieved. The algorithm shows only the calculation of unavailability for a single transmission line but can be repeatedly applied to any number of components.

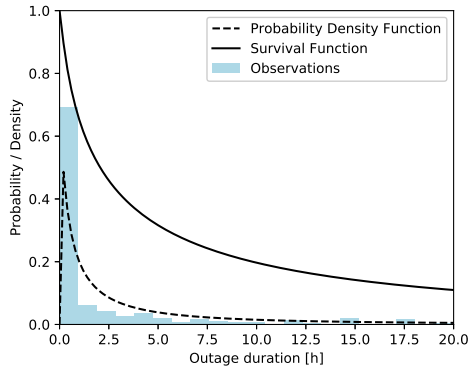

Fig. 2. Observed outage duration of power lines (132-420kV) 2006-2016.

The algorithm appends the expected unavailability at time t to a given number of time-steps x ahead of time up until a given cutoff, taking into account the probability that the line is already unavailable due to a previous failure. The cutoff in forward looking time-steps is a trade-off between computational efficiency and accuracy, and is set to 1000 hours after the failure in this example.

To correct for the accuracy impact of the chosen 1000 hour cutoff, we need to compare the area under the SF-curve when considering the integration of the curve towards infinity versus an upper bound of 1000 hours. For the former, the alternative expectation formula (see e.g. [22]) is used, which states that the integral from zero to infinity of the SF for a continuous non-negative random variable equals the expected value of the distribution (7). For the latter, numerical integration is used to approximate the area under the curve. The ratio of these two areas, k in (8), can then be used to inflate numbers before the cutoff. This ensures that the sum of outage duration is kept the same as without a cutoff.

$$E(X) = \int_0^\infty [1 - F(x)]dx \tag{7}$$

$$\frac{E(D)}{\int_0^{1000}[1-F(x)]dx} = k \tag{8}$$

The result of running the algorithm is given in Fig. 3, which shows the hourly expected unavailability due to wind for a single transmission line using the proposed method. The figure is based on the failure probabilities found in Fig. 1 and outage duration curve in Fig. 2.

Algorithm 1 Algorithm for calculating unavailability

Input: time-series of t failure probabilities
Output: time-series of t unavailability probabilities
Initialisation:
$p_t \leftarrow$ failure probability at time t
$S(x) \leftarrow$ outage survival function at time x since failure
$u_t \leftarrow$ unavailability probability at time t
cutoff $\leftarrow$ limit to forward propagating time-steps
$k \leftarrow$ inflation factor due to cutoff
LOOP Process:
for all increasing time steps t **do**
  for x in $range(0, cutoff)$ **do**
    $u_{t+x} += p_t \cdot (1 - u_t) \cdot S(x) \cdot k$
  end for
end for
return u_t

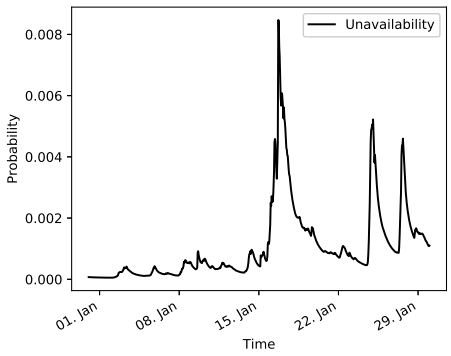

Fig. 3. Hourly probability of line unavailability. Sample.

III. Sample case

The goal of this approach is to better capture spatio-temporal correlations in unavailability due to weather. A test case is presented to exemplify. Unavailability is calculated using both the proposed method, and a traditional analytical method paired with a contingency enumeration approach [23] as the base case. The results are then compared.

A 4-bus test network, given in [24], presented in [25], is used to illustrate the test case. The 4-bus test network can be seen in Fig. 4. Every line in the test-network is given a capacity of 135 MW. Both generators have the capacity to cover all demand on their own. Load point 1 (L1) is the prioritized load point due to a higher cost of Energy Not Supplied (ENS). Only minimal cutsets are enumerated. Two operating states (OS) are considered, a high- and a light-load state, which have their own minimal cuts. The high demand state (OS2) covers the months December, January and February, while the light-load state (OS1) covers the remaining months.

A divergence from the original test case is that individual reliability input data for overhead transmission lines in the test network is calculated, based on historical weather and outage durations. This is done to ensure that the same mean values are used in both the base case and the proposed method. The modified rating and reliability data is given in Table I. The delivery point load demand for the different operating states are given in Table II. Minimal cut-sets (MC) are associated with an interrupted power (P_{interr}) at specific delivery points (DP) in different operating states (OS), given in Table III.

The base case is a contingency enumeration approach using average failure rates and outage durations as input to the evaluation of the unavailability of the components. Approximate methods are used to calculate equivalent failure rates, outage durations and unavailability for higher order contingencies. Equations for this can be found in any number of reliability textbooks, see e.g. [26]. Expected annual unavailability for each operating state and delivery point is calculated as the product of the annual failure rate and outage duration weighted according to the duration of each operating state, exemplified

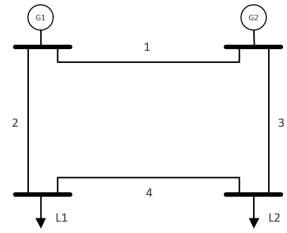

Fig. 4. 4-bus OPAL network [24].

TABLE I
Modified rating and reliability data, transmission lines

Line	Rating [MW]	Failure rate [failures/year]	Outage time [hours/failure]
1	135	0.118	11.42
2	135	0.375	11.42
3	135	0.069	11.42
4	135	0.229	11.42

TABLE II
Delivery point load demand

DP	Light load (OS1) [MW]	Heavy load (OS2) [MW]
L1	60	100
L2	30	75

TABLE III
Interrupted power [MW] due to minimal cutsets (MC)

	Light load (OS1)		Heavy load (OS2)	
MC\DP	L1	L2	L1	L2
{*2*}	-	-	-	40
{*3*}	-	-	-	40
{*2,3*}	60	30	100	-
{*2,4*}	60	-	100	-
{*3,4*}	-	30	-	-

in (9) for OS1 (9 out of 12 months). Expected Annual ENS (AENS) is calculated as in (10).

$$U_{MC,OS1} = \lambda_{MC} \cdot r_{MC} \cdot \frac{9}{12} \tag{9}$$

$$AENS_{MC,OS,DP} = U_{MC,OS} \cdot P_{interr,MC,OS,DP} \tag{10}$$

The proposed method relies on the same minimal cutsets and power interrupted, and has the same average failure rates and outage times as the base case. However, the input to the reliability evaluation is time series of failure probabilities and distributions of outage durations. Time series of hourly unavailability covering 25 years of observations for four transmission lines is constructed using historical weather data and outage durations. Single line contingencies are calculated using the proposed algorithm. The correlation of failure probabilities between lines are given in Table IV. Higher order contingencies can be calculated as a system of independent components in parallel (see e.g. [27]) given the weather exposure. The expected unavailability of the resulting time series, u_t, in the months of the different operating states can be summed up and adjusted for the number of years of observations, y, to find annual unavailability of the cutsets in the associated operating states, as seen in (11).

$$U_{OS} = \frac{\sum_{t=1,t\in OS}^{n} u_t}{y} \tag{11}$$

TABLE IV
CORRELATION OF FAILURE PROBABILITIES BETWEEN LINES

		Line			
		1	*2*	*3*	*4*
Line	*1*	1.00	0.74	0.17	0.60
	2	0.74	1.00	0.11	0.57
	3	0.17	0.11	1.00	0.21
	4	0.60	0.57	0.21	1.00

The calculated expected annual unavailability and AENS are compared in the different approaches. Single line unavailability can be seen in Fig. 5. Numbers in bars represent the percentage difference in unavailability when comparing the proposed method to the base case for each operating state. Although single line contingencies occur with the same expected number of hours each year in the two approaches, the displacement of when unavailability occurs has an effect on ENS, as single line contingencies only cause ENS in OS2. The difference in ENS as a result of this displacement can be observed in Table V. ENS during OS2 for line 2 and 3 is 82% and 79% higher respectively, using the proposed method than in the base case. This is a reflection of harsher weather during the winter months which is more accurately captured by the time-series unavailability in the proposed method.

Spatio-temporal correlations and the associated failure bunching come into play for second order contingencies. The total unavailability of second order contingencies have notably lower estimates during the winter months in the base case compared to the proposed method, especially when failure

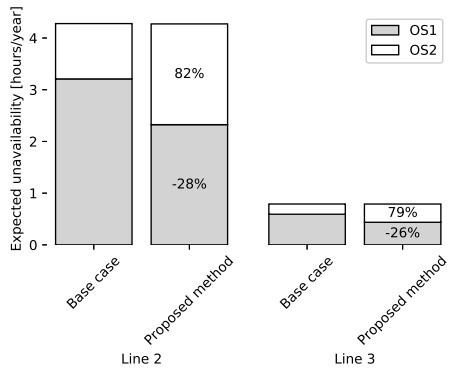

Fig. 5. Single line unavailability in different operating states.

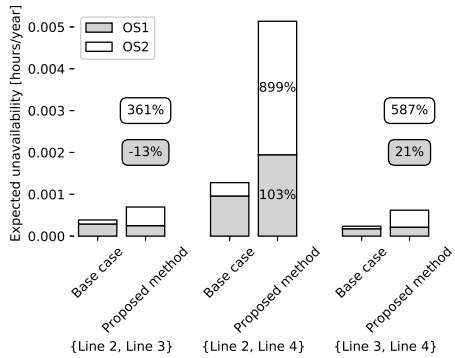

Fig. 6. Unavailability due to second order contingencies

probabilities are highly correlated. Results in Fig. 6 illustrate this: Unavailability of the minimal cutset lines 2 and 4 due to wind in OS2 is 899% higher than in the base case, and the annual ENS is 387% higher. The reason for this increase is two-fold. First, the hourly average expected unavailability is higher during the winter months in this sample. Secondly, periods of high expected unavailability for the two components coincide due to spatio-temporal correlation in weather exposure for this cutset, thus causing the product of the two probabilities to sum to larger values than if this was not the case. This effect is not captured by the base case method.

Single line contingencies dominate the expected annual unavailability and ENS, compared to the second order contingencies. However, the effects of higher order contingencies are more relevant to consider in a N-1 secure transmission grid. The difference in expected annual unavailability and ENS is 239% and 290% higher, respectively, compared with the base case for second order contingencies.

TABLE V
SUMMARY RESULTS

	Base case	Proposed method	Δ
Unavailability [h/y]			
Line 2	4.2789	4.2726	0 %
Line 3	0.7901	0.7897	0 %
Line 2 Line 3	0.0004	0.0007	80 %
Line 2 Line 4	0.0013	0.0051	302 %
Line 3 Line 4	0.0002	0.0006	163 %
Single lines	5.0689	5.0623	0 %
2nd order contingencies	0.0019	0.0065	239 %
Total	5.0708	5.0687	0 %
AENS [MWh/y]			
Line 2	42.7886	77.9177	82 %
Line 3	7.9005	14.1269	79 %
Line 2 Line 3	0.0357	0.0670	88 %
Line 2 Line 4	0.0895	0.4358	387 %
Line 3 Line 4	0.0053	0.0064	21 %
Single lines	50.6891	92.0445	82 %
2nd order contingencies	0.1305	0.5093	290 %
Total	50.8195	92.5538	82 %

IV. CONCLUSION

In this paper we have developed a method of calculating time-series unavailability of components in the electrical transmission system due to external threats that exhibit spatio-temporal correlation. The solution is exemplified in a test case, which shows that the proposed method captures spatio-temporal correlation in threat exposure more accurately than the base case method. When combining the time-series output of expected unavailability with a consequence analyses we get a more complete view of the associated risks. In the test case, this results in an almost four times higher AENS due to a second order cutset with highly correlated wind exposure.

The proposed method must make a trade-off between the need for accuracy and computational efficiency, and as a consequence it relies on several approximations in distributing outage durations in time. However, comparison of single line contingencies show that there are small differences in annual expected unavailability in the approaches, which indicates that the effects of the approximations are limited. It can be argued that the benefits of capturing the spatio-temporal correlations in the analysis of higher order contingencies outweighs the negative impact of these approximations.

By identifying lines that has a high impact on a given consequence metric, such as ENS, in conjunction with other lines, strengthening measures can be prioritized and initiated on lines that have the greatest consequence reducing effects. The proposed method is a useful approach that may contribute to reducing the probability of HILP events and thereby, to a more resilient grid.

REFERENCES

[1] Y. Wang, C. Chen, J. Wang, and R. Baldick, "Research on Resilience of Power Systems Under Natural Disasters—A Review," *IEEE Transactions on Power Systems*, vol. 31, no. 2, pp. 1604–1613, Mar. 2016.

[2] E. Bompard, T. Huang, Y. Wu, and M. Cremenescu, "Classification and trend analysis of threats origins to the security of power systems," *International Journal of Electrical Power & Energy Systems*, vol. 50, pp. 50–64, Sep. 2013.

[3] M. Panteli, P. Mancarella, D. Trakas, E. Kyriakides, and N. Hatziargyriou, "Metrics and quantification of operational and infrastructure resilience in power systems," *IEEE Transactions on Power Systems*, vol. 32, no. 6, pp. 4732–4742, 2017.

[4] A. Stankovic, "The Definition and Quantification of Resilience," IEEE PES Industry Tech. Support Task Force, Tech. Rep. PES-TR65, 2018.

[5] R. Rocchetta, E. Zio, and E. Patelli, "A power-flow emulator approach for resilience assessment of repairable power grids subject to weather-induced failures and data deficiency," *Applied Energy*, vol. 210, pp. 339–350, Jan. 2018.

[6] GARPUR, "D1.1 State of the art on reliability assessment in power systems," SINTEF Energi AS, Tech. Rep. 608540, Mar. 2014.

[7] R. Billinton, C. Wu, and G. Singh, "Extreme adverse weather modeling in transmission and distribution system reliability evaluation," in *PSCC*, Sevilla, 2002.

[8] A. M. Rei, M. T. Schilling, and A. C. G. Melo, "Monte Carlo Simulation and Contingency Enumeration in Bulk Power Systems Reliability Assessment," in *PMAPS*, Stockholm, 2006.

[9] M. Panteli and P. Mancarella, "Influence of extreme weather and climate change on the resilience of power systems: Impacts and possible mitigation strategies," *Electric Power Systems Research*, vol. 127, pp. 259–270, Oct. 2015.

[10] M. Panteli and P. Mancarella, "Modeling and Evaluating the Resilience of Critical Electrical Power Infrastructure to Extreme Weather Events," *IEEE Systems Journal*, vol. PP, no. 99, pp. 1–10, 2015.

[11] S. Kaplan and B. J. Garrick, "On The Quantitative Definition of Risk," *Risk Analysis*, vol. 1, no. 1, pp. 11–27, Mar. 1981.

[12] R. Billinton, G. Singh, and J. Acharya, "Failure Bunching Phenomena in Electric Power Transmission Systems," *Proceedings of the Institution of Mechanical Engineers, Part O: Journal of Risk and Reliability*, vol. 220, no. 1, pp. 1–7, Jan. 2006.

[13] International Electrotechnical Commission, "International Electrotechnical Vocabulary. IEV number 192-08-04."

[14] Ø. R. Solheim, G. Kjølle, and T. Trötscher, "Wind dependent failure rates for overhead transmission lines using reanalysis data and a Bayesian updating scheme," in *PMAPS*, Beijing, 2016.

[15] Ø. R. Solheim and T. Trötscher, "Modelling transmission line failures due to lightning using reanalysis data and a Bayesian updating scheme," in *PMAPS*, Boise, 2018.

[16] Kjeller Vindteknikk, "Long-term data series, WRF ERA-Interim." [Online]. Available: http://www.vindteknikk.com/services/analyses/wind-power/pre-construction/long-term-series-2

[17] G. Kjølle, A. O. Eggen, H. M. Vefsnmo, J. Heggset, A. Bostad, T. Trötscher, and Ø. R. Solheim, "Norwegian disturbance management system and database," in *CIGRE, Session Proceedings 2016*, Paris, 2016.

[18] E. Hillberg, "Perception, Prediction and Prevention of Extraordinary Events in the Power System," Doctoral Theses, Norwegian University of Science and Technology, Trondheim, Norway, Jan. 2016.

[19] J. Heggset, G. Kjolle, and K. Sagen, "FASIT - a tool for collection, calculation and reporting of reliability data," in *IET Conference Publications*. Prague, Czech Republic: IET, 2009, pp. 716–716.

[20] A. Arif and Z. Wang, "Distribution Network Outage Data Analysis and Repair Time Prediction Using Deep Learning," in *PMAPS*, Boise, 2018.

[21] B. Shen, D. Koval, and S. Shen, "Modelling extreme-weather-related transmission line outages," in *1999 IEEE Canadian Conference on Electrical and Computer Engineering*, vol. 3. Edmonton, Alta., Canada: IEEE, 1999, pp. 1271–1276.

[22] S. Chakraborti, F. Jardim, and E. Epprecht, "Higher-Order Moments Using the Survival Function: The Alternative Expectation Formula," *The American Statistician*, pp. 1–4, Jul. 2017.

[23] O. Gjerde, G. Kjølle, S. H. Jakobsen, and V. V. Vadlamudi, "Enhanced method for reliability of supply assessment - an integrated approach," in *PSCC*. IEEE, 2016.

[24] G. Kjølle and O. Gjerde, "The OPAL methodology for reliability analysis of power systems," SINTEF Energy Research, Technical Report TR A7175, Jul. 2012.

[25] G. H. Kjølle, I. B. Sperstad, and S. H. Jakobsen, "Interruption costs and time dependencies in quality of supply regulation," in *PMAPS*, Durham, 2014.

[26] R. Billinton and R. N. Allan, *Reliability Evaluation of Power Systems*, 2nd ed. New York, NY, USA: Plenum Press, 1996.

[27] M. Rausand and A. Høyland, *System reliability theory: models, statistical methods, and applications*, 2nd ed., ser. Wiley series in probability and statistics. Hoboken, NJ: Wiley-Interscience, 2004.

Paper II

Cite as:
E. S. Kiel, G. H. Kjølle
"Reliability of Supply and the Impact of Weather Exposure and Protection System Failures"
Applied Sciences 11, no. 1 (2021): 182.
DOI: 10.3390/app11010182
URL: `https://doi.org/10.3390/app11010182`

Co-author declaration:
The publication was conceptualized by the candidate, who was the main contributor to the literary review, methodology, writing of associated computer programs and visualizations, as well as the analysis of the results. This was done with contributions from the second author in the form of supervision, discussions and input on prepared material. The candidate produced an original draft, and incorporated review comments and editing.

applied sciences

MDPI

Article

Reliability of Supply and the Impact of Weather Exposure and Protection System Failures †

Erlend Sandø Kiel [1,*] and Gerd Hovin Kjølle [2]

[1] Department of Electric Power Engineering, Faculty of Information Technology and Electrical Engineering, Norwegian University of Science and Technology (NTNU), 7491 Trondheim, Norway
[2] SINTEF Energy Research, 7034 Trondheim, Norway; gerd.kjolle@sintef.no
* Correspondence: erlend.kiel@ntnu.no

† This paper is an extended version of our paper published in 2019 IEEE International Conference on Environment and Electrical Engineering and 2019 IEEE Industrial and Commercial Power Systems Europe (EEEIC/I&CPS Europe), Genova, Italy, 13 June 2019.

Abstract: Extreme weather is known to cause failure bunching in electrical transmission systems. However, protection systems can also contribute to the worsening of the system state through various failure modes—spontaneous, missing or unwanted operation. The latter two types of failures only occur when an initial failure has happened, and thus are more likely to happen when the probability of failure of transmission lines is high, such as in an extreme weather scenario. This causes an exacerbation of failure bunching effects, increasing the risk of blackouts, or High Impact Low Probability (HILP) events. This paper describes a method to model transmission line failure rates, considering both protection system reliability and extreme weather exposure. A case study is presented using the IEEE 24 bus Reliability Test System (RTS) test system. The case study, using both an approximate method as well as a time-series approach to calculate reliability indices, demonstrates both a compact generalization of including protection system failures in reliability analysis, as well as the interaction between weather exposure and protection system failures and its impact on power system reliability indices. The results show that the inclusion of protection system failures can have a large impact on the estimated occurrence of higher order contingencies for adjacent lines, especially for lines with correlated weather exposure.

Keywords: protection systems; failure bunching; extreme weather; reliability; HILP; extraordinary events

Citation: Kiel, E.S.; Kjølle, G.H. Reliability of Supply and the Impact of Weather Exposure and Protection System Failures. *Appl. Sci.* **2021**, *11*, 182. https://dx.doi.org/10.3390/app11010182

Received: 20 November 2020
Accepted: 23 December 2020
Published: 27 December 2020

1. Introduction

Society is dependent on a reliable supply of electricity for its normal operation, and thus power outages can have severe consequences. Major blackouts are often due to multiple component outages, caused by environmental factors [1–5], and/or dependent failures such as protection system failures [6]. The increased probability of failure of one or more components in a short period of time due to extreme weather has been termed failure bunching, and models have been developed to capture such effects in power system reliability studies by using both analytical methods and Monte Carlo simulation methods [7–10]. Large blackouts are often a consequence of complex series of events, such as cascading failures [11]. A distinction in the structure of cascading blackouts is made in [12] between a triggering event, which can be simple component failure(s), and generation of propagating events, caused by preceding events and a change in the power system state.

One of the causes of propagating events is the misoperation of protection systems [4,11,13]. Overlapping outages of highly reliable components, whose probability is the product of the individual component outage probabilities, can be rather small even if their individual probabilities are relatively high. Dependent failures, such as protection system failures, can however lead to the same set of simultaneous component outages with a much higher probability than

what the simultaneous independent outages might suggest [14]. This will in turn increase the risk of the scenario, as a function of its probability and consequence [15]. Previous studies have shown how protection system failures can have a significant impact on system reliability evaluation [16,17]. Combining the effects of failure bunching with protection system failures may give more realistic picture of the power system reliability assessment.

The hypothesis in this paper is that the combination of failure bunching effects and protection system failures will increase the risk of blackout events. To the best of our knowledge, this hypothesis was not investigated before in a quantifiable manner with respect to system reliability. The goal of this paper is to carry out investigations to verify the proposed hypothesis. The unique contributions made in this paper are as follows: A generalized compact system of equations using graph theory has been formulated to quantify the impact of protection system failures on power system reliability, based on [17]. Graph theory helps establish a systematic identification of propagation of transmission line failures due to misoperation of protection systems. These equations are then used to incorporate the effects of failure bunching due to harsh weather on the system reliability. Subsequently, these equations are applied to time-series of failure probability of transmission lines specifically due to wind conditions. It should be noted that the procedure is not only applicable to wind-dependent threats but can be used with any time-varying threats, e.g., due to other weather conditions.

The paper is structured as follows: In Section 2, previous work on failure bunching effects and protection system reliability is presented, together with a short review of graph theory and its use in this study of power systems reliability. In Section 3, a general and compact method for calculating reliability indices including protection system misoperations is presented, using both approximate methods and a time-series method. Section 4 presents a case study where the method is applied, before the paper is concluded in Section 5. This paper is an extension of the work presented in [18], incorporating an extended literature review, updated equations, calculation of unavailability for the time-series method, additional illustrations as well as an extended case study and results.

2. Failure Bunching and Protection System Failures

Harsh weather has long been known to cause common cause failures within short periods of time, often termed failure bunching. One way of incorporating such effects is to use multi-state Markov models or similar approximate methods when calculating reliability, another is to utilize Monte Carlo simulation techniques [3,19,20]. In [19], the effect of failure bunching due to wind exposure is captured using historical failure data and a Bayesian updating scheme to estimate annual wind dependent failure rates of transmission lines. The annual failure rate is then spread out in time by combining fragility curve modeling and a dataset of historical wind speeds for the lines in question. This results in hourly time-series of wind dependent failure probability for the lines. This approach has been applied to create similar time-series of failure probability due to other weather effects such as icing and lightning, which is further used together with a Monte Carlo-based tool to calculate system consequences in terms of interrupted power and interruption costs in [21].

In [10] an analytical technique is used to calculate time-series of expected unavailability of transmission lines due to wind conditions, instead of using a Monte Carlo approach. For each hour, the probability of failure of the transmission line is paired with a distribution of outage duration. An iterative algorithm then appends the probability of the component being unavailable due to a failure at a specific time for a given number of hours ahead in time. A contingency enumeration approach, defining outage combinations as cut-set structures [22,23] is used together with the time-series of expected unavailability of transmission lines to calculate annual Energy Not Supplied (ENS) for the system.

In this paper, a failure of a component is understood as a loss of ability to perform as required, leading to a fault, where the former is understood as an event, while the latter is understood as a state [24]. An outage is understood as the loss of ability of a component to deliver power, which may or may not cause an interruption of service to customers [25].

A contingency is understood as an outage occurrence of a single system component, or the concurrent outage of two or more system components [24]. A set is sometimes used interchangeably with a contingency. A cut-set is understood as a contingency which causes end-user consequences in terms of interrupted power. A cut-set is said to be minimal if the set cannot be reduced without loosing its status as a cut-set [26].

Protection systems are expected to be both dependable and secure [6,17]. Missing operation of the protection system occurs if it fails to react appropriately to a situation it is designed to respond to and would be a shortfall of the dependability of the system. Similarly would an unwanted operation occur if the protection system reacts to conditions it is not designed to react to, and is a shortfall of the security of the system [17]. This corresponds to the protection system misoperation types defined in [27]. Protection systems have previously been incorporated in power systems reliability analysis in multiple ways, such as through Markov models [14,16] and approximate methods [17,28].

Dependability and security were the basis in [17] to construct different scenarios in which protection system reliability can cause a transmission line to be isolated from the network. This gave rise to four fault types [17]: Fault type 1 (FT1) is the failure rate of the transmission line in focus. Fault type 2 (FT2) represents failures due to the spontaneous unwanted operation of a line's own protection system. Fault type 3 (FT3) is explained by a situation where a failure occurs on a neighboring line but is not correctly cleared due to missing operation of the neighboring line's protection system, and thus causes the line in focus to be isolated from the system. Fault Type 4 (FT4) is a result of a fault on the neighboring line that is correctly cleared by the neighboring line's protection system but causes an unwanted non-selective tripping of the line in focus. An equivalent failure rate for each line is then constructed as a summation of these four failure type contributions. The method is a contingency enumeration approach, where an approximate system reliability evaluation is used to obtain reliability indices for predefined minimal cut-sets. A more detailed presentation of the approach can be found in [17].

Complex network theory and graph-theoretic approaches have been used in the literature on cascading failures to study the power system, e.g., to identify critical components [29–31]. Protection system failures and misoperation have a propagating effect between components, and it is similarly necessary to consider the adjacency between them. The power system lends itself to a graph-based representation. A graph (G) is an object consisting of an ordered vertex set (V) and edge set (E) joining the vertices through its two connected buses u and v, as seen in (1)–(3), where n is the number of vertices in the graph and m is the number of edges in the graph, see e.g., [32,33]. Intuitively, it is natural to think of buses, b, as vertices and components such as transmission lines, l, as edges when it comes to representing the power system as a graph. An illustrative graph representation of a 4-bus power system following these conventions can be seen in Figure 1.

In the following, the graph-based representation of relationships between components is a useful tool to incorporate protection system failures into power system reliability analysis.

$$G = (V, E) \tag{1}$$

$$V = \{b_1, b_2, \ldots, b_n\} \tag{2}$$

$$E = \{l_1, l_2, \ldots, l_m\} = \{\{u_1, v_1\}, \{u_2, v_2\}, \ldots, \{u_m, v_m\}\} \tag{3}$$

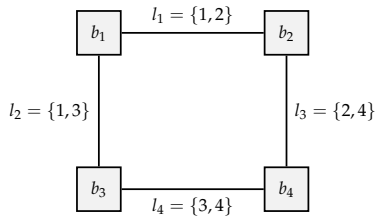

Figure 1. Illustrative graph of a 4-bus power system.

3. Method

In this section, a general and compact method for calculating reliability indices including protection system misoperations is postulated, using both approximate methods and a time-series method, based on the definitions of fault types as originally proposed in [17]. The basis for approximate methods is [34] in Section 3.1, and that for a time-series approach is [10] in Section 3.2.

In power systems, we normally look at buses as vertices and transmission lines as edges. However, the idea behind the proposed methodology in this paper is to see vertices as transmission lines and edges as dependencies. This structure can then be utilized to calculate the contribution to failure rates at a given transmission line, given failures at adjacent lines.

When including protection system failures into the system, we consider two different types of lines in each case: the target line i, for which we wish to calculate the failure rates, and the source line j, which is adjacent to the target line and contributes to the failure rate of the target line through propagation of protection system failures. The target- and source lines are adjacent lines if they are connected to a common bus, as seen in Figure 2. The subscript l is used when it is not specific if the line is a target or a source line.

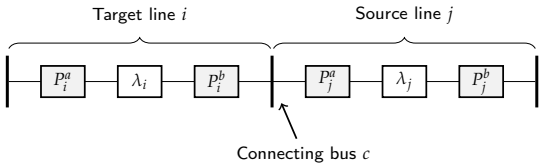

Figure 2. Two adjacent transmission lines, i and j.

A line is associated with a protection system on each end. These are referred to as the a-side and the b-side protection system, represented as the set $s = \{a, b\}$ for simplicity. For a line l, the failure rate of the line λ_l, and the two protection systems, P_l^s are considered. The protection systems have three parameters: (1) a specific annual failure rate, λ_l^s, (2) a conditional probability of missing operation, $p_l^{s,m}$, if the line experiences a failure, and (3) upon a correctly cleared failure of an adjacent line, a conditional probability of unwanted non-selective tripping at the target line, $p_l^{s,u}$. The associated outage duration, r, is denoted with a subscript indicating which line is considered, and a superscript indicating which fault type it is applicable to. All line- and protection system specific information is represented as ordered column vectors.

The primary concern is how misoperation of the protection system of one transmission line can cause an adjacent line to be isolated from the system. The system can initially be considered a graph G, where each edge $l = \{u, v\}$ represents a transmission line, and the buses are represented by vertices, which are unique observations of u and v. Let u represent the a-side connecting bus of a transmission line, and v the b-side connecting bus of the line. An adjacency matrix indicates connections between vertices and is used to represent the system in a form where vertices are transmission lines and edges are directed paths of failure propagation between the lines. An adjacency matrix is constructed for

each side of the source line, A^s in (4), to take into account which side of the source line is connected to the target line. The adjacency matrix is an ordered $l * l$-matrix, where rows represent a target line i and columns represent a source line j. If line j is connected to line i through its s-side, it is marked with a digit 1 in the appropriate element of the matrix, 0 otherwise. Matrices are typeset in uppercase regular font, vectors are typeset in lowercase bold italic, while scalar values such as specific elements of vectors or matrices are typeset with italic fonts.

$$A^s = [a^s_{i,j}] = \begin{bmatrix} a_{1,1} & \dots & a_{1,l} \\ \vdots & \ddots & \vdots \\ a_{l,l} & \dots & a_{l,l} \end{bmatrix} \quad , where: \tag{4}$$

$$a^a_{i,j} = \begin{cases} 1 & \text{if } u_j \in \{u_i, v_i\} \\ 0 & \text{Otherwise} \end{cases}$$

$$a^b_{i,j} = \begin{cases} 1 & \text{if } v_j \in \{u_i, v_i\} \\ 0 & \text{Otherwise} \end{cases}$$

$$s \in \{a, b\}$$
$$i \in \{1, \dots, l\}$$
$$j \in \{1, \dots, l\}$$

The system can now be represented as a transformed graph, where transmission lines are represented as vertices, and directed edges are possible paths of failure propagation due to protection system failures. Figure 3 gives a visual representation of the 4-bus system presented in Figure 1, where the adjacency matrices defines the directed edges between the source line and the target line in the graph.

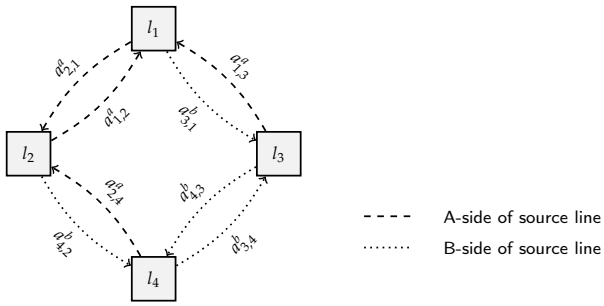

Figure 3. Transformed 4-bus system. Transmission lines as vertices, edges as propagation paths. Labeled edges correspond to elements in the resulting adjacency matrices marked with a digit 1.

The adjacency matrix can then be further modified to incorporate the probability that a failure on a source line will propagate to a target line. From the initial equations in [17], it is clear that only FT3 and FT4 stem from adjacent lines and as such these fault types will receive the primary focus in this paper.

FT3 is related to a failure on an adjacent line, which is not correctly cleared by the adjacent line's protection system. The probability of missing operation of the protection system on the s side for a given line is represented by the column vector $p^{s,m}_l$. A matrix containing the probability that a failure propagates from the source line j to the target line i through the FT3 mechanism is created, named $PT3$, by modifying the adjacency matrix (5).

$$\text{PT3} = \sum_s \left[A^s \cdot \text{diag}(\boldsymbol{p}^{s,m}) \right] \tag{5}$$

PT3 only takes into consideration the properties of line j's protection systems. The same probability matrix for FT4, a failure on the source line causing an unwanted non-selective tripping of the protection systems at the target line, $PT4$, must consider protection system properties of both the target line and the source line. The probability of line j successfully clearing a failure on its own line is included first in (6), followed by the probability of an unwanted non-selective tripping at line i, incorporated through transposing the matrix. Note that the probability of spontaneous unwanted operation is represented by a single column vector since the target line response is considered side-independent, where $p_l^u = P(p_l^{a,u} \cup p_l^{b,u})$.

$$\mathrm{PT4} = \sum_s \left[\left[\mathrm{A}^s \cdot \mathrm{diag}(1 - \boldsymbol{p}^{s,m}) \right]^T \cdot \mathrm{diag}(\boldsymbol{p}^u) \right]^T \tag{6}$$

Matrices representing the probability of different fault types propagating from a source line to a target line have now been established. These can be applied to calculate systems reliability indices for cut-sets. Two methods are presented here: an approximate method of system reliability using annual failure rates including protection system failures, and a method to calculate time series of probability of failure due to different fault types, which can be used together with [10] to calculate unavailability of cut-sets.

3.1. Approximate Method

This approach starts by calculating the equivalent failure rate of each line by considering each line a target line. The equivalent failure rate is calculated based on the failure rate of the line itself (FT1) and its protection systems (FT2), and the fault types FT3 and FT4 propagating from adjacent lines, following the method in [17]. FT1 and FT2 are only dependent on information of the line itself and is repeated for reference here (7) and (8). FT3 and FT4 are calculated by using the associated probability matrices (9) and (10). The multiplication of the matrices with the line failure rate vectors gives vectors of FT3 and FT4 failure rate contributions from all source lines at the target line.

$$\boldsymbol{ft1}_i = \boldsymbol{\lambda}_l \tag{7}$$

$$\boldsymbol{ft2}_i = \sum_s \boldsymbol{\lambda}_l^s \tag{8}$$

$$\boldsymbol{ft3}_i = \mathrm{PT3} \cdot \boldsymbol{\lambda}_l \tag{9}$$

$$\boldsymbol{ft4}_i = \mathrm{PT4} \cdot \boldsymbol{\lambda}_l \tag{10}$$

Equivalent failure rate, incorporating protection system failures is then calculated as λ' in (11).

$$\boldsymbol{\lambda'} = \boldsymbol{ft1} + \boldsymbol{ft2} + \boldsymbol{ft3} + \boldsymbol{ft4} \tag{11}$$

From this, equivalent unavailability and outage durations for all target lines is found in (12) and (13), where the vectors of fault type contributions are paired with vectors of the associated repair or switching times using element-wise Hadamard operations ($\circ$ signifies the Hadamard product, where $c_{ij} = a_{ij} \cdot b_{ij}$, and $\oslash$ is used for Hadamard division, see e.g., [35] for an introduction). A slight adjustment is made when incorporating unavailability due to FT3. As opposed to the other fault types, FT3 is dependent on the switching time at the source line, j, rather than that at the target line i. To include this, the contribution of the unavailability from the source line to target line is carried through the probability matrix for FT3.

$$\boldsymbol{U'} = \boldsymbol{ft1} \circ \boldsymbol{r}^{\boldsymbol{FT1}} + \boldsymbol{ft2} \circ \boldsymbol{r}^{\boldsymbol{FT2}} + \mathrm{PT3} \cdot [\boldsymbol{\lambda} \circ \boldsymbol{r}^{\boldsymbol{FT3}}] + \boldsymbol{ft4} \circ \boldsymbol{r}^{\boldsymbol{FT4}} \tag{12}$$

$$\boldsymbol{r'} = \boldsymbol{U'} \oslash \boldsymbol{\lambda'} \tag{13}$$

Vectors containing reliability indices for single lines are now established. Second order cut-sets involving two lines x and y can now be calculated in a general form, avoiding a distinction in equations between adjacent and non-adjacent lines by utilizing the matrix of adjacency adjusted probabilities. If two lines in a cut-set are adjacent and they experience a FT3 or a FT4 where the source line is the other line in the cut-set, they will both surely be unavailable. This means that these dependent failures should be treated separately from the independent failures. Adjustments for dependent failures between individual lines in the cut-set are created in (14) and (15) before calculating the new expected restoration time of the cut-set due to independent failures in (16).

$$\lambda_x^a = \left(pt3_{x,y} + pt4_{x,y}\right) \cdot ft1_y \tag{14}$$

$$U_x^a = \left(pt3_{x,y} \cdot r_y^{FT3} + pt4_{x,y} \cdot r_x^{FT4}\right) \cdot ft1_y \tag{15}$$

$$r_x^n = \left(U_x' - U_x^a\right) / \left(\lambda_x' - \lambda_x^a\right) \tag{16}$$

However, to account for both lines in the cut-set failing simultaneously due to the occurrence of a FT3 or FT4 of an adjacent line also in the cut-set, an added dependency mode failure rate, λ^D, is created in (17). The dependency mode failure rate and the expected unavailability due to these dependent events is used to calculate the associated expected restoration time in (18). It is important to note that if the lines are not adjacent, the elements $\{x, y\}$ and $\{y, x\}$ in the probability matrices will be zero, and hence all adjustments and the dependency mode failure rate will be zero. The failure rate of the cut-set will be calculated on the basis of independent component failures if the components are not adjacent.

$$\lambda_{\{x,y\}}^D = \lambda_x^a + \lambda_y^a \tag{17}$$

$$r_{\{x,y\}}^D = \begin{cases} \left(U_x^a + U_y^a\right) / \lambda_{\{x,y\}}^D & \text{if } \lambda_{\{x,y\}}^D > 0 \\ 0 & \text{Otherwise} \end{cases} \tag{18}$$

The equivalent annual failure rate, expected annual unavailability and expected restoration time for the cut-set including any potential dependent failures are then calculated in (19)–(21).

$$\lambda_{\{x,y\}}' = \frac{\left(\lambda_x' - \lambda_x^a\right)\left(\lambda_y' - \lambda_y^a\right)\left(r_x^n + r_y^n\right)}{8760} + \lambda_{\{x,y\}}^D \tag{19}$$

$$U_{\{x,y\}}' = \frac{\left(\lambda_x' - \lambda_x^a\right)\left(\lambda_y' - \lambda_y^a\right)\left(r_x^n \cdot r_y^n\right)}{8760} + \lambda_{\{x,y\}}^D \cdot r_{\{x,y\}}^D \tag{20}$$

$$r_{\{x,y\}}' = \frac{U_{\{x,y\}}'}{\lambda_{\{x,y\}}'} \tag{21}$$

3.2. Time Series Method

Time series of failure probability can be used to incorporate varying failure probabilities due to exposure to external threats, e.g., wind, lightning, icing etc., leading to failure bunching effects. For time series, unavailability and associated reliability indices for cut-sets are calculated using the time series of different fault types, dependent on adjacency, as explained in this subsection. The algorithmic method outlined in [10] is used to calculate resulting unavailability and further reliability indices.

The addition of a time dimension to failure rates makes it necessary to make alterations to the equations in Section 3.1. The probability matrices established in Section 3 can still be used, assuming that the probability of a failure propagating is time independent. Time-series of hourly failure probabilities for a set of lines, as presented in (22), is now considered.

When referring to the time-series of failure probability for a single line, the column vector is denoted $\lambda_{:,l}$. The fault types for a single target line i are given in (23)–(27).

$$\lambda^{s} = \left[\lambda^{s}_{t,l}\right] = \begin{bmatrix} \lambda_{1,1} & \dots & \lambda_{1,l} \\ \vdots & \ddots & \vdots \\ \lambda_{t,1} & \dots & \lambda_{t,l} \end{bmatrix} \tag{22}$$

$$\mathrm{FT1}_{:,\mathrm{i}} = \lambda_{:,\mathrm{l}} \tag{23}$$

$$\mathrm{FT2}_{:,\mathrm{i}} = [ft2_{t,i}], \text{where } ft2_{t,i} = \frac{\sum_s \lambda^s_l}{8760} \tag{24}$$

$$\mathrm{FT3}_{:,\mathrm{i}} = \sum_j [\lambda_{:,\mathrm{j}} \cdot pt3_{i,j}] \tag{25}$$

$$\mathrm{FT4}_{:,\mathrm{i}} = \sum_j [\lambda_{:,\mathrm{j}} \cdot pt4_{i,j}] \tag{26}$$

$$\lambda'_{:,\mathrm{i}} = \mathrm{FT1}_{:,\mathrm{i}} + \mathrm{FT2}_{:,\mathrm{i}} + \mathrm{FT3}_{:,\mathrm{i}} + \mathrm{FT4}_{:,\mathrm{i}} \tag{27}$$

When calculating the unavailability and failure probability of second order cut-sets it is necessary to adjust FT3 and FT4 to account for adjacency as was done in the approximate equations, for both lines x and y, as seen in (28) and (29). A time series of dependency mode failure probability for the two lines in conjunction is calculated in (30). Again, the adjustments and dependency mode failure rate are equal to zero if the lines are not adjacent.

$$\mathrm{FT3}'_{:,\mathrm{x}} = \mathrm{FT3}_{:,\mathrm{x}} - \mathrm{FT1}_{:,y} \cdot pt3_{x,y} \tag{28}$$

$$\mathrm{FT4}'_{:,\mathrm{x}} = \mathrm{FT4}_{:,\mathrm{x}} - \mathrm{FT1}_{:,y} \cdot pt4_{x,y} \tag{29}$$

$$\lambda^{\mathrm{D}}_{:,\{\mathrm{x,y}\}} = \mathrm{FT1}_{:,y} \cdot pt3_{x,y} + \mathrm{FT1}_{:,y} \cdot pt4_{x,y} + \mathrm{FT1}_{:,\mathrm{x}} \cdot pt3_{y,x} + \mathrm{FT1}_{:,\mathrm{x}} \cdot pt4_{y,x} \tag{30}$$

For the cut-set itself, time-series of unavailability of individual lines with updated fault type values for FT3 and FT4 is calculated. The unavailability due to dependent faults is calculated as a separate time series, using restoration times according to the relevant line and the fault type. The calculation of unavailability is done using the method outlined in [10]. The result is a time series of the probability of the component being unavailable at a given point in time, which together with the unavailability due to the dependency mode failure probability is combined to the unavailability of the cut-set in (31). Once the time-series of unavailability is established, this is used to calculate the failure probability of the cut-set in (32).

$$\mathrm{U}'_{:,\{\mathrm{x,y}\}} = \mathrm{U}'_{:,\mathrm{x}} \circ \mathrm{U}'_{:,y} + \mathrm{U}^{\mathrm{D}}_{:,\{\mathrm{x,y}\}} \tag{31}$$

$$\lambda'_{:,\{\mathrm{x,y}\}} = \mathrm{U}'_{:,\mathrm{x}} \circ \lambda_{:,y} + \mathrm{U}_{:,y} \circ \lambda_{:,\mathrm{x}} + \lambda^{\mathrm{D}}_{:,\{\mathrm{x,y}\}} \tag{32}$$

4. Case Study

A test case is constructed to exemplify the combined effect of failure bunching due to weather and protection system failures on power systems reliability. The test case is based on the topology and annual failure rates from the 24-bus IEEE Reliability Test System (RTS) [36] with added protection systems. Only Permanent Outage Rates (POR) for the branches are considered. A representation of the system with numbered branches can be seen in Figure 4. A contingency enumeration approach is employed to evaluate the reliability of the system. A consequence analysis is performed at peak load, using an AC OPF algorithm with load shedding, as described in [37] yielding interrupted power at load points for the different cut-sets. The calculated interrupted power is used together with the unavailability of the cut-sets to calculate their respective contributions to annual Expected Energy Not Supplied (ENS) of the system.

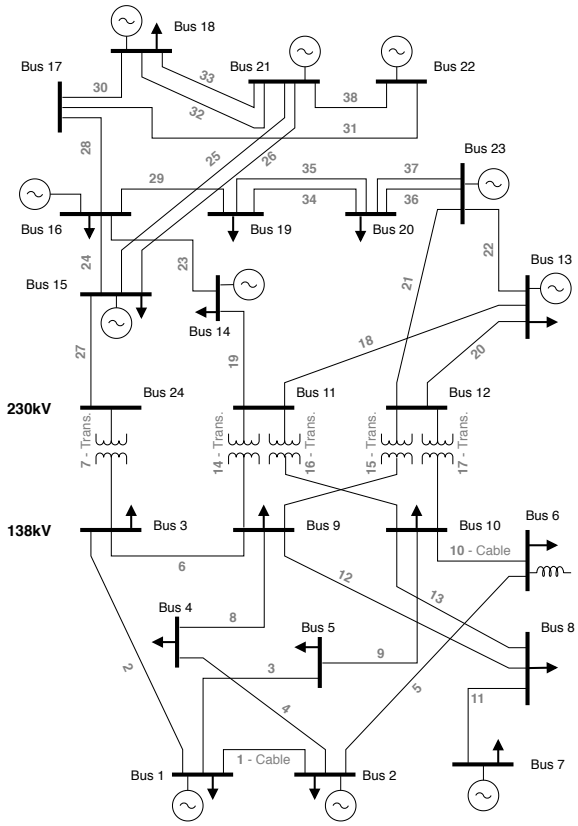

Figure 4. Twenty-four-bus Reliability Test System (RTS) [36] with component labels. Overhead transmission line unless otherwise noted.

Time series of hourly probability of failure due to wind conditions is calculated according to the method outlined in [19]. The time series covers 30 years of hourly estimated failure probabilities due to wind for actual lines in the Norwegian transmission system based on historical weather. This incorporates correlated weather exposure between lines in the data material. For the time-series, 75 percent of the failure probability is assumed to be constant, while 25 percent is scaled wind dependent failure probability varying at an hourly interval. Transformers and cables are assumed unaffected by wind, and are given a constant failure rate throughout the year. Annual failure rates due to permanent outages for the branches and the associated outage durations can be found in [36]. All protection systems are assumed to have an annual failure rate $\lambda_l^s = 0.025$. The probability of missing operation of the protection system is assumed to be $P_s^{s,m} = 0.0205$. The probability of unwanted non-selective tripping of the protection systems is assumed to be $P_l^{s,u} = 0.007$. Repair of protection system units, relevant to FT2, is assumed to be 2 h. FT3 and FT4 are associated with a 0.5 h switching time. These parameter values are in line with the case study presented in [17].

Unavailability of the different cut-sets are calculated in four ways: (1) A base case using an approximate method of reliability evaluation not including protection system failures [34]. (2) An approximate method including protection systems failures, as outlined in Section 3.1. (3) A time-series method including wind-dependent failure rates, as outlined in [10]. (4) A time-series method including wind-dependent failure rates adjusted for protection system faults, as outlined in Section 3.2. A simplification is done compared

to the original approach in [10] when calculating time-series of unavailability, where restoration times are assumed to be constant values, rather than distributions.

Adjacency matrices are created and weighted according to dependent probabilities and failure rates following the procedure in Section 3 to incorporate protection system reliability into the analysis. The results can be illustrated for the single line, branch 35, in Figure 5, where vertices are transmission lines and the directed edges show the adjacency between the lines. The line-style of the edges indicates the source line protection system side (A-side is dashed, B-side is dotted). To accumulate results, all edges leading into a vertex are summed up to see the contribution of FT3 and FT4 from the adjacent lines. Note the double connection between lines 34 and 35 appearing, causing line 34 to contribute to FT3 and FT4 at line 35 through two separate paths.

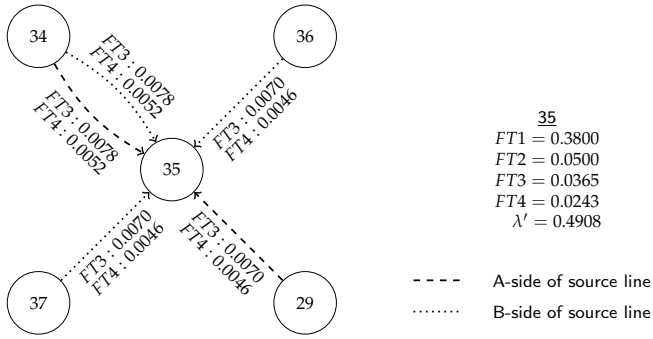

Figure 5. Contributions to fault type 3 (FT3) and FT4 for line 35 from adjacent lines. FT1–FT4 and adjusted failure rate for line 35. Annual values.

Figure 6 shows a 40 hour sample of the probability of failure for the individual components in the cut-set $\{26, 27\}$, as well as the calculated unavailability of the cut-set, to illustrate the method. The lines in the cut-set are adjacent at a single bus. In the top panel, the independent failure probabilities of the lines are relatively high, peaking around the tenth hour, while the dependency mode failure probability is comparably low. The dependency mode failure rate does however have a large impact on the failure probability of the cut-set due to its additive nature, as seen in the mid panel, where the failure probability of the cut-set is calculated with and without the inclusion of protection system failures. The resulting unavailability of the cut-set, illustrated in the lower panel, shows the impact of protection system failures as a short spike in unavailability compared to the case excluding protection system failures. This spike is due to the notably shorter outage durations associated with FT3 and FT4 of only thirty minutes, as compared with the permanent outage duration of independent faults for the lines at 11 hours. The unavailability only considering independent failures, with longer outage durations, is illustrated by the more rounded, dotted line.

The failure rates for sets of components in different categories are summarized in Table 1. These are not necessarily cut-sets causing load curtailment for the RTS at peak load, however, but show the impact on failure rate and unavailability of the methods described in the paper on different sets of network components in different topologies. For single lines, the approximate and time-series methods yield similar results. This is expected, as the time-series method only points out when the failure occurs but does not alter the annual failure rate in any way. The inclusion of protection systems has a limited impact on the annual failure rate for individual cables and lines but a large impact for transformers. This is due to the initially low failure rate of the transformers, when paired with a comparably high failure rate of its protection systems affecting FT2 in addition to contributions from adjacent lines through FT3 and FT4. For second order sets where the components are not adjacent, the sets containing at least one component with a constant failure rate, e.g., cables, are similar across the methods. The inclusion of protection systems causes a small increase

in the failure rate but there is no effect due to weather. However, when looking at sets including two overhead transmission lines, the effect of correlated weather causes a large increase in failure rate from the approximate method to the time series method, both not including protection systems. The failure rate increases sharply for sets where components are adjacent when protection systems are included in the evaluation. More importantly, the frequency of occurrence of some states is notably greater when protection systems and weather effects are both taken into consideration.

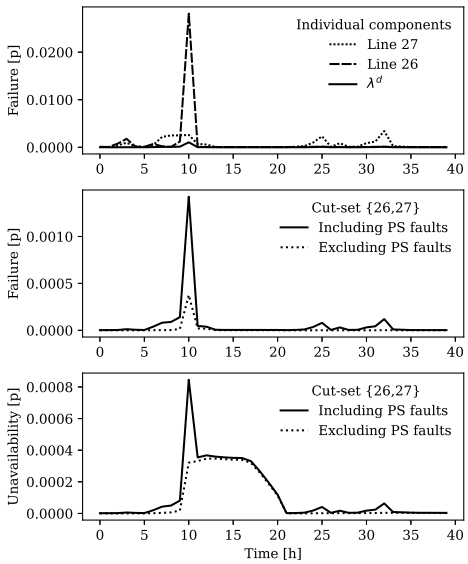

Figure 6. Individual failure probability of components in cut-set {26, 27} and dependency mode failure probability for a 40 hour time-window. Failure probability and unavailability of cut-set, including and excluding protection system failures.

Table 1. Annual failure rate for outages within different set categories [λ/y].

Set Information		Method [1]			
		Approximate		Time Series	
Connection	Components	No PS	PS	No PS	PS
-	Cable	0.570	0.773	0.570	0.773
-	Line	12.250	15.534	12.250	15.534
-	Transformer	0.100	0.673	0.100	0.673
None	Cable-Cable	0.000	0.001	0.000	0.001
None	Cable-Line	0.027	0.035	0.027	0.038
None	Cable-Trans	0.004	0.006	0.004	0.006
None	Line-Line	0.155	0.202	0.627	0.755
None	Line-Trans	0.094	0.127	0.093	0.138
None	Trans-Trans	0.000	0.003	0.000	0.003
1 bus	Cable-Line	0.003	0.172	0.003	0.173
1 bus	Cable-Trans	0.001	0.026	0.001	0.026
1 bus	Line-Line	0.020	1.477	0.111	1.581
1 bus	Line-Trans	0.015	0.330	0.015	0.332
1 bus	Trans-Trans	0.000	0.007	0.000	0.007
2 buses	Line-Line	0.001	0.204	0.010	0.214

[1] Approximate and time-series method, excluding and including protection system failures (PS).

In terms of unavailability of sets of components, Table 2 shows a somewhat different story. The single contingency of a transformer has a 5.7 times increase in failure probability when protection systems are included in the analysis but has nearly no change in expected unavailability. This is due to the short outage durations associated with protection systems failures in the model. Again, sets of components which are both exposed to correlated weather, such as overhead transmission lines, experience the largest increase in annual unavailability. The most extreme being the case of two overhead lines sharing both buses, where the time-series method including protection systems reliability has an expected unavailability 20 times higher than what is found using the approximate method without including protection systems failures.

ENS for the system calculated using the different methods is shown in Table 3. The transmission system is usually operated by the N-1 criterion, and only second order contingencies are considered here. Considering cut-sets consisting of two components with no shared buses, the majority of increase in ENS stems from the inclusion of weather effects in the model, affecting overhead transmission line cut-sets. For cut-sets with adjacent components, the inclusion of protection systems has the largest impact compared to the base case, although weather effects have almost the same impact as the inclusion of protection systems for overhead transmission line cut-sets within this category. The impact seen in second order cut-sets suggests that protection systems and weather effects are important aspects to consider when evaluating the reliability of supply.

Table 2. Annual unavailability for outages within different set categories [h/y].

Set Information		Method			
		Approximate		Time Series	
Connection	Components	No PS	PS	No PS	PS
-	Cable	15.390	15.641	15.372	15.624
-	Line	130.780	134.747	129.571	133.921
-	Transformer	76.800	77.462	76.570	77.230
None	Cable-Cable	0.005	0.005	0.005	0.005
None	Cable-Line	0.206	0.215	0.203	0.212
None	Cable-Trans	0.094	0.097	0.094	0.096
None	Line-Line	0.826	0.876	3.415	3.575
None	Line-Trans	0.988	1.027	0.976	1.009
None	Trans-Trans	0.162	0.164	0.161	0.163
1 bus	Cable-Line	0.024	0.109	0.024	0.109
1 bus	Cable-Trans	0.041	0.053	0.040	0.053
1 bus	Line-Line	0.111	0.842	0.630	1.395
1 bus	Line-Trans	0.158	0.319	0.156	0.318
1 bus	Trans-Trans	0.108	0.112	0.107	0.111
2 buses	Line-Line	0.008	0.109	0.057	0.161

Table 3. Energy Not Supplied (ENS) due to second order cut-sets, calculated using different methods; in MWh/year.

Cut-Set Information	Method			
	Approximate		Time Series	
Connection	No PS	PS	No PS	PS
Unconnected	373	390	999	1032
of which is Line-Line	211	222	839	867
Connected at 1 bus	22	125	107	214
of which is Line-Line	9	71	94	160
Total	395	515	1107	1246

The approach can support decision makers in taking appropriate actions based on risk and socioeconomic considerations. The revelation of cut-sets with a high ENS may guide prioritization in grid hardening efforts, such as enhancing robustness of lines, undergrounding of overhead transmission lines, or investment in new transmission routes. Identification of adjacent cut-sets with high failure rates due to propagating failures may similarly support prioritized inspection and maintenance efforts of the associated protection systems.

5. Conclusions

In this paper we have shown a compact and generalized method of including protection system failures in power system reliability analysis, based on a graph-theoretical approach. The use of adjacency matrices in the approach is novel. This incorporates the topology of the grid and possible paths of failure propagation due to protection system misoperation into the reliability analysis as a set of matrix operations. The method was extended further to account for time-series of failure probability in the analysis, allowing for inclusion of both protection system misoperation and time-varying failure probabilities throughout the year due to weather exposure.

Our investigations confirm the hypothesis that the combination of failure bunching effects and protection system failures adversely impact power system reliability. A case study was presented to show the effect on reliability of supply when weather exposure and protection system misoperation were implemented into the analysis. The case study shows that taking protection system reliability and the adjacency of transmission lines into account can have a large impact on the contribution to annual ENS from certain cut-sets due to the propagation of protection system failures. Since protection system misoperation follows an initial failure, propagating failures cluster around periods of high failure probability from other causes, and further increase risks associated with failure bunching effects. Thus, taking a time-series approach to capture time-varying failure rates including protection system failures can more accurately quantify the reliability of supply. This is especially important for more frequently occurring second order cut-sets. Taking the time-series approach would also be especially relevant when considering multiple operating states throughout the year. The results of the analysis can support decision makers in risk-based prioritization of grid hardening, inspection or maintenance efforts.

The compact and generalized method presented can be implemented with ease on large power systems. The results can be used to prioritize preventive and corrective measures aiming to reduce risks associated with unwanted events in the power system. The use of adjacency matrices to incorporate dependencies between component outages in the reliability evaluation was exemplified using an approximate method and an analytical time-series method. The use of the probability matrices could, however, also be implemented into Monte Carlo based tools to the same effect.

Author Contributions: Conceptualization, E.S.K.; methodology, E.S.K.; original draft preparation, E.S.K.; review and editing, G.H.K.; visualization, E.S.K.; supervision, G.H.K. All authors have read and agreed to the published version of the manuscript.

Funding: The research leading to these results has received funding through the project "Analysis of extraordinary events in power systems" (HILP) (Grant No. 255226), co-funded by the Research Council of Norway, Statnett and Fingrid.

Institutional Review Board Statement: Not applicable.

Informed Consent Statement: Not applicable.

Data Availability Statement: Not applicable.

Conflicts of Interest: The authors declare no conflict of interest. The funders had no role in the design of the study; in the collection, analyses, or interpretation of data; in the writing of the manuscript, or in the decision to publish the results.

References

1. Bompard, E.; Huang, T.; Wu, Y.; Cremenescu, M. Classification and trend analysis of threats origins to the security of power systems. *Int. J. Electr. Power Energy Syst.* **2013**, *50*, 50–64. [CrossRef]
2. Wang, Y.; Chen, C.; Wang, J.; Baldick, R. Research on Resilience of Power Systems under Natural Disasters—A Review. *IEEE Trans. Power Syst.* **2016**, *31*, 1604–1613. [CrossRef]
3. Panteli, M.; Mancarella, P. Influence of extreme weather and climate change on the resilience of power systems: Impacts and possible mitigation strategies. *Electr. Power Syst. Res.* **2015**, *127*, 259–270. [CrossRef]
4. Pourbeik, P.; Kundur, P.S.; Taylor, C.W. The anatomy of a power grid blackout. *IEEE Power Energy Mag.* **2006**, *4*, 22–29. [CrossRef]
5. Hines, P.; Apt, J.; Talukdar, S. Large blackouts in North America: Historical trends and policy implications. *Energy Policy* **2009**, *37*, 5249–5259. [CrossRef]
6. Papic, M.; Agarwal, S.; Allan, R.N.; Billinton, R.; Dent, C.J.; Ekisheva, S.; Gent, D.; Jiang, K.; Li, W.; Mitra, J.; et al. Research on Common-Mode and Dependent (CMD) Outage Events in Power Systems: A Review. *IEEE Trans. Power Syst.* **2017**, *32*, 1528–1536. [CrossRef]
7. Billinton, R.; Singh, G.; Acharya, J. Failure Bunching Phenomena in Electric Power Transmission Systems. *Proc. Inst. Mech. Eng. Part O J. Risk Reliab.* **2006**, *220*, 1–7. [CrossRef]
8. Billinton, R. Basic models and methodologies for common mode and dependent transmission outage events. In Proceedings of the 2012 IEEE Power and Energy Society General Meeting, San Diego, CA, USA, 22–26 July 2012; IEEE: Piscataway, NJ, USA, 2012. [CrossRef]
9. Panteli, M.; Mancarella, P. Modeling and evaluating the resilience of critical electrical power infrastructure to extreme weather events. *IEEE Syst. J.* **2017**, *11*, 1733–1742. [CrossRef]
10. Kiel, E.S.; Kjølle, G.H. Transmission line unavailability due to correlated threat exposure. In Proceedings of the 2019 IEEE Milan PowerTech, PowerTech 2019, Milano, Italy, 23–27 June 2019; IEEE: Milano, Italy, 2019. [CrossRef]
11. Guo, H.; Zheng, C.; Iu, H.H.C.; Fernando, T. A critical review of cascading failure analysis and modeling of power system. *Renew. Sustain. Energy Rev.* **2017**, *80*, 9–22. [CrossRef]
12. Dobson, I.; Newman, D.E. Cascading blackout overall structure and some implications for sampling and mitigation. *Int. J. Electr. Power Energy Syst.* **2017**, *86*, 29–32. [CrossRef]
13. Phadke, A.G.; Thorp, J.S. Expose hidden failures to prevent cascading outages. *IEEE Comput. Appl. Power* **1996**, *9*, 20–23. [CrossRef]
14. Billinton, R.; Tatla, J. Composite generation and transmission system adequacy evaluation including protection system failure modes. *IEEE Trans. Power Appar. Syst.* **1983**, *PAS-102*, 1823–1830. [CrossRef]
15. Kaplan, S.; Garrick, B.J. On The Quantitative Definition of Risk. *Risk Anal.* **1981**, *1*, 11–27. [CrossRef]
16. Jiang, K.; Singh, C. New models and concepts for power system reliability evaluation including protection system failures. *IEEE Trans. Power Syst.* **2011**, *26*, 1845–1855. [CrossRef]
17. Vadlamudi, V.V.; Gjerde, O.; Kjølle, G.H. Dependability and security-based failure considerations in protection system reliability studies. In Proceedings of the 2013 4th IEEE/PES Innovative Smart Grid Technologies Europe, ISGT Europe 2013, Lyngby, Denmark, 6–9 October 2013; IEEE: Lyngby, Denmark, 2013. [CrossRef]
18. Kiel, E.S.; Kjølle, G.H. The impact of protection system failures and weather exposure on power system reliability. In Proceedings of the 2019 IEEE International Conference on Environment and Electrical Engineering and 2019 IEEE Industrial and Commercial Power Systems Europe (EEEIC/I&CPS Europe), Genoa, Italy, 11–14 June 2019; IEEE: Piscataway, NJ, USA, 2019. [CrossRef]
19. Solheim, Ø.R.; Kjølle, G.H. Wind dependent failure rates for overhead transmission lines using reanalysis data and a Bayesian updating scheme. In Proceedings of the 2016 International Conference on Probabilistic Methods Applied to Power Systems (PMAPS), Beijing, China, 16–20 October 2016. [CrossRef]
20. Billinton, R.; Singh, G. Application of adverse and extreme adverse weather: Modelling in transmission and distribution system reliability evaluation. *IEEE Proc. Gener. Transm. Distrib.* **2006**, *153*, 115–120. [CrossRef]
21. Solheim, Ø.R.; Warland, L.; Trotscher, T. A holistic simulation tool for long-term probabilistic power system reliability analysis. In Proceedings of the 2018 IEEE International Conference on Probabilistic Methods Applied to Power Systems (PMAPS), Boise, ID, USA, 24–28 June 2018. [CrossRef]
22. Kjølle, G.H.; Gjerde, O. Integrated approach for security of electricity supply analysis. *Int. J. Syst. Assur. Eng. Manag.* **2010**, *1*, 163–169. [CrossRef]
23. Gjerde, O.; Kjølle, G.H.; Jakobsen, S.H.; Vadlamudi, V.V. Enhanced method for reliability of supply assessment—An integrated approach. In Proceedings of the 19th Power Systems Computation Conference, PSCC 2016, Genova, Italy, 20–24 June 2016; IEEE: Genoa, Italy, 2016. [CrossRef]
24. IEC 60050. *Electropedia—International Electrotechnical Vocabulary*; International Electrotechnical Commission: Geneva, Switzerland, 2009.
25. IEEE Standards Association. *Proceedings of the 1366–2012—IEEE Guide for Electric Power Distribution Reliability Indices*; IEEE Standards Association: Piscataway, NJ, USA, 2012. [CrossRef]
26. Rausand, M.; Høyland, A. *System Reliability Theory: Models, Statistical Methods, and Applications*, 2nd ed.; John Wiley & Sons: New York, NY, USA, 2004.
27. Bian, J.J.; Slone, A.D.; Tatro, P.J. Protection system misoperation analysis. In Proceedings of the 2014 IEEE PES General Meeting | Conference & Exposition, National Harbor, MD, USA, 27–31 July 2014; IEEE: Piscataway, NJ, USA, 2014; pp. 1–5. [CrossRef]

28. Vadlamudi, V.V.; Gjerde, O.; Kjølle, G.H. Impact of protection system reliability on power system reliability: A new minimal cutset approach. In Proceedings of the 2014 International Conference on Probabilistic Methods Applied to Power Systems, PMAPS 2014, Durham, UK, 7–10 July 2014; IEEE: Durham, UK, 2014. [CrossRef]
29. Sun, K. Complex networks theory: A new method of research in power grid. In Proceedings of the IEEE Power Engineering Society Transmission and Distribution Conference, Dalian, China, 15–18 August 2005; IEEE: Piscataway, NJ, USA, 2005; pp. 1–6. [CrossRef]
30. Arianos, S.; Bompard, E.; Carbone, A.; Xue, F. Power grid vulnerability: A complex network approach. *Chaos* **2009**, *19*, 13119. [CrossRef] [PubMed]
31. Pagani, G.A.; Aiello, M. The Power Grid as a complex network: A survey. *Phys. A Stat. Mech. Appl.* **2013**, *392*, 2688–2700. [CrossRef]
32. Diestel, R. *Graph Theory*, 5th ed.; Graduate Texts in Mathematics; Springer: Berlin/Heidelberg, Germany, 2017; Volume 173, pp. xviii + 428. [CrossRef]
33. Chartrand, G.; Zhang, P. *A First Course in Graph Theory—Chartrand, Zhang*; Dover Publications: New York, NY, USA, 2012; p. 450.
34. Billinton, R.; Allan, R.N. *Reliability Evaluation of Power Systems*; Plenum Press: New York, NY, USA, 1996.
35. Styan, G.P. Hadamard products and multivariate statistical analysis. *Linear Algebra Appl.* **1973**, *6*, 217–240. [CrossRef]
36. IEEE Probability Methods Subcommittee. IEEE reliability test system. *IEEE Trans. Power Appar. Syst.* **1979**, *PAS-98*, 2047–2054. [CrossRef]
37. Sperstad, I.B.; Jakobsen, S.H.; Gjerde, O. Modelling of corrective actions in power system reliability analysis. In Proceedings of the 2015 IEEE Eindhoven PowerTech, Eindhoven, The Netherlands, 29 June–2 July 2015; IEEE: Piscataway, NJ, USA, 2015. [CrossRef]

Paper III

The paper **"A Bayesian Network approach to predicting transmission line down times"** is published by **Research Publishing** in the proceedings of **30th European Safety and Reliability Conference and 15th Probabilistic Safety Assessment and Management Conference (ESREL2020 PSAM15)**.

The paper is not included in the text due to copyright reasons. The paper can be accessed through the URL found below.

Cite as:
E. S. Kiel, G. H. Kjølle
"A Bayesian Network approach to predicting transmission line down times"
Proceedings of 30th European Safety and Reliability Conference and 15th Probabilistic Safety Assessment and Management Conference (ESREL2020 PSAM15)
edited by Piero Baraldi, Francesco Di Maio and Enrico Zio, nov 2020
DOI: 10.3850/978-981-14-8593-0
URL: `https://www.rpsonline.com.sg/proceedings/esrel2020/pdf/3776.pdf`

Co-author declaration:
The publication was conceptualized by the candidate, who was the main contributor to the literary review, methodology, writing of associated computer programs and visualizations, as well as the analysis of the results. The candidate prepared and conducted interviews. This was done with contributions from the second author in the form of supervision, discussions and input on prepared material. The candidate produced an original draft, and incorporated review comments and editing.

Paper IV

Cite as:
E. S. Kiel, G. H. Kjølle
"Identification, visualization and reduction of risk related to HILP events in power systems"
54th International Universities Power Engineering Conference (UPEC), sept 2019
DOI: 10.1109/UPEC.2019.8893553
URL: `https://doi.org/10.1109/UPEC.2019.8893553`

Co-author declaration:
The publication was conceptualized by the candidate, who was the main contributor to the literary review, methodology, writing of associated computer programs and visualizations, as well as the analysis of the results. This was done with contributions from the second author in the form of supervision, discussions and input on prepared material. The candidate produced an original draft, and incorporated review comments and editing.

Paper A

The paper **"Development of a qualitative framework for analysing high-impact low probability events in power systems"** is published by **CRC Press** in the proceedings of the **28th European Safety and Reliability Conference (ESREL2018)**. It is published under a open access license: Creative Commons, CC BY-NC-ND.

Cite as:
I.B. Sperstad, E. S. Kiel
"Development of a qualitative framework for analysing high-impact low probability events in power systems"
Safety and Reliability - Safe Societies in a Changing World - Proceedings of the 28th International European Safety and Reliability Conference, ESREL 2018, 2018
DOI: 10.1201/9781351174664-201

Co-author declaration:
The contribution of the candidate was input and discussions in conceptualizing the article. The candidate contributed to the literature review for the article and contributed with writing several parts of the article. This includes, but is not limited, to portions of the text on handling uncertainties in the modeling. The candidate contributed to the review and editing, and presented the published work at the relevant conference.

Development of a qualitative framework for analysing high-impact low-probability events in power systems

I.B. Sperstad
SINTEF Energy Research, Trondheim, Norway

E.S. Kiel
Norwegian University of Science and Technology, Trondheim, Norway

ABSTRACT: High-impact low-probability (HILP) events in power systems historically involve a multitude of aspects, including diverse and disparate threats, failures and sequences of events. Each of these aspects are associated with different types of uncertainties. In practice, the analyst has to make trade-offs between computational efficiency and accuracy in the different aspects that are included in the analysis. Without a clear understanding of the specific problem to be solved and which aspects that are important to capture, elaborate quantitative analysis may be of limited value. This paper presents the development of a *qualitative* framework for analysing HILP events in power systems. By mapping aspects of power system HILP events to a bow-tie model, it provides a framework for defining, decomposing and delimitating decision problems related to such events. The framework may guide the analyst in the development and application of methods for quantitative analysis and for considering different types of uncertainties.

1 INTRODUCTION

A *high-impact low-probability* (HILP) event, also referred to as an *extraordinary event*, is an event with a high societal impact and a low probability to occur. In power systems, such events are often understood as *blackouts*, i.e. wide-area power interruptions. A number of such major blackout events have occurred in the last few decades (Bompard *et al.* 2013, Hillberg 2016), each resulting in critical consequences to society. Such events therefore receive great attention both by power system operators and other stakeholders, such as researchers and the general public, despite their low probability of occurrence. Partly due to this low probability, these events typically are not captured in conventional reliability and risk analyses, which calls for analysis approaches specific to HILP events.

HILP events historically involve a multitude of diverse and disparate threats and complex sequences of events, which present the analysts and researchers studying them with numerous uncertainties. Relevant aspects that can be taken into account in quantitative modelling of HILP events include: failure bunching due extreme weather (Panteli and Mancarella 2015), other natural hazards, cascading outages (Vaiman *et al.* 2012, Dobson and Newman 2017), dynamic phenomena, system protection schemes (Hillberg *et al.* 2012), corrective actions (Vadlamudi *et al.* 2016), and valuation of the societal impact. Different approaches and methodologies exist for quantitatively analysing these events (Gjerde *et al.* 2011), including methods of identifying unwanted events, causal analysis, consequence analysis, and risk and vulnerability evaluation. Such methods typically focus on one or a subset of all potentially relevant aspects. The realization is that there is no single methodology covering all these aspects that is suitable for analyzing HILP events in power systems (Kjølle *et al.* 2013), and the full set of aspects is too comprehensive to analyse quantitatively. Without a clear understanding of what specifically is the problem to be solved or decision to be supported, and consequently which aspects are important to capture, elaborate quantitative analysis may be of limited value.

In this paper, we take a broader view on HILP events and present the development of a *qualitative* framework for analysing HILP events in power systems. A qualitative framework provides the analyst with a more complete overview of the set of problems and a starting point for detailed analysis. Previous work on HILP events largely focus on methods of detailed, quantitative analysis (Vaiman *et al.* 2012), but some work on the more conceptual level also exists. For instance, (Watson *et al.* 2014) developed a framework for resilience metrics for energy infrastructures. In (Veeramany *et al.* 2016), an overarching modelling framework is formulated under which different models can be integrated for an multi-hazard risk assessment of power system HILP events. The cascading

aspect of some HILP events is discussed conceptually in (Vaiman *et al.* 2012, Dobson and Newman 2017).

The qualitative framework presented in this paper is based on an existing framework for power system vulnerability analysis (Kjølle *et al.* 2013, Kjølle and Gjerde 2015). The present paper advance previous work and attempts to consolidate relevant aspects of HILP events in a consistent and all-encompassing mapping. This framework explicitly discusses and structures uncertainties related to different decision problems. The framework is presented in Section 2, which forms the bulk of this paper. Subsection 2.1 shows how mapping relevant aspects and their relationships to a bow tie model provides a more complete overview of HILP events. Subsection 2.2 to Subsection 2.4 presents an approach to defining, delimitating and decomposing decision problems related to HILP events. This provides a starting point for quantitative analysis, as discussed in Section 2.4, and a basis for taking into account uncertainties, which is discussed in Section 2.5. Throughout these subsections, concrete examples of problems are discussed to illustrate the application of the framework. Finally, Subsection 3 concludes the paper and indicates future work in refining and applying the framework.

2 QUALITATIVE FRAMEWORK FOR HILP EVENTS

The qualitative framework presented in this paper is based on the conceptual bow tie model and a previously developed framework for power system vulnerability analysis (Kjølle *et al.* 2013, Kjølle and Gjerde 2015). The bow tie model describes the relationship between causes and consequences of unwanted events, which are here defined as power system failures. Note that the unwanted event in the centre of the bow-tie is not by itself a HILP event, but it could be the initiating event of a sequence of events with critical consequences that constitutes the HILP event.

2.1 *Getting a better overview of relevant aspects*

The bow tie model can be used as a visual aid in structuring the causes and consequences of unwanted events as illustrated in Figure 1. This figure gives a comprehensive overview of aspects relevant to HILP events in power systems and how these relate to each other. Such an overview is useful when structuring an analysis of HILP events.

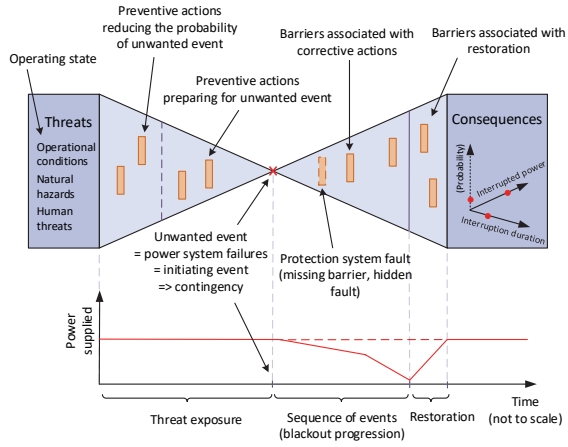

Figure 1. Overview of a relevant aspects of HILP events in power systems mapped to a bow-tie model.

The left-hand part of the figure shows schematically how the exposure of the power system to different threats can cause power system failures, and the right-hand part shows how power system failures can result in consequences external to the power system, i.e. societal impact. The criticality of the consequences can be measured along different dimensions, but for the illustrations in this paper we will consider total end-user power interruption (MW) and interruption duration (hours) as the two principal dimensions. Each HILP event could, in principle, also be associated with a probability. Other relevant factors include the types of end-users affected and the dependence of the society on electricity supply; for further discussion of the definition of "critical", we refer to (Kjølle *et al.* 2013, Kjølle and Gjerde 2015).

Relevant threats on the left-hand side include conditions related to the operating state of the power system (e.g. challenges related to the power import/export situation, prior outages, etc.), natural hazards such as major storms and human threats. Barriers on the left-hand side of the bow tie reduce the susceptibility of the power system to threats. These barriers reduce the probability of unwanted events through preventive actions such as condition monitoring, preventive maintenance and vegetation management. Some barriers also preemptively increase the coping capacity of the system to reduce the probability of critical consequences in case an unwanted event does occur. This category of barriers includes preventive scheduling, grid reconfiguration and islanding in preparation for a major storm.

Barriers on the right-hand side of the bow-tie are intended to reduce the consequence of power system failures and correspond to the coping capacity of the power system with respect to these unwanted events. Examples of such barriers are corrective actions such as emergency generation rescheduling, controlled load shedding, controlled islanding, and various system protection schemes. Other barriers are associated

with the restoration of system operation after power has been interrupted, for instance the black-start capability of generators and the availability of spare parts, equipment and competent personnel.

To illustrate the distinction between these two types of barriers, we have in Figure 1 superimposed a timeline with an example of how the interrupted power could develop as a function of time throughout the course of the HILP event. The sequence of events after the occurrence of the initiating event can be broadly separated in a blackout progression phase and a restoration phase. Corrective action barriers are associated with the blackout progression phase and primarily intended to reduce the amount of interrupted power, whereas barriers associated with the restoration phase generally intended to reduce the restoration time and thus the interruption duration.

2.2 *Defining and framing the problem*

The analysis of HILP events in power systems is a broad problem area involving different decision problems as well as more fundamental research problems. The question one needs to ask is why one is interested in analyzing HILP events the first place. It is necessary with a clear definition the problem and a clear understanding of the motivation and purpose of solving the problem.

Figure 2 shows two dimensions that can be used to frame problems related to HILP events: The time scales for power system-related decisions and relevant stakeholders or decision makers. The figure also indicates the motivation of the stakeholders with regards to HILP events. The two dimensions in Figure 2 determine what information is available to the analyst and thus what uncertainties must be taken into account. This will be discussed in more detail in Section 2.5.

Here we will distinguish between operational, tactical and strategic decisions by the time scale of the planning horizon that is considered. Following the classification in (GARPUR Consortium 2016), these three time scales correspond to system operation (including both real-time operation and day-ahead operational planning), asset management, and system development or planning, respectively. Note that other references may use other terms and definitions for the time scales. For instance, (Watson *et al.* 2014) distinguishes between system planning decisions and policy decisions, and (Yang and Haugen 2015) defines both strategic and operational decisions as planning decision, which are in turn distinguished from instantaneous or emergency decisions.

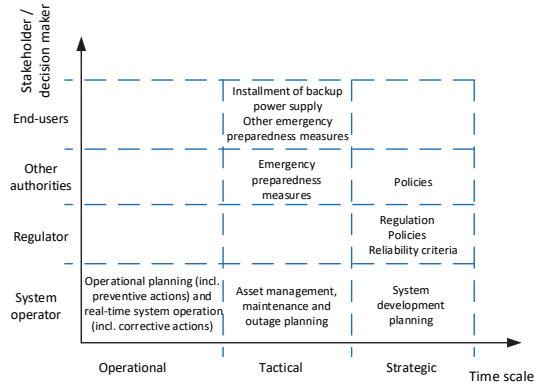

Figure 2. Two dimensions relevant for framing problems related to HILP events: The stakeholder or decision maker, and the time scale of relevant decision problems.

Stakeholders can be differentiated in terms of their influence over power system related decisions, and since system operators have the most direct influence, we will in the following take the perspective of the system operator as a decision maker. Furthermore, we will focus on transmission system operators (TSOs) since distribution system operators (DSOs) have less influence over decisions relevant for wide-area power interruptions. In practice, decisions will be taken by different departments and at different levels in the organisation, but in the following we simply refer to the decision maker as "the system operator".

To put the more general problem of analysing HILP events in a decision-making context, Figure 3 shows some examples of relevant decision problems for system operators, sorted by time scale. These decision problems will be defined in broad terms below and be used in the following sections to illustrate the qualitative framework. Although we do not define the decision problems formally in terms of their objective function etc. as done e.g. in (GARPUR Consortium 2016), it is important to keep in mind that these reliability management decisions typically involve some form of trade-off between costs and reliability of supply. The value of reliability of supply is sometimes monetized in the form of expected interruption costs, i.e. the cost of energy not supplied.

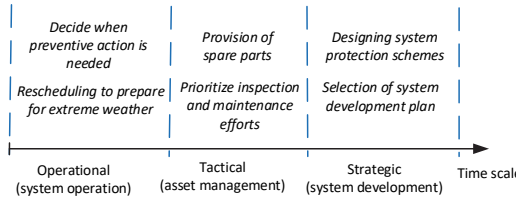

Figure 3. Examples of decision problems for transmission system operators with relevance for the analysis of HILP events.

Selection of system development plan: An example of a strategic decision problem is the evaluation of candidate system development plans (e.g. for new

transmission lines) and selection of the best candidate. Regulation may dictate that a socio-economic cost-benefit analysis of the candidates is performed. Ideally, the cost of energy not supplied associated with possible HILP events should be included in such an analysis.

Designing system protection schemes: System protection schemes (SPSs) are important examples of barriers on the right-hand side of the bow-tie, and the system operator has to plan which SPSs to implement. The motivation of implementing an SPS could be to increase the transmission capacity of the system as well as to increase the coping capacity of the system with respect to the occurrence of contingencies that would otherwise result in critical consequences (Hillberg *et al.* 2012).

Prioritize inspection and maintenance efforts: The system operator has to decide how to best allocate limited resources for preventive actions such as intensified inspection and maintenance and improved condition monitoring of power system components. Mitigating certain susceptibilities could help reduce the risk of HILP events as well as more ordinary events.

Spare parts etc. for critical components: If the power system is vulnerable to the loss of certain component, e.g. a transformer, the decision can be made to provide for spare parts to reduce the duration of potential power interruptions.

Decide when preventive action is needed: During operation, preventive actions such as generation rescheduling may be needed e.g. due to the development of threat exposure and/or the operating state. The first step for the system operator is to correctly assess the situation and decide whether or not to effectuate preventive actions.

Rescheduling generation e.g. to prepare for extreme weather: During an extreme weather event the near-simultaneous failure of multiple transmission lines (failure bunching) is more likely. In this case, one relevant preventive action is to reschedule generation in a way that makes the power system better able to cope with failures on one or several transmission lines.

2.3 *Defining and delimiting the analysis*

Decision making for problems as exemplified above can be supported by the analysis of HILP events. One way of defining and delimitating "analysis of HILP events" is to consider sub-problems distinguished by the objective of the analysis. One possible classification is:

1) identifying critical contingencies
2) identifying critical operating states
3) identifying critical barriers
4) assessing the contributions to the overall reliability of supply

Each of these sub-problems can be associated with different parts of the bow-tie model as illustrated in Figure 4. In practice, the objectives may be overlapping and the sub-problems may be combined in one of the same analysis. The classification may nevertheless be useful in discussing specific decision problems and the underlying motivation.

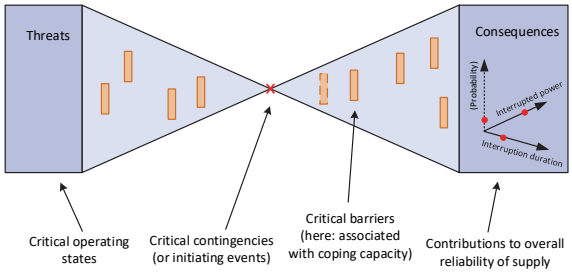

Figure 4. The placement in the bow tie model of different criticalities and sub-problems relevant in the analysis of HILP events.

2.3.1 *Identify critical contingencies*

A critical contingency is here understood as a failure or unplanned outage of a power system component that may potentially result in critical consequences. One purpose of identifying critical contingencies is to identify critical power system components with the motivation to strengthen or introduce appropriate barriers, cf. Section 2.3.3.

One example of a system operation decision involving the identification of critical contingencies is the (optimal) preventive rescheduling of generation in preparation for an extreme weather event. In this case, the system operator should ideally know which (critical) higher-order contingencies to take into account when rescheduling. In the context of system development, one would like to identify critical contingencies in the candidate development plans to reduce the vulnerabilities of the development plan that is selected. Another purpose of identifying critical contingencies can be to screen contingencies to be considered as input to more detailed (e.g. dynamic) analysis.

2.3.2 *Identify critical operating states*

We here understand a critical operating state as an operating state which in combination with a critical contingency potentially result in critical consequences. The motivation for identifying these could be to increase the situational awareness of the system operators, which has previously been identified as being crucial to avoid HILP events (Johansson, E. *et al.* 2010). Situational awareness is relevant for operational decisions on which corrective actions to carry out after a contingency has occurred. Identifying critical operating states prior to contingencies may also be important to be able to decide when preventive action is needed.

2.3.3 *Identify critical barriers*

The identification of critical barriers may be used in selecting barriers to strengthen, and the identification of critical barriers that are missing may be used in proposing new barriers to put in place. This involves corrective barriers such as well-designed system protection schemes, or preventive barriers such as inspection and maintenance. For the latter example, the decision of which components to prioritize also depends on the identification of critical contingencies.

2.3.4 *Assessing the contributions to the overall reliability of supply*

An underlying premise of this work is that conventional power system reliability analysis methods do not fully capture HILP events. The reliability of a power system can be defined as "the probability of its satisfactory operation over the long run. It denotes the ability to supply adequate electric service on a nearly continuous basis, with few interruptions over an extended time period" (Kundur *et al.* 2004). The overall reliability of supply may be quantified by reliability indices such as the expected annual energy not supplied. Over the long run, HILP events do contribute to these reliability indices, but their contribution may be underestimated by conventional reliability analysis methods. For instance, this may happen when the methods do not capture failure bunching, protection system failures, or any of the other aspects and dependencies that may conspire to result in a HILP event. Furthermore, the short-term impact of a HILP event may be disproportional to their long-run visibility in expected values of reliability indices and therefore warrant separate treatment (Vaiman *et al.* 2012). These are some of the reasons why methods of vulnerability analysis focusing on HILP events have been advocated to complement traditional risk and reliability analysis methods (Johansson *et al.* 2013, Kjølle and Gjerde 2015).

Nevertheless, estimates of reliability indices are used by system operators as part of their reliability management processes also for decisions relating to HILP events. An example is the selection of system development plans for a given region, supported by a socio-economic cost-benefit analysis including expected interruption costs. If the region is exposed to strong winds, this could motivate capturing the contribution of HILP events due to failure bunching effects in the estimated interruption costs.

2.4 *Decomposition in quantitative analysis*

After defining the purpose of the analysis, one needs to consider which quantities the analysis method needs to estimate and which of them is most important to estimate accurately. Here we will consider three primary output parameters: 1) The probability of an event and its consequence in terms of 2) power interrupted and 3) interruption duration. As illustrated in Figure 5, these output parameters are broadly speaking associated with different parts of the bow-tie model. To assess the consequences of an unwanted event, it is sufficient to consider the right-hand side of the bow-tie: The interrupted power is primarily determined by the sequence of events within the phase labelled "blackout progression", and the interruption duration is primarily determined by the events in the restoration phase. On the other hand, to determine the probability of a HILP event, characterized by a given consequence, one has to consider both the left-hand side (with the label "threat exposure" in Figure 5) and the right-hand side of the bow-tie.

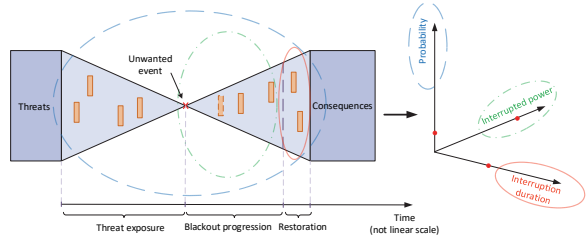

Figure 5. Illustration of how the problem of analysing extraordinary events can be decomposed and delimitated based on what quantity one is focusing on estimating.

To approach more quantitative analysis and consideration of different uncertainties, we overlay the bow tie model with a schematic data flow diagram for the analysis in Figure 6. A cause analysis is depicted on the left-hand side of the bow tie that gives as output the failure rate (or the probability of failure during a certain time interval) for a given unwanted event (i.e. a given power system failure). Such a module could for instance be based on a fault tree. Failure bunching effects, for example due to major storms, could be incorporated in this step using existing tools for estimation of wind-dependent failure rates, as done in (Solheim *et al.* 2016).

The consequence analysis on the right-hand side of Figure 6 is divided in two modules representing the blackout progression phase and the restoration phase, respectively. The module for the blackout progression phase models system responses and resulting power interruptions. It could be based on an event tree model, power flow analysis, dynamic analysis, etc. This module can take as input electrotechnical parameters describing the power system and its operational limits as well as parameters describing the actions and responses in the system. For instance, if the analysis method is based on an event tree accounting for corrective action failures (Vadlamudi *et al.* 2016), input parameters can be conditional probabilities determining the probability of different sequences of events. The restoration phase module represents the restoration process. For instance, the restoration time could be modelled by average outage times of the components involved, in which case such outage times are needed as input. Alternatively, the restoration process

could be modelled in more detail, which would require additional input parameters.

When analyzing system protection schemes to identify critical barriers for certain unwanted events, it may not be important for the purpose of the analysis to consider what caused these unwanted events. For such an analysis, one could omit the left-hand side of Figure 6 and focus on the first part of the consequence analysis, e.g. using dynamic analysis to estimate the power interrupted. On the other hand, if the objective is to assess the contribution to the overall reliability of supply, one would typically also have to represent power system restoration in the analysis.

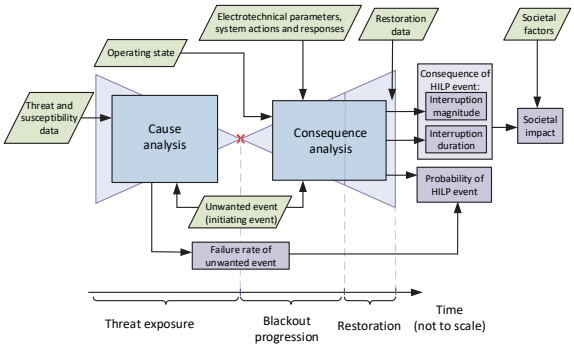

Figure 6. Schematic of quantitative analysis (blue, within the bow-tie) with input data (green parallelograms) and output data (purple).

In the determination of the consequences illustrated in Figure 6, the consequence analysis stops after finding the interruption magnitude and duration. However, as mentioned in Section 2.1, the societal impact of an HILP event is not determined by these two parameters alone. The box labeled societal factors in Figure 6 represent other factors determining the societal impact, such as the type of customers (end-users) and the criticality of the loads that are interrupted. Consequences of power interruptions are typically monetized using interruption cost functions determined by customer surveys, but these interruption costs give only a lower bound for the total socio-economic costs of the power interruption (GARPUR Consortium, 2016). Estimating quantitatively the impact on society more widely might involve modelling of the interactions between the power system and other infrastructures (Johansson *et al.* 2015).

2.5 *Taking into account uncertainties*

HILP events can be argued to be inherently associated with uncertainties (Taleb 2010, p. xxviii). Factors such as the operating state, the technical condition of components and failure bunching effects due to adverse weather all have their own individual uncertainties. HILP events are often the results of multiple, interacting factors and circumstances. As such, their combined uncertainty is larger than the uncertainty of the individual factors.

First, it is common to classify uncertainties as either aleatory, i.e. associated with random variability, or epistemic, i.e. associated with a lack of knowledge. Given that HILP events are characterized by a scarce experience base and severe lack of knowledge, epistemic uncertainties are especially important to consider. Next, following a similar classification as in (Rausand 2013), we will broadly distinguish between three types of uncertainties:

- Input data uncertainties
- Modelling uncertainties
- Completeness uncertainties

For the analysis of HILP events in power systems, these types of uncertainties can be related to Figure 6 as follows. Input data uncertainties and modelling uncertainties are related to green and blue boxes, respectively. The additional category that we have here chosen to label "completeness uncertainty" represents uncertainty associated with the completeness of the models of the system. Although there are different ways to understand this term (Rausand 2013, Aven 2016), and "completeness uncertainty" may not be unambiguously distinguished from "modelling uncertainty", we find the term useful to describe uncertainty associated with aspects omitted and/or outside the scope of the analysis. As an example, a consequence analysis starting from a given set of contingencies (i.e. covering only the right-hand side of Figure 6) does not explicitly consider what might have caused the contingencies. If the problem was to identify effective system protection schemes, for instance, threat and susceptibility aspects may not have been within the scope of the analysis.

Sources of incompleteness in the analysis can be either known or unknown to the analyst (Aven 2016). If the analyst is unaware that an aspect is not considered in the analysis, this uncertainty can be labelled an "unknown unknown" (Feduzi and Runde 2014). Here, we use this term in a wider sense to refer to lack of knowledge that is implicit, i.e. a form of epistemic uncertainty associated with "what we don't know we don't know". Furthermore, we focus on "unknown unknowns" that are "knowable", i.e. that can in principle be transformed into "known unknowns" (Feduzi and Runde 2014).

Another way to classify uncertainties related to an analysis of HILP events that is more specific to the domain of power systems is to consider uncertainties related to the aspects discussed in Section 2.1. An example of such a classification is illustrated in Figure 7. Here, each of the categories along the vertical axis corresponds to one of the components of quantitative analysis that were illustrated in Figure 6. This shows how a domain-specific classification can be combined with the generic uncertainty classification discussed above: For each category, a given analysis is associated with uncertainty (indicated along the horizontal axis) related to the accuracy of modelling assumptions and the input data.

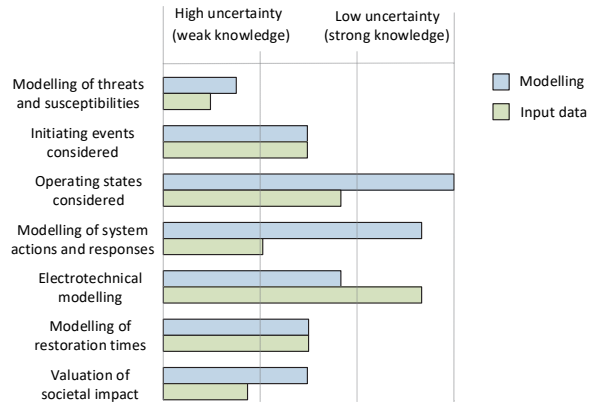

Figure 7. Example of classification and assessment of uncertainties associated with analyses of HILP events.

This multi-dimensional classification of uncertainties can be used to structure a qualitative assessment of the strength of background knowledge (Aven *et al.* 2014, p. 87) underlying a given analysis: If an aspect is modelled in a simplified or inaccurate manner, the knowledge of this aspect that is represented in the analysis is weak and the uncertainty is correspondingly high. Even if the modelling of an aspect is accurate, the uncertainty is still high if the associated input data represented in the analysis is inaccurate.

Such a structured assessment of the uncertainties of a HILP event analysis can be used by the analyst to rank which uncertainties are most important (Aven *et al.* 2014) to improve the overall accuracy and suitability of the analysis. More accurate modelling of an aspect often implies longer computation times. In practice, a trade-off must therefore be made between computational efficiency and accuracy, and trade-offs must be made between the modelling accuracy for the different aspects considered in the analysis.

An explicit qualitative assessment of uncertainties can also be used as a basis for comparing different analyses and informing the decision maker of their uncertainties (Aven *et al.* 2014). As an example, one can consider methods designed to analyse cascading outages. A number of such methods have been developed, each focusing on different subsets of the mechanisms and aspects involved in cascading outages. Considerable efforts have already been devoted to reviewing and validating such methods (Vaiman *et al.* 2012, Bialek *et al.* 2016), but there are still many open questions that may limit their credibility in decision making. More explicit classification and assessment of their uncertainties, scope and purpose could help inform system operators of which methods are most suitable for different problems.

Completeness uncertainty is not included as a separate dimension in Figure 7, but if an aspect is not covered in an analysis, the modelling uncertainties related to this aspect can be regarded as high. However, to fully characterize the completeness uncertainty dimension of the analysis one needs to identify and uncover "unknown unknowns". It has been argued that to do so, the analysis needs to be placed in a sufficiently broad framework and avoid starting out with a too narrow view of the problem (Feduzi and Runde 2014, Aven 2016). A qualitative mapping of relevant aspects to the analysis as proposed in this paper can contribute to transforming "unknown unknowns" to "known unknowns", or in other words making implicit assumptions and uncertainties explicit. Communicating such uncertainties associated with the completeness of the analysis can change, from the perspective of the decision maker, a "unknown unknown" to a "known unknown". To give a simple example: When deciding on system protection schemes to mitigate cascading outages and the analysis does not model the dynamics of rotor angle stability, the decision maker should be aware that the type of cascading events characterized by generators losing synchronism is omitted from the analysis.

As mentioned in Section 2.2, the time scale of the decision problem is relevant for what information is available during the analysis and hence what is uncertain and what is known. For instance, the system operator knows the operating state to a good approximation during real-time system operation, whereas this information is not available for an analysis for long-term planning purposes (Vaiman *et al.* 2012). For the example of cost-benefit analysis including the contributions of wind-related failures, the analyst needs to assume a selection of operating states expected to be representative of the future, and this is associated with additional uncertainties. For the example of preventive rescheduling in preparation of a major storm, more information is available on the operating state over the planning horizon, although this is still imperfect information as one may have to consider the forecast uncertainties.

3 CONCLUSIONS AND FUTURE WORK

This paper proposes a qualitative framework for analysing HILP events in power systems that may complement or guide more quantitative analysis. Mapping relevant aspects of such HILP events to a bow tie model provides the analyst with a broad overview of the set of problems at hand and a starting point for detailed analysis. Although the full set of aspects is too comprehensive to analyse quantitatively, the qualitative framework provides a basis for decomposing and delimitating the problem: Defining precisely the purpose of the analysis, one can then choose what aspects need to be modelled accurately and which aspects one is choosing to omit. Omitting and neglecting aspects of the overall problem introduce uncertainties in the analysis, but by being explicit about what is omitted and assumed one reduces the

amount of "unknown unknowns" in the analysis and may thus support more well-informed decisions.

Further work will test the applicability of the framework in case studies of real problems related to HILP events. The approach for defining the purpose of an analysis and delimitating the problem presented will also be used to guide the development and application of methods for quantitative analysis of HILP events. Furthermore, the classification of models and input data for the analysis may form the basis for considering which methods are most appropriate for handling different types of uncertainties related to modelling choices and input data.

REFERENCES

Aven, T., 2016. Ignoring scenarios in risk assessments: Understanding the issue and improving current practice. *Reliability Engineering & System Safety*, 145, 215–220.

Aven, T., Zio, E., Baraldi, P., & Flage, R., 2014. *Uncertainty in Risk Assessment: The Representation and Treatment of Uncertainties by Probabilistic and Non-Probabilistic Methods*. Chichester, UK: Wiley.

Bialek, J., Ciapessoni, E., Cirio, D., Cotilla-Sanchez, E., Dent, C., I. Dobson, P. Henneaux, P. Hines, J. Jardim, S. Miller, M. Panteli, M. Papic, A. Pitto, J. Quiros-Tortos, & D. Wu, 2016. Benchmarking and Validation of Cascading Failure Analysis Tools. *IEEE Transactions on Power Systems*, PP, 1–14.

Bompard, E., Huang, T., Wu, Y., & Cremenescu, M., 2013. Classification and trend analysis of threats origins to the security of power systems. *International Journal of Electrical Power & Energy Systems*, 50 (Supplement C), 50–64.

Dobson, I. and Newman, D.E., 2017. Cascading blackout overall structure and some implications for sampling and mitigation. *International Journal of Electrical Power & Energy Systems*, 86, 29–32.

Feduzi, A. & Runde, J., 2014. Uncovering unknown unknowns: Towards a Baconian approach to management decision-making. *Organizational Behavior and Human Decision Processes*, 124 (2), 268–283.

GARPUR Consortium, 2016. *D2.2: Guidelines for implementing the new reliability assessment and optimization methodology*.

GARPUR Consortium, 2016. *D3.2: Recommendations for implementing the socio-economic impact assessment methodology over the pan-European system in a tractable way*.

Gjerde, O., Kjølle, G.H., Detlefsen, N.K., & Brønmo, G., 2011. Risk and vulnerability analysis of power systems including extraordinary events. Presented at the PowerTech 2011, Trondheim.

Hillberg, E., 2016. Perception, Prediction and Prevention of Extraordinary Events in the Power System. PhD thesis. Norwegian University of Science and Technology, Trondheim.

Hillberg, E., Trengereid, F., Breidablik, Ø., Uhlen, K., Kjølle, G., Løvlund, S., & Gjerde, J.O., 2012. System integrity protection schemes - Increasing operational security and system capacity. Presented at the CIGRE Session, Paris.

Johansson, E., Uhlen, K., Nybø, A., Kjølle, G., & Gjerde, O., 2010. Extraordinary events: understanding sequence, causes, and remedies. Presented at the European Safety & Reliability Conference (ESREL) 2010, Rhodes.

Johansson, J., Hassel, H., Cedergren, A., Svegrup, L., & Arvidsson, B., 2015. Method for describing and analysing cascading effects in past events: Initial conclusions and findings. Presented at the European Safety & Reliability Conference (ESREL) 2015, Zürich, Switzerland.

Johansson, J., Hassel, H., & Zio, E., 2013. Reliability and vulnerability analyses of critical infrastructures: Comparing two approaches in the context of power systems. *Reliability Engineering & System Safety*, 120, 27–38.

Kjølle, G.H. & Gjerde, O., 2015. Vulnerability analysis related to extraordinary events in power systems. Presented at the PowerTech 2015, Eindhoven.

Kjølle, G.H., Gjerde, O., & Hofmann, M., 2013. *Vulnerability and security in a changing power system – Executive summary*. Trondheim: SINTEF Energy Research, Report No. TR A7278.

Kundur, P., Paserba, J., Ajjarapu, V., Andersson, G., Bose, A., Canizares, C., Hatziargyriou, N., Hill, D., Stankovic, A., Taylor, C., van Cutsem, T., & Vittal, V., 2004. Definition and classification of power system stability IEEE/CIGRE joint task force on stability terms and definitions. *IEEE Transactions on Power Systems*, 19, 1387–1401.

Panteli, M. & Mancarella, P., 2015. Influence of extreme weather and climate change on the resilience of power systems: Impacts and possible mitigation strategies. *Electric Power Systems Research*, 127, 259–270.

Rausand, M., 2013. *Risk assessment: theory, methods, and applications*. John Wiley & Sons.

Solheim, Ø.R., Kjølle, G., & Trötscher, T., 2016. Wind dependent failure rates for overhead transmission lines using reanalysis data and a Bayesian updating scheme. Presented at the 2016 International Conference on Probabilistic Methods Applied to Power Systems (PMAPS), Beijing: IEEE.

Taleb, N.N., 2010. *The black swan: The impact of the highly improbable*. Revised edition. London: Penguin Books.

Vadlamudi, V.V., Hamon, C., Gjerde, O., Kjølle, G., & Perkin, S., 2016. On Improving Data and Models on Corrective Control Failures for Use in Probabilistic Reliability Management. Presented at the 2016 International Conference on Probabilistic Methods Applied to Power Systems (PMAPS), Beijing: IEEE.

Vaiman, M., Bell, K., Chen, Y., Chowdhury, B., Dobson, I., Hines, Papic, Miller, & Zhang, 2012. Risk Assessment of Cascading Outages: Methodologies and Challenges. *IEEE Transactions on Power Systems*, 27, 631–641.

Veeramany, A., Unwin, S.D., Coles, G.A., Dagle, J.E., Millard, D.W., Yao, J., Glantz, C.S., & Gourisetti, S.N.G., 2016. Framework for modeling high-impact, low-frequency power grid events to support risk-informed decisions. *International Journal of Disaster Risk Reduction*, 18, 125–137.

Watson, J.-P., Guttromson, R., Silva-Monroy, C., Jeffers, R., Jones, K., Ellison, J., Rath, C., Gearhart, J., Jones, D., Corbet, T., Hanley, C., & Walker, L.T., 2014. *Conceptual Framework for Developing Resilience Metrics for the Electricity, Oil, and Gas Sectors in the United States*. Albuquerque, New Mexico and Livermore, California: Sandia National Laboratories, Report No. SAND2014-18019.

Yang, X. & Haugen, S., 2015. Classification of risk to support decision-making in hazardous processes. *Safety Science*, 80 (Supplement C), 115–126.

Appendices

Appendix A: Historical events

Table A.1: Historical extraordinary events.

Country	*Year*	*ID*	*Average interruption duration [h]*	*Disconnected load [MW]*	*Category*	*Sources*
India	2012	IN 2012	5.0	48000	Technical	[123, 124]
Chile	2010	CL 2010	72.0	3000	Natural	[125]
New Zealand	2011	NZ 2011	24.0	255	Natural	[126]
Turkey	2015	TR 2015	5.0	32200	Technical	[127]
Netherlands	2015	NL 2015	3.0	1500	Technical	[128]
UK	2019	UK 2019	0.7	2000	Natural	[28]
Argentina	2019	AR 2019	5.0	13000	Technical	[129]
USA	2021	US 2021	60.0	20000	Natural	[130]
Sweden	2005	SE 2005	79.3	1400	Natural	[16, 131]
Sweden	1983	SE 1983	2.1	11920	Technical	[16, 132]
Swe./Den.	2003	SE/DK 2003	2.7	6600	Technical	[2, 16, 131, 133]
Norway	2004	NO 2004	0.5	2400	Technical	[16, 132]
Norway	2011	NO 2011	15.0	1152	Natural	[3]
USA	1977	US 1977	13.0	6000	Natural	[1, 16]
USA	1998	US 1998	9.5	950	Natural	[1, 16]
USA	1965	US 1965	6.5	20000	Technical	[1, 16]
USA/Canada	2003	US/CA 2003	16.0	61800	Technical	[1, 16]
Italy	2003	IT 2003	6.7	27000	Technical	[16, 132]
Finland	2011	FI 2011	11.0	13649	Natural	[3]
France	1999	FR 1999	100.0	4000	Natural	[16, 134]
France	1978	FR 1978	4.1	29000	Technical	[16, 132]
Belgium	1982	BE 1982	6.0	2400	Technical	[16, 135]
Canada	1998	CA 1998	125.0	8000	Natural	[16, 131]

Appendix B: Expert elicitation

The following appendix describes the expert elicitation process, following the guidance of the SHELF protocol [114]. Table B.1 provides a introduction to the elicitation workshop. Table B.2 describes the variables of interest, and the questions posed to the experts. Table B.3 gives a summary of the elicited individual expert judgments. The group discussion and process of developing the final distributions is presented in the following paragraph. The final distributions after processing can be found in Paper IV [41]. The experts' names have been omitted for the purpose of privacy.

After the individual expert elicitations were conducted, the results were given to the facilitator without sharing information between the experts. Each elicited distribution was presented to the group and discussed. A linear interpolation of the parameters of the distributions was decided upon for in most cases. The discussions were supported by a third person acting as a Rational Impartial Observer (RIO) with knowledge of the failure statistics, giving input on values that seemed improbable or could indicate that the question may have been misinterpreted. It became apparent that some of the categories posed some challenges in interpretation. Expert A had included considerations such as weather and lack of available transport into the variables related to accessibility. After discussing the comparison with Expert B an agreement was reached that Expert B's judgments for this category were more applicable to the scenario described. Expert A also had no input on the nighttime delay, and Expert B's judgment was decided upon for this category as well. During the elicitation process, it also became clear that the experts could not differentiate between Saturdays and Sundays in terms of delays. As a result, the same elicited values were used to form a single variable for "weekend".

Table B.1: SHELF elicitation record - Part 1: General

Workshop	Expert elicitation - Transmission line down times
Date	21.11.2019
Attendance, roles and expertise	Facilitator: PhD Candidate. Expert 1: Line man organizer (Northern Norway). Expert 2: Line man organizer (Southwestern Norway). Rational Impartial Observer (RIO): Leader, fault statistics.
Purpose of elicitation	To build a model of transmission line down times due to permanent failures. The purpose of the model is to alleviate some of the challenges related to lack of data. This is especially relevant for long outage durations which can have severe consequences for affected customers. The contribution of the experts' judgments will give a more realistic picture of the potential consequences of such events.
This record	Participants are aware that this elicitation will be conducted using the Sheffield Elicitation Framework, and that this document, including attachments, will form a record of the session.
Orientation, training and evidence	RIO was included in the process of developing the conceptual model from which the elicited variables were decided. Experts were sent a brief description of the variables, the elicitation process, and the quantities of interests of a scaled beta and a triangular distribution ahead of the workshop. The participants were encouraged not to discuss between themselves until after the individual elicitation process was finished.
Strengths and weaknesses	Participants have strong knowledge of overhead transmission line repairs. RIO has strong knowledge of the definitions and processes related to transmission line down times. Participants come from different regions in Norway, which is a strength in terms of variety in different geographical and environmental conditions. However, it can also be a potential weakness that experienced processes can be substantially different based on location. To avoid an overly complex model, all processes that are not specifically weather dependent are assumed to be under ideal conditions. This can lead to inaccuracies. Weather effects are incorporated in the larger model through component dependence and weather delays.

Table B.2: SHELF elicitation record - Part 1: Definitions

General	It is to be assumed that each elicited variable reflects the duration in ideal conditions, and should not explicitly incorporate considerations such as harsh weather or other external factors. Failures can be at any location in the geographical area. All elicited distributions represents a duration of a process or delay expressed in hours.
Time of day	Duration from failure until personnel are available at rally point, ready to travel to the fault location due to a failure at different times of the day. Assume that the failure occurs during a weekday. This is divided into three variables: Working hours (07.00-16.00), Evening (16.00-22.00), Night (22.00-07.00).
Weekend	Assume that the failure takes place during a weekend. How much time is added to when the personnel are available at the rally point compared to during a weekday?
Daylight	Assume that the failure occurs when there is no daylight. How much extra time will this cause in terms of fault finding and delays in the reparation process?
Repair	Assume that a permanent failure occurs. Equipment and personnel are at the fault site, and there is ideal weather. How much time will it take to repair the fault for the different components: tower, insulator, phase line, top line, other (e.g. loop, etc.)?
Weather delay	Assume that the failure occurs due to one of the following causes: wind, snow/ice, lightning, landslide. How much extra time should be expected in involuntary delays before transport from the rally point to the fault location?
Accessibility	Consider potential line segment locations where a failure can occur. Categorize how easy it is to access the fault locations. "High" is the location of the most accessible locations, "Low" is the location of the most difficult to access locations, while "Medium" characterizes the average accessibility of all line segments. "Medium high" and "Medium low" represents the areas in between. How long will it take to travel from the rally-point to the fault location in the different accesibility categories?

Table B.3: SHELF elicitation record - Part 2: Eliciting a Continuous Distribution

Introduction	It was initially planned to elicit a scaled beta distribution for the variables. However, when introducing the scaled beta, some challenges became apparent. There was uncertainty among experts as to how to fit the distribution 25 and 75 percentage values, and to what extent they were comfortable with placing these values to begin with. Following the advice of [136] the more intuitive and easier to parameterize triangular distribution was opted for instead.			
Distribution	*Triangular.* Elicited quantities are plausible lower and upper limits, and the most likely value. The elicited values are presented below in the form "Category - Variable - l m u", where l is the set of plausible lower bound, m is the median and u is the plausible upper bound. The elicited values are ordered according to which expert submitted the value. No response is symbolized with a dash (-).			
Category	*Variable*	*Lower*	*Median*	*Upper*
Time of day	Working hours	1,2	2,4	4,8
	Evening	4,4	4,8	6,10
	Night	-,4	-,10	-,20
Weekend	Saturday	4,5	4,18	6,24
	Sunday	4,5	4,18	6,24
Daylight	Darkness	6,5	8,12	8,16
Repair	Tower	96,72	200,180	450,240
	Insulator	6,12	6,30	24,48
	Phase line	8,24	36,100	96,150
	Top line	6,24	14,72	24,96
	Other	3,6	4,12	8,24
Accessibility	High	60,0.5	120,2	240,4
	Medium high	-,0.5	-,3	-,5
	Medium	-,1	-,4	-,6
	Medium low	-,2	-,6	-,10
	Low	96,5	126,10	330,15

Appendix C: CENS correction factors

Table C.1: CENS correction factor by month.

Month	Agriculture	Residential	Industry	Commercial	Public service	Energy-intensive industry
1	1.00	1.00	1.00	1.00	1.00	1.00
2	1.10	1.00	1.00	1.00	1.00	1.00
3	1.10	0.90	0.87	1.00	0.67	1.00
4	1.10	0.90	0.87	1.00	0.67	1.00
5	0.90	0.80	0.87	1.00	0.67	1.00
6	0.90	0.70	0.86	1.02	0.51	1.00
7	0.90	0.60	0.86	1.02	0.51	1.00
8	0.90	0.60	0.86	1.02	0.51	1.00
9	1.00	0.70	0.88	1.06	0.58	1.00
10	1.00	0.90	0.88	1.06	0.58	1.00
11	1.10	0.90	0.88	1.06	0.58	1.00
12	1.10	1.00	1.00	1.00	1.00	1.00

Table C.2: CENS correction factor by day of week.

Day	Agriculture	Residential	Industry	Commercial	Public service	Energy-intensive industry
Weekday	1.00	1.00	1.00	1.00	1.00	1.00
Saturday	1.10	1.15	0.13	0.45	0.30	1.00
Sunday/Holiday	1.10	1.15	0.14	0.11	0.29	1.00

Table C.3: CENS correction factor by hour.

Time	Agriculture	Residential	Industry	Commercial	Public service	Energy-intensive industry
0000–0600	0.80	0.65	0.12	0.11	0.43	1.00
0600–0800	1.00	1.05	1.00	1.00	1.00	1.00
0800–0900	0.90	1.05	1.00	1.00	1.00	1.00
0900–1200	0.90	0.75	1.00	1.00	1.00	1.00
1200–1600	0.70	0.75	1.00	1.00	1.00	1.00
1600–1800	1.00	1.05	1.00	1.00	1.00	1.00
1800–2000	1.00	1.05	0.14	0.30	0.31	1.00
2000–2100	0.80	1.05	0.14	0.29	0.31	1.00
2100–2400	0.80	0.80	0.14	0.29	0.31	1.00

ISBN 978-82-326-6111-4 (printed ver.)
ISBN 978-82-326-6358-3 (electronic ver.)
ISSN 1503-8181 (printed ver.)
ISSN 2703-8084 (online ver.)

NTNU
Norwegian University of
Science and Technology